Syracuse University

SURFACE

Dissertations - ALL

SURFACE

8-2014

Transient electromagnetic scattering by a radially uniaxial dielectric sphere: Debye series, Mie series and ray tracing methods

Mohsen Yazdani
Syracuse University

Follow this and additional works at: https://surface.syr.edu/etd

Part of the Engineering Commons

Recommended Citation

Yazdani, Mohsen, "Transient electromagnetic scattering by a radially uniaxial dielectric sphere: Debye series, Mie series and ray tracing methods" (2014). *Dissertations - ALL*. 154.
https://surface.syr.edu/etd/154

Abstract

Transient electromagnetic scattering by a radially uniaxial dielectric sphere is explored using three well-known methods: Debye series, Mie series, and ray tracing theory.

In the first approach, the general solutions for the impulse and step responses of a uniaxial sphere are evaluated using the inverse Laplace transformation of the generalized Mie series solution. Following high frequency scattering solution of a large uniaxial sphere, the Mie series summation is split into the high frequency (HF) and low frequency terms where the HF term is replaced by its asymptotic expression allowing a significant reduction in computation time of the numerical Bromwich integral.

In the second approach, the generalized Debye series for a radially uniaxial dielectric sphere is introduced and the Mie series coefficients are replaced by their equivalent Debye series formulations. The results are then applied to examine the transient response of each individual Debye term allowing the identification of impulse returns in the transient response of the uniaxial sphere.

In the third approach, the ray tracing theory in a uniaxial sphere is investigated to evaluate the propagation path as well as the arrival time of the ordinary and extraordinary returns in the transient response of the uniaxial sphere. This is achieved by extracting the reflection and transmission angles of a plane wave obliquely incident on the radially oriented air-uniaxial and uniaxial-air boundaries, and expressing the phase velocities as well as the refractive indices of the ordinary and extraordinary waves in terms of the incident angle, optic axis and propagation direction. The results indicate a satisfactory agreement between Debye series , Mie series and ray tracing methods.

Transient electromagnetic scattering by a radially
uniaxial dielectric sphere: Debye series, Mie series
and ray tracing methods

By

Mohsen Yazdani

M.S. IUST, 2009

Dissertation

Submitted in partial fulfillment of the requirements
for the degree of Doctor of Philosophy in Electrical
Engineering

Syracuse University

August 2014

Acknowledgement

I am deeply thankful of many individuals who have continually supported my work. First and foremost, I am forever indebted to my advisor Dr. Ercument Arvas for his unreserved support, advice and most importantly for creating a research environment in which my Ph.D. experience became exciting and productive.

I am sincerely appreciative to my co-advisor, Dr. Joseph Mautz, for his inspirational and timely advice. I learned many great lessons from his unique perspective of research, his meticulousness and expecting excellence in the research quality.

I would like to extend my thanks to Dr. Jay Lee who first introduced and thought me the wave analysis in anisotropic medium and provided encouraging and constructive feedbacks on my scientific papers and thesis.

I would like to thank the members of my defense committee for taking their time, Dr. Agraval, Dr. Dang and specifically Dr. Elsherbeni and Dr. Demir who travel long distances to take part in my Ph.D. defense.

My Last and especial appreciation is for my loving and caring family and friends. I would not have completed this long but fulfilling journey without the constant love and support of my parents specifically my mom who always inspired and supported me in my academic pursuits. To my siblings particularly my older brother Mahdi thanks for always being supportive. I want to thank my close friend and colleague Dr. Luke Murphy who was always available for discussion and brain storming suggestions.

Contents

Table of figures

Chapter 1

Chapter 2

Chapter 3

Chapter 4

Chapter 5

Chapter 1 Prior work

1.1 Motivation

The transient electromagnetic wave scattering by a radially uniaxial dielectric sphere using three well-known methods, the generalized Lorenz-Mie theory, Debye series and ray tracing is the subject of this dissertation. The work is motivated by the increasing use of ultra-short pulse RADAR technology on target identification and the broad application of anisotropic materials in the field of scattering, e.g., cloaking of the targets in which RCS reduction became a challenge in recent years.

The existing frequency domain scattering solutions, while offering numerous applications on particle sizing and target identifications, fail to provide a physical interpretation and simple explanation of the scattering mechanism especially in the case of anisotropic material in which electric permittivity is characterized by a square matrix with the elements determined by constitutive relations of the medium. To overcome this difficulty, the time domain solution sounds a promising approach where both scattering amplitude and phase responses are used to generate the transient electromagnetic scattering response by different objects and therefore more information can be extracted using this solution. It is known that the transient scattering solution can be derived by either solving the problem directly in time domain using numerical techniques, e.g., FDTD or by inverse Laplace transformation of the frequency domain solution. This dissertation concerns the second approach in which two well-known frequency domain solutions, generalized Mie and Debye series, are introduced to investigate the influence of uniaxiality on the transient scattering response of various uniaxial dielectric spheres.

1

1.2   Introduction

The electromagnetic scattering of plane waves by anisotropic and isotropic dielectric spheres has been an attractive subject over the past few decades. A rigorous solution for scattering from an isotropic sphere was first developed by Lorenz and Mie in the form of an infinite series of partial wave contributions [1]. This is achieved by expressing the incident and scattered electromagnetic waves in terms of infinite series of spherical Bessel and Hankel functions and extracting the well-known Mie series coefficients by deriving the tangential electric and magnetic field components both inside and outside of the sphere. Wong and Chen [2] developed a generalized Mie series scattering solution for the anisotropic dielectric sphere by deriving the spherical potential wave functions in a radially uniaxial sphere and computing the scattered wave amplitudes in the uniaxial-air boundary surface of the sphere. A significant difference between backscattering by the uniaxial and isotropic dielectric spheres were reported in their paper. However, as stated in the paper, there is no general rule for scattering by the non-absorbing uniaxial dielectric sphere and therefore further work in this area was required. This difficulty is partially resolved by introducing other methods e.g., ray tracing Debye series solution. By means of the Debye series formulation, the Mie series scattering wave amplitudes, b_n and c_n, are decomposed into a series of partial wave contributions that are diffracted, reflected and refracted following by P−1 internal reflections in the sphere of Fig. 1.1. Lock and Laven used this theory to investigate the contribution of different p-waves on the scattering from dielectric and coated dielectric spheres [3]. Investigating each individual term of the Debye series can also improve our understanding of complex scattering processes e.g., the mechanisms causing the atmospheric optical phenomena

such as primary/secondary rainbow, corona and glory, as well as the deformation of intricate ripples in the curve associated with bistatic RCS of the dielectric sphere in Fig. 1.2 [4].

In [5] the calculation of scattering from a water droplet using the Debye series resulted the better understanding of light scattering by spherical particles, e.g., the colored rings of glories seem to be generated by rays that have been reflected once within the water drops while the bright white central feature is mainly due to higher-order terms.
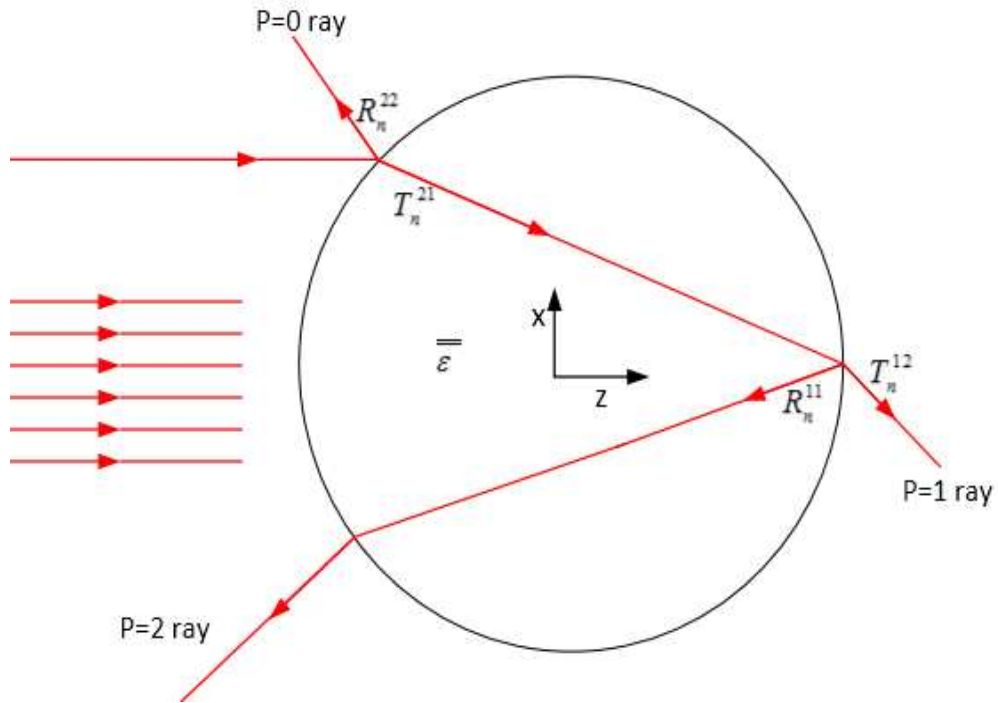
Fig. 1. 1. A plane wave approaching a uniaxial dielectric sphere

However, there are a number of processes that cannot be examined by Debye series in the frequency domain such as the separation of geometrical wave contributions that belong to the same term of the Debye series and same scattering angle but travel along

different path lengths as shown in Fig. 1.3. These types of problems have been solved by time domain approach where a short electromagnetic pulse is incident upon the sphere and the delay time is measured for each individual reflected ray [6]–[7].

Perhaps the first attempt to calculate the time domain response waveform in the radar scattering context was that of Kennaugh who estimated the impulse response of the field scattered from a perfectly conducting sphere using an extremely simple approximation [8]–[9]. The first order approximation to the impulse response of a perfectly conducting sphere was proposed in his paper using the Rayleigh scattering approximation in the low frequency region and the geometric optics solution in the high frequency region. Aly and Wong [10] obtained the transient response of a dielectric sphere using a high frequency scattering approximation. They have shown that the high frequency asymptotic form of the frequency domain representation can be applied beyond a certain point of the contour of the inverse Laplace transformation integral which results in a significant reduction of computation time. According to the high frequency scattering solution of an isotropic sphere, [11], the infinite Mie series summation can be replaced by a rapidly converging contour integral using the modified Watson transformation method. The resulting function is then split into the geometric optics and diffracted field contributions. The coefficients associated with the geometric optics portion (high frequency solution) are replaced by their equivalent Debye series formulation and the results are simplified and then computed using the saddle point method.

The time domain backscattering by perfectly conducting and dielectric spheres illuminated by modulated pulse trains is also investigated by Rheinstein [12]. Using the Fourier series method, the scattering of a transient EM wave was estimated and various

4

returns were observed in his solutions. However, his achievements were not fully understood due to employing Lorenz-Mie theory which provides no physical interpretation of the scattering mechanisms.
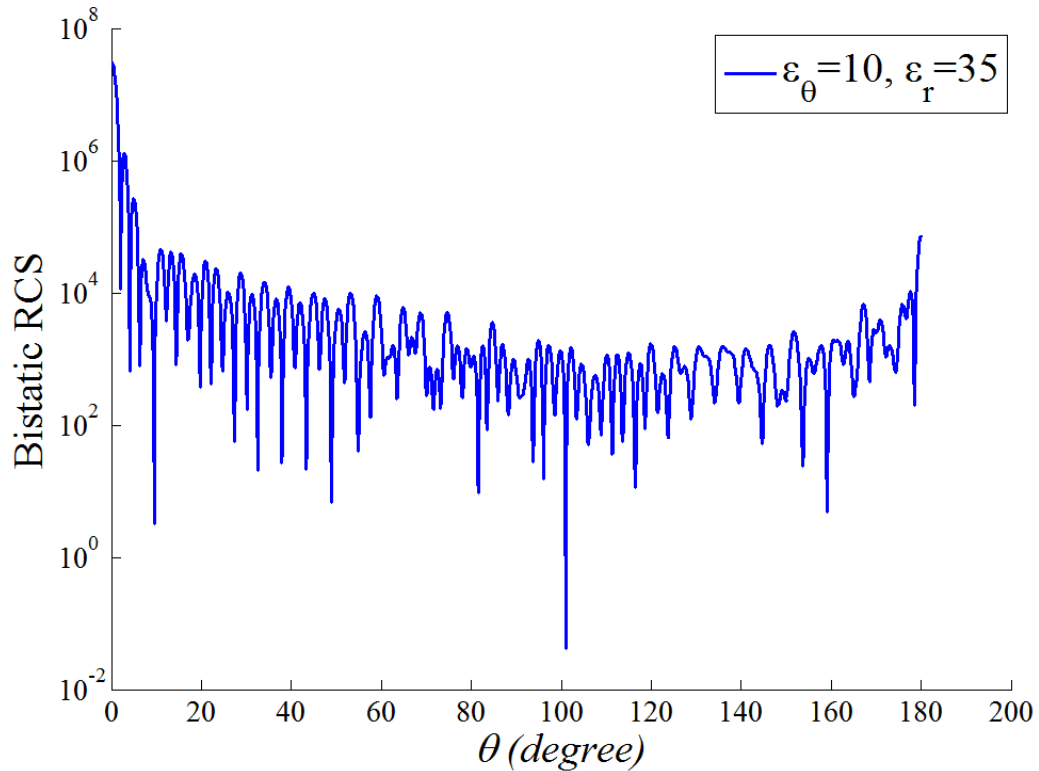
Fig. 1. 2. Bistatic RCS of uniaxial dielectric sphere calculated using Mie series, and $k_0 a = 100$ [4].

To overcome this difficulty, Lock and Laven [6]–[7] estimated the signature of various scattering processes from the isotropic dielectric sphere using the time domain Debye series formulation. This allows the calculation of only a single term of the Debye series at each time rather than the entire Mie series time domain solution which leads to the identification of each individual return in the transient scattering response of the dielectric sphere.
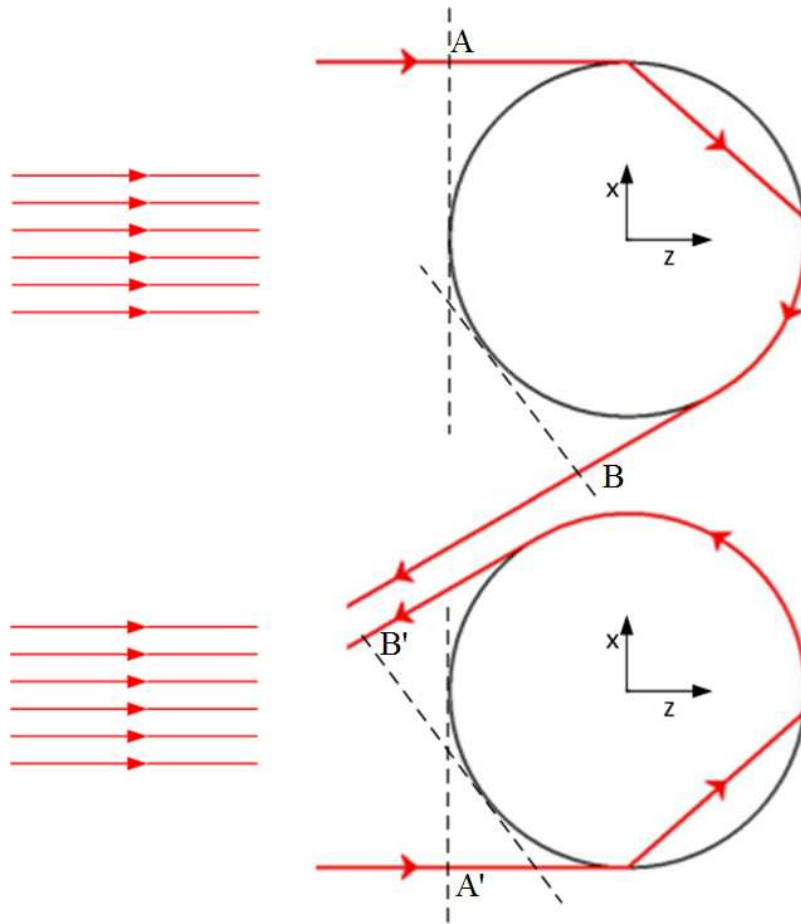
Fig. 1. 3. Pictorial representation of p=1 wave, Shortcut wave

The time domain scattering solution using Mie and Debye series was also studied for various isotropic bodies of revolution. The transient electromagnetic wave scattering by arbitrarily shaped cylindrical conducting structures for different observation points was investigated in [13]. The solution was achieved by introducing an integral equation that was numerically computed in the time domain. The method was particularly well suited for computing electromagnetic impulse response of finite numbers of cylindrical scatterers with arbitrary shaped cross section.

The time domain scattering by a thin dielectric coated sphere and a plate coated with a thin dielectric layer is also investigated by Strifors and Gaunaurd [14]. After deriving the frequency domain solution of the dielectric coated sphere, the time domain scattering by this object is computed using the inverse discrete Fourier transformation and the results are compared with the time domain scattering by the conducting plate coated with the same dielectric material. The transient scattering by the coated sphere is also studied by Laven and Lock using the Debye series solution [15]. For the fixed core and coating radii, the Debye series terms that most strongly contribute to the scattered intensity were identified for different angles of observation. This achievement, which was obtained by investigating each individual Debye term, offered a good physical interpretation of the scattering from dielectric coated sphere.

The Mie and Debye theories are successful in describing several certain features of the transient EM scattering by isotropic sphere however lack of a simple graphical computation to determine the features of impulse returns, e.g., arrival time, travel path, velocity, refractive index, etc., indicates that the ray tracing modeling is needed for uniaxial dielectric sphere.

In the past, ray tracing has been frequently used to describe many complex scattering problems. In 1637, Descartes used ray tracing to understand the formation of primary and secondary rainbows [1]. Newton subsequently extended the theory to explain the colors of the rainbow. In[4], [6], and [7]the ray tracing along with the Debye series solution is applied to compute the arrival time of each individual ray of order p in the transient response of the isotropic dielectric sphere and propose a simple description for the formation of optical phenomena such as primary and secondary rainbow, glory and

corona. Ray tracing is also studied for the anisotropic plane parallel-plates by Simon in [16]. This was achieved by computation of the reflection and refraction wave angles in the air-anisotropic medium and the possible reflection cases in anisotropic-air boundaries reported in [17]. For the most general form of the refraction and reflection in the air-anisotropic boundary, the readers are encouraged to explore [18]–[19].

To improve our understanding of scattering from the anisotropic sphere, the transient scattering by the uniaxial sphere using both Mie and Debye series along with ray tracing is investigated in this dissertation.

In Chapter 2, the Maxwell equations in a radially uniaxial medium are introduced and the scalar potential wave equations representing TE and TM waves are evaluated. The vector potentials A and F both inside and outside of a uniaxial sphere are also derived in this chapter and the general formulations for the scattering and traveling wave amplitudes are obtained.

In Chapter 3, in addition to exploring the bistatic Radar Cross Section (RCS) of a uniaxial dielectric sphere using Lorenz-Mie theory, the generalized Debye series for a radially uniaxial sphere is introduced. It is shown that the generalized Mie series coefficients b_n and c_n are the decomposition of a series of partial wave contributions that are diffracted, reflected and refracted following by p-1 internal reflections in the sphere. The monostatic and bistatic RCS are then examined for each term of the Debye series, and compared with those of computed in isotropic case.

In Chapter 4, the Watson transformation method is briefly studied and it is used to transform the slowly converging Mie series summation into a rapidly converging contour

integral. Applying the Debye's asymptotic formula for alternative spherical Hankel functions, the problem reduces to a form that can be computed using the saddle point method. An approximate formula for high frequency backscattering from the uniaxial dielectric sphere is proposed and the results are compared with those computed using the Lorenz-Mie theory.

In Chapter 5, the impulse and step responses of a radially uniaxial sphere are calculated using the inverse Laplace transformation and the Mie series-asymptotic combination method. The time domain Debye series is also introduced to evaluate the impulse response of each individual term of the Debye series.

In Chapter 6, the ray tracing is introduced in a uniaxial dielectric sphere. The generalized Snell's laws for air-uniaxial and uniaxial-air boundaries of the sphere are briefly studied and the general formulations for velocity and refractive indices of ordinary and extraordinary waves are derived. The ray tracing for ordinary and extraordinary wave returns of order p=1–2 are also investigated and the results are applied to obtain the general formulations for computing the arrival times of extraordinary and ordinary waves in the uniaxial sphere. The results are validated by satisfactory agreement between Mie, Debye and ray tracing methods.

Chapter 2   Electromagnetic scattering by a radially uniaxial sphere

2.1   Introduction

Electromagnetic plane wave scattering by a radially uniaxial dielectric sphere is studied in this chapter. Starting from the Maxwell equations, the general solutions for TE_r and TM_r scalar potentials in an unbounded radially uniaxial medium are evaluated and the electric and magnetic field components are expressed in terms of alternative spherical Bessel and Hankel functions, similar to the isotropic case, but with the order of functions determined by the anisotropic ratio ($AR = \frac{\varepsilon_\theta}{\varepsilon_r}$). Proceeding with the solution for a uniaxial dielectric sphere immersed in an unbounded air region, the electric and magnetic vector potentials both inside and outside of the sphere are derived, and the tangential electric and magnetic field components are computed. After applying the boundary conditions on the interface of the uniaxial sphere, the scattering and traveling wave amplitudes are extracted and the results are compared with those computed for the isotropic sphere.

This chapter is organized as follows: In Section 2.2 the constitutive relations for a radially uniaxial medium are substituted into the source free Maxwell equations and the scalar potential wave equations for TE and TM waves are obtained. Sections 2.3 and 2.4 propose the general solutions for the scalar potential wave equations using the separation of variables method. In Section 2.5, the vector potentials A and F are calculated and the results are applied to compute the E and H field components. In Section 2.6, the vector potentials A and F both inside and outside of a uniaxial sphere are derived and the general formulas for the scattering and traveling wave amplitudes are extracted.

2.2 The derivation of Maxwell equations in a radially uniaxial medium

Consider a radially uniaxial medium characterized by the constitutive relations

$$\boldsymbol{D} = (\bar{\bar{\varepsilon}} \cdot \boldsymbol{E})$$

(2-1)

$$\boldsymbol{B} = \mu_0 \boldsymbol{H}$$

(2-2)

where $\bar{\bar{\varepsilon}}$ is the permittivity tensor given by

$$\bar{\bar{\varepsilon}} = \varepsilon_0 \begin{bmatrix} \varepsilon_r & 0 & 0 \\ 0 & \varepsilon_\theta & 0 \\ 0 & 0 & \varepsilon_\theta \end{bmatrix}$$

(2-3)

and μ_0 and ε_0 are, respectively, the permeability and permittivity of free space. The source-free Maxwell equations are

$$\nabla \times \boldsymbol{E} = -j\omega \boldsymbol{B}$$

(2-4)

$$\nabla \times \boldsymbol{H} = j\omega \boldsymbol{D}.$$

(2-5)

Substitution of (2-1) into (2-4) and (2-2) into (2-5) give

$$\nabla \times (\bar{\bar{\varepsilon}}^{-1} \cdot \boldsymbol{D}) = -j\omega \boldsymbol{B}$$

(2-6)

$$\nabla \times \boldsymbol{B} = j\omega \mu_0 \boldsymbol{D}.$$

(2-7)

2.2.1 A TM solution of Maxwell equations in a radially uniaxial medium

In a source free region, the magnetic flux density is solenoidal and can be represented as the curl of the vector potential $\boldsymbol{A}$. Therefore

11

$$\boldsymbol{B}^{\text{TM}} = \nabla \times \boldsymbol{A}$$

(2-8)

Substituting (2-8) into (2-6) and (2-7), we obtain the following

$$\nabla \times \{(\bar{\bar{\varepsilon}}^{-1} \cdot \boldsymbol{D}^{\text{TM}}) + j\omega \boldsymbol{A}\} = \boldsymbol{0}.$$

(2-9)

and

$$\boldsymbol{D}^{\text{TM}} = \frac{1}{j\omega\mu_0} \nabla \times \nabla \times \boldsymbol{A}$$

(2-10)

Equation (2-9) implies that

$$(\bar{\bar{\varepsilon}}^{-1} \cdot \boldsymbol{D}^{\text{TM}}) + j\omega \boldsymbol{A} = -\nabla \phi^{\text{TM}}$$

(2-11)

where ϕ^{TM} is an arbitrary scalar function of r, θ, and ϕ. Multiplication of (2-11) by $\bar{\bar{\varepsilon}}$

gives

$$\boldsymbol{D}^{\text{TM}} + j\omega\bar{\bar{\varepsilon}} \cdot \boldsymbol{A} = -\bar{\bar{\varepsilon}} \cdot (\nabla \phi^{\text{TM}}).$$

(2-12)

Substitution of (2-10) into (2-12) yields

$$\nabla \times \nabla \times \boldsymbol{A} + j\omega\mu_0 \bar{\bar{\varepsilon}} \cdot (\nabla \phi^{\text{TM}}) - k_0^2 \bar{\bar{\varepsilon}}/\varepsilon_0 \cdot \boldsymbol{A} = \boldsymbol{0}$$

(2-13)

where $k_0^2 = \omega^2 \mu_0 \varepsilon_0$. Let

$$\boldsymbol{A} = \hat{\boldsymbol{r}} r \psi^{\text{TM}}.$$

(2-14)

Using vector identities in [20], it can be shown that

$$\nabla \times \nabla \times (\hat{\boldsymbol{r}} r \psi^{\text{TM}}) = \hat{\boldsymbol{r}}(-\frac{1}{r^2}\frac{\partial^2 (r\psi^{TM})}{\partial \theta^2}$$

(2-15)

$$-\frac{1}{r^2 \tan \theta}\frac{\partial (r\psi^{TM})}{\partial \theta} - \frac{1}{r^2 \sin^2 \theta}\frac{\partial^2 (r\psi^{TM})}{\partial \phi^2}) + \hat{\theta}\left(\frac{1}{r}\frac{\partial^2 (r\psi^{TM})}{\partial r \partial \theta}\right)$$

$$+ \hat{\phi}\left(\frac{1}{r\sin \theta}\frac{\partial^2 (r\psi^{TM})}{\partial \phi \partial r}\right)$$

$$\nabla \phi^{\mathrm{TM}(i)} = \hat{r}\frac{\partial \phi^{TM}}{\partial r} + \hat{\theta}\left(\frac{1}{r}\frac{\partial \phi^{TM}}{\partial \theta}\right) + \hat{\phi}\left(\frac{1}{r\sin \theta}\frac{\partial \phi^{TM}}{\partial \phi}\right). \qquad (2\text{-}16)$$

with $\boldsymbol{A}$ given by (2-14), and after use of (2-3), (2-15) and (2-16), the r-, θ-, and ϕ-components of (2-13) are the respective equations

$$-\frac{1}{r^2}\frac{\partial^2 (r\psi^{TM})}{\partial \theta^2} - \frac{1}{r^2 \tan \theta}\frac{\partial (r\psi^{TM})}{\partial \theta} - \frac{1}{r^2 \sin^2 \theta}\frac{\partial^2 (r\psi^{TM})}{\partial \phi^2} - k_0^2 \varepsilon_r r\psi^{\mathrm{TM}}$$

$$+ j\omega\mu_0\varepsilon_0\varepsilon_r \frac{\partial \phi^{TM}}{\partial r} = 0 \qquad (2\text{-}17)$$

$$\frac{1}{r}\frac{\partial^2 (r\psi^{TM})}{\partial r \partial \theta} + j\omega\mu_0\varepsilon_0\varepsilon_\theta \left(\frac{1}{r}\frac{\partial \phi^{TM}}{\partial \theta}\right) = 0 \qquad (2\text{-}18)$$

$$\frac{1}{r\sin \theta}\frac{\partial^2 (r\psi^{TM})}{\partial \phi \partial r} + j\omega\mu_0\varepsilon_0\varepsilon_\theta \left(\frac{1}{r\sin \theta}\frac{\partial \phi^{TM}}{\partial \phi}\right) = 0. \qquad (2\text{-}19)$$

Equations (2-18) and (2-19) will be satisfied if

$$\phi^{\mathrm{TM}} = -\frac{1}{j\omega\mu_0\varepsilon_0\varepsilon_\theta}\frac{\partial (r\psi^{TM})}{\partial r}. \qquad (2\text{-}20)$$

Substitution of the partial derivative with respect to r of (2-20) into (2-17) leads to

13

$$-\frac{1}{r^2}\frac{\partial^2(r\psi^{TM})}{\partial\theta^2} - \frac{1}{r^2\tan\theta}\frac{\partial(r\psi^{TM})}{\partial\theta} - \frac{1}{r^2\sin^2\theta}\frac{\partial^2(r\psi^{TM})}{\partial\phi^2}$$

$$-\left(\frac{\varepsilon_r}{\varepsilon_\theta}\right)\frac{\partial^2}{\partial r^2}(r\psi^{TM}) - k_0^2\varepsilon_r r\psi^{TM} = 0. \tag{2-21}$$

Equation (2-21) can be expressed as

$$-r\left(\frac{1}{r^2}\frac{\partial^2\psi^{TM}}{\partial\theta^2} + \frac{1}{r^2\sin^2\theta}\frac{\partial\psi^{TM}}{\partial\theta} + \frac{1}{r^2\sin^2\theta}\frac{\partial^2\psi^{TM}}{\partial\phi^2} + \left(\frac{\varepsilon_r}{\varepsilon_\theta}\right)\frac{1}{r}\frac{\partial^2}{\partial r^2}(r\psi^{TM})\right.$$

$$\left. + k_0^2\varepsilon_r\psi^{TM}\right) = 0. \tag{2-22}$$

Knowing that $\tan\theta = \frac{\sin\theta}{\tan\theta}$, one can observe in (2-22) that

$$\frac{\partial^2\psi^{TM}}{\partial\theta^2} + \frac{1}{\tan\theta}\frac{\partial\psi^{TM}}{\partial\theta} = \frac{1}{\sin\theta}\frac{\partial}{\partial\theta}\left(\sin\theta\frac{\partial\psi^{TM}}{\partial\theta}\right). \tag{2-23}$$

$$\frac{\partial^2}{\partial r^2}(r\psi^{TM}) = \frac{1}{r}\frac{\partial}{\partial r}\left(r^2\frac{\partial\psi^{TM}}{\partial r}\right). \tag{2-24}$$

Substitution of (2-23) and (2-24) into (2-22) gives, after deletion of the factor of $-r$,

$$\left(\frac{\varepsilon_r}{\varepsilon_\theta}\right)\frac{1}{r^2}\frac{\partial}{\partial r}\left(r^2\frac{\partial\psi^{TM}}{\partial r}\right) + \frac{1}{r^2\sin\theta}\frac{\partial}{\partial\theta}\left(\sin\theta\frac{\partial\psi^{TM}}{\partial\theta}\right) + \frac{1}{r^2\sin^2\theta}\frac{\partial^2\psi^{TM}}{\partial\phi^2}$$

$$+ k_0^2\varepsilon_r\psi^{TM} = 0. \tag{2-25}$$

Equation (2-25) is the wave equation for ψ^{TM} and recast as

$$\left(\frac{\varepsilon_r}{\varepsilon_\theta}\right)\frac{1}{r^2}\frac{\partial}{\partial r}\left(r^2\frac{\partial\psi^{TM}}{\partial r}\right) + \nabla_t^2\psi^{TM} + k_0^2\varepsilon_r\psi^{TM} = 0 \tag{2-26}$$

where

14

$$\nabla_t^2 \psi^{TM} = \frac{1}{r^2 \sin\theta} \frac{\partial}{\partial\theta}\left(\sin\theta \frac{\partial\psi^{TM}}{\partial\theta}\right) + \frac{1}{r^2 \sin^2\theta} \frac{\partial^2\psi^{TM}}{\partial\phi^2}. \tag{2-27}$$

Equation (2-27) can also be rewritten as

$$\nabla_t^2 \psi^{TM} = \nabla^2 \psi^{TM} - \frac{1}{r^2} \frac{\partial}{\partial r}\left(r^2 \frac{\partial\psi^{TM}}{\partial r}\right) \tag{2-28}$$

where, from the last of (A-12) in [21],

$$\nabla^2 \psi^{TM} = \frac{1}{r^2} \frac{\partial}{\partial r}\left(r^2 \frac{\partial\psi^{TM}}{\partial r}\right) + \frac{1}{r^2 \sin\theta} \frac{\partial}{\partial\theta}\left(\sin\theta \frac{\partial\psi^{TM}}{\partial\theta}\right)$$

$$+ \frac{1}{r^2 \sin^2\theta} \frac{\partial^2\psi^{TM}}{\partial\phi^2}. \tag{2-29}$$

2.2.2 A TE solution of Maxwell equations subject to the constitutive relations

In a source free region, the electric flux density is solenoidal and can be represented as the curl of the vector potential $\boldsymbol{F}$. Therefore

$$\boldsymbol{D}^{\mathrm{TE}} = -\nabla \times \boldsymbol{F} \tag{2-30}$$

$$\boldsymbol{B}^{\mathrm{TE}} = \frac{1}{j\omega} \nabla \times (\bar{\bar{\varepsilon}}^{-1} \cdot \nabla \times \boldsymbol{F}) \tag{2-31}$$

substituting (2-30) into (2-6) and (2-7), we obtain the following solution to (2-6) and (2-7)

$$\nabla \times (\boldsymbol{B}^{\mathrm{TE}} + j\omega\mu_0\boldsymbol{F}) = \boldsymbol{0}. \tag{2-32}$$

Equation (2-32) implies that

15

$$\boldsymbol{B}^{\mathrm{TE}} + j\omega\mu_0\boldsymbol{F} = -\mu_0\nabla\phi^{\mathrm{TE}} \qquad (2\text{-}33)$$

where ϕ^{TE} is an arbitrary scalar function of r, θ, and ϕ. Use of (2-33) in (2-31) gives

$$\nabla \times (\bar{\bar{\varepsilon}}^{-1} \cdot \nabla \times \boldsymbol{F}) + j\omega\mu_0\nabla\phi^{\mathrm{TE}} - \frac{k_0^2}{\varepsilon_0}\boldsymbol{F} = \boldsymbol{0}. \qquad (2\text{-}34)$$

Let

$$\boldsymbol{F} = \hat{\boldsymbol{r}}r\psi^{\mathrm{TE}}. \qquad (2\text{-}35)$$

Substitution of (2-35) into (2-34) gives

$$\nabla \times \left(\bar{\bar{\varepsilon}}^{-1} \cdot \nabla \times (\hat{\boldsymbol{r}}r\psi^{\mathrm{TE}})\right) + j\omega\mu_0\nabla\phi^{\mathrm{TE}} - \frac{k_0^2}{\varepsilon_0}\hat{\boldsymbol{r}}r\psi^{\mathrm{TE}} = \boldsymbol{0}. \qquad (2\text{-}36)$$

From the third of (A-12) in [21],

$$\nabla \times (\hat{\boldsymbol{r}}r\psi^{\mathrm{TE}}) = \hat{\theta}\frac{1}{r\sin\theta}\frac{\partial}{\partial\phi}(r\psi^{\mathrm{TE}}) - \hat{\phi}\frac{1}{r}\frac{\partial}{\partial\theta}(r\psi^{\mathrm{TE}}) \qquad (2\text{-}37)$$

which reduces to

$$\nabla \times (\hat{\boldsymbol{r}}r\psi^{\mathrm{TE}}) = \hat{\theta}\frac{1}{\sin\theta}\frac{\partial\psi^{TE}}{\partial\phi} - \hat{\phi}\frac{\partial\psi^{TE}}{\partial\theta}. \qquad (2\text{-}38)$$

Multiplying (2-38) by $\bar{\bar{\varepsilon}}^{-1}$ where $\bar{\bar{\varepsilon}}$ is given by (2-3), we obtain

$$\bar{\bar{\varepsilon}}^{-1} \cdot \left(\nabla \times (\hat{\boldsymbol{r}}r\psi^{\mathrm{TE}})\right) = \hat{\theta}\frac{1}{\varepsilon_0\varepsilon_\theta\sin\theta}\frac{\partial\psi^{TE}}{\partial\phi} - \hat{\phi}\frac{1}{\varepsilon_0\varepsilon_\theta}\frac{\partial\psi^{TE}}{\partial\theta}. \qquad (2\text{-}39)$$

Using the third of (A-12) in [21] to evaluate the curl of (2-39), we obtain

$$\nabla \times \left(\bar{\bar{\varepsilon}}^{-1} \cdot \left(\nabla \times (\hat{\boldsymbol{r}} r \psi^{\mathrm{TE}})\right)\right) = \hat{\boldsymbol{r}} \frac{1}{\varepsilon_0 \varepsilon_\theta r \sin \theta}$$

$$\cdot \left(-\frac{\partial}{\partial \theta}\left(\sin \theta \frac{\partial \psi^{TE}}{\partial \theta}\right) - \frac{\partial}{\partial \phi}\left(\frac{1}{\sin \theta}\frac{\partial \psi^{TE}}{\partial \phi}\right)\right) + \hat{\theta} \frac{1}{\varepsilon_0 \varepsilon_\theta r}\frac{\partial}{\partial r}\left(r \frac{\partial \psi^{TE}}{\partial \theta}\right)$$

$$+ \hat{\phi} \frac{1}{\varepsilon_0 \varepsilon_\theta r}\frac{\partial}{\partial r}\left(\frac{r}{\sin \theta}\frac{\partial \psi^{TE}}{\partial \phi}\right). \tag{2-40}$$

Equation (2-16) with ϕ^{TM} replaced by ϕ^{TE} is

$$\nabla \phi^{\mathrm{TE}} = \hat{\boldsymbol{r}} \frac{\partial \phi^{TE}}{\partial r} + \hat{\theta}\left(\frac{1}{r}\frac{\partial \phi^{TE}}{\partial \theta}\right) + \hat{\phi}\left(\frac{1}{r \sin \theta}\frac{\partial \phi^{TE}}{\partial \phi}\right). \tag{2-41}$$

The r-, θ-, and ϕ-components of (2-36) are, after use of (2-40) and (2-41), the respective equations

$$-\frac{1}{\varepsilon_\theta r \sin \theta}\left(\frac{\partial}{\partial \theta}\left(\sin \theta \frac{\partial \psi^{TE}}{\partial \theta}\right) + \frac{\partial}{\partial \phi}\left(\frac{1}{\sin \theta}\frac{\partial \psi^{TE}}{\partial \phi}\right)\right) + j\omega\mu_0\varepsilon_0 \frac{\partial \phi^{TE}}{\partial r}$$
$$- k_0^2 r \psi^{\mathrm{TE}} = 0 \tag{2-42}$$

$$\frac{1}{\varepsilon_\theta r}\frac{\partial}{\partial r}\left(r \frac{\partial \psi^{TE}}{\partial \theta}\right) + j\omega\mu_0\varepsilon_0 \left(\frac{1}{r}\right)\frac{\partial \phi^{TE}}{\partial \theta} = 0 \tag{2-43}$$

$$\frac{1}{\varepsilon_\theta r}\frac{\partial}{\partial r}\left(\frac{r}{\sin \theta}\frac{\partial \psi^{TE}}{\partial \phi}\right) + j\omega\mu_0\varepsilon_0 \left(\frac{1}{r \sin \theta}\right)\frac{\partial \phi^{TE}}{\partial \phi} = 0. \tag{2-44}$$

Equations (2-42)–(2-44) are rewritten as

$$-\frac{r}{\varepsilon_\theta}\left(\frac{1}{r^2 \sin\theta}\frac{\partial}{\partial\theta}\left(\sin\theta\,\frac{\partial\psi^{TE}}{\partial\theta}\right) + \frac{1}{r^2\sin^2\theta}\frac{\partial^2\psi^{TE}}{\partial\phi^2} - \frac{j\omega\mu_0\varepsilon_0\varepsilon_\theta}{r}\frac{\partial\phi^{TE}}{\partial r}\right.$$

$$\left. + k_0^2 \varepsilon_\theta \psi^{\text{TE}}\right) = 0 \tag{2-45}$$

$$\frac{1}{\varepsilon_\theta r}\frac{\partial}{\partial\theta}\left(\frac{\partial}{\partial r}(r\psi^{\text{TE}}) + j\omega\mu_0\varepsilon_0\varepsilon_\theta\phi^{\text{TE}}\right) = 0 \tag{2-46}$$

$$\frac{1}{\varepsilon_\theta r \sin\theta}\frac{\partial}{\partial\phi}\left(\frac{\partial}{\partial r}(r\psi^{\text{TE}}) + j\omega\mu_0\varepsilon_0\varepsilon_\theta\phi^{\text{TE}}\right) = 0. \tag{2-47}$$

Equations (2-46) and (2-47) will be satisfied if

$$j\omega\mu_0\varepsilon_0\varepsilon_\theta\phi^{\text{TE}} = -\frac{\partial}{\partial r}(r\psi^{\text{TE}}). \tag{2-48}$$

Discarding the factor of $-\frac{r}{\varepsilon_0}$ in (2-45) and then substituting the partial derivative with respect to r of (2-48) into the resulting equation, we obtain

$$\frac{1}{r}\frac{\partial^2}{\partial r^2}(r\psi^{\text{TE}}) + \frac{1}{r^2\sin\theta}\frac{\partial}{\partial\theta}\left(\sin\theta\,\frac{\partial\psi^{TE}}{\partial\theta}\right)$$

$$+\frac{1}{r^2\sin^2\theta}\frac{\partial^2\psi^{TE}}{\partial\phi^2} + k_0^2\varepsilon_\theta\psi^{\text{TE}} = 0. \tag{2-49}$$

Modifying (2-24) by replacing ψ^{TM} by ψ^{TE} and then substituting the modified (2-24) into (2-49), we obtain

$$\frac{1}{r^2}\frac{\partial}{\partial r}\left(r^2\,\frac{\partial\psi^{TE}}{\partial r}\right) + \frac{1}{r^2\sin\theta}\frac{\partial}{\partial\theta}\left(\sin\theta\,\frac{\partial\psi^{TE}}{\partial\theta}\right) + \frac{1}{r^2\sin^2\theta}\frac{\partial^2\psi^{TE}}{\partial\phi^2}$$

$$+ k_0^2\varepsilon_\theta\psi^{\text{TE}} = 0. \tag{2-50}$$

Equation (2-50) is the wave equation for ψ^{TE}.

2.3 A general solution for $\boldsymbol{\psi^{\text{TM}}}$ using the method of separation of variables

By introducing the electric anisotropy ratio

$$AR = \frac{\varepsilon_\theta}{\varepsilon_r} \tag{2-51}$$

(2-25) can be written as

$$\frac{1}{(AR)r^2}\frac{\partial}{\partial r}\left(r^2\frac{\partial \psi^{TM}}{\partial r}\right) + \frac{1}{r^2 \sin\theta}\frac{\partial}{\partial\theta}\left(\sin\theta\,\frac{\partial\psi^{TM}}{\partial\theta}\right) + \frac{1}{r^2 \sin^2\theta}\frac{\partial^2\psi^{TM}}{\partial\phi^2}$$

$$+ k_0^2\varepsilon_r\psi^{\text{TM}} = 0. \tag{2-52}$$

Substituting

$$\psi^{\text{TM}} = R(r)H(\theta)\Phi(\phi) \tag{2-53}$$

into (2-52) and dividing the resulting equation by $RH\Phi$, we obtain [[21], Section 6-1]

$$\frac{1}{(AR)r^2 R}\frac{d}{dr}\left(r^2\frac{dR}{dr}\right) + \frac{1}{r^2 \sin\theta\,H}\frac{d}{d\theta}\left(\sin\theta\,\frac{dH}{d\theta}\right) + \frac{1}{r^2 \sin^2\theta\,\Phi}\frac{d^2\Phi}{d\phi^2}$$

$$+ k_0^2\varepsilon_r = 0. \tag{2-54}$$

Multiplying (2-54) by $r^2 \sin^2\theta$, we obtain

$$\frac{\sin^2\theta}{(AR)R}\frac{d}{dr}\left(r^2\frac{dR}{dr}\right) + \frac{\sin\theta}{H}\frac{d}{d\theta}\left(\sin\theta\,\frac{dH}{d\theta}\right) + \frac{1}{\Phi}\frac{d^2\Phi}{d\phi^2} + k_0^2\varepsilon_r r^2 \sin^2\theta = 0. \tag{2-55}$$

In (2-55), $\frac{1}{\Phi}\frac{d^2\Phi}{d\phi^2}$ has to be a constant. Let

$$\frac{1}{\Phi}\frac{d^2\Phi}{d\phi^2} = -m^2. \tag{2-56}$$

Multiplying (2-56) by Φ, we obtain

$$\frac{d^2\Phi}{d\phi^2} + m^2\Phi = 0. \tag{2-57}$$

Substituting (2-56) into (2-55) and then dividing the resulting equation by $\sin^2\theta$, gives

$$\frac{1}{(AR)R}\frac{d}{dr}\left(r^2\frac{dR}{dr}\right) + \frac{1}{H\sin\theta}\frac{d}{d\theta}\left(\sin\theta\frac{dH}{d\theta}\right) - \frac{m^2}{\sin^2\theta} + k_0^2\varepsilon_r r^2 = 0. \tag{2-58}$$

Seeking to derive the associated Legendre equation, [[21], Appendix E] we let

$$\frac{1}{H\sin\theta}\frac{d}{d\theta}\left(\sin\theta\frac{dH}{d\theta}\right) - \frac{m^2}{\sin^2\theta} = -n(n+1). \tag{2-59}$$

Multiplying (2-59) by H, we obtain the associated Legendre equation which is [[21], Appendix E]

$$\frac{1}{\sin\theta}\frac{d}{d\theta}\left(\sin\theta\frac{dH}{d\theta}\right) + \left(n(n+1) - \frac{m^2}{\sin^2\theta}\right)H = 0. \tag{2-60}$$

Substituting (2-59) into (2-58) yields

$$\frac{1}{(AR)R}\frac{d}{dr}\left(r^2\frac{dR}{dr}\right) - n(n+1) + k_0^2\varepsilon_r r^2 = 0. \tag{2-61}$$

The product of (2-61) with $(AR)R$ is

$$\frac{d}{dr}\left(r^2\frac{dR(r)}{dr}\right) + ((AR)k_0^2\varepsilon_r r^2 - n(n+1)(AR))R(r) = 0. \tag{2-62}$$

20

Substituting (2-51) for the first *(AR)* in (2-62) gives

$$\frac{d}{dr}\left(r^2\frac{dR(r)}{dr}\right) + (k_0^2\varepsilon_\theta r^2 - n(n+1)(AR))R(r) = 0. \qquad (2\text{-}63)$$

Substitution of

$$r = \frac{x}{k_0\sqrt{\varepsilon_\theta}} \qquad (2\text{-}64)$$

into (2-63) obtains

$$\frac{d}{dx}\left(x^2\frac{dR(r)}{dx}\right) + (x^2 - n(n+1)(AR))R(r) = 0 \qquad (2\text{-}65)$$

where r is given by (2-64). If $AR= 1$, then (2-65) would be the differential equation for the spherical Bessel functions of argument x and of order n [[24], Formula 10.1.1].Therefore, if $AR= 1$, a solution of (2-65) would be

$$R(r) = j_n(k_0\sqrt{\varepsilon_\theta}\, r) \qquad (2\text{-}66)$$

where j_n is the spherical Bessel of the first kind. If $AR \neq 1$, then there is a new variable v that satisfies

$$n(n+1)(AR) = v(v+1). \qquad (2\text{-}67)$$

Equation (2-67) is rewritten as

$$\left(v + \frac{1}{2}\right)^2 = \frac{1}{4} + n(n+1)(AR). \qquad (2\text{-}68)$$

Taking the square root of both sides of (2-68), we have

21

$$v = -\frac{1}{2} \pm \sqrt{n(n+1)(AR) + \frac{1}{4}}. \qquad (2\text{-}69)$$

Choosing the positive square root in (2-69) so that, v is positive when n is positive, we obtain

$$v = -\frac{1}{2} + \sqrt{n(n+1)(AR) + \frac{1}{4}}. \qquad (2\text{-}70)$$

Substitution of (2-67) into (2-64) gives

$$\frac{d}{dx}\left(x^2 \frac{dR}{dx}\right) + (x^2 - v(v+1))R = 0. \qquad (2\text{-}71)$$

Since (2-71) is (2-65) with *(AR)* replaced by 1 and n replaced by v, it follows that a solution of (2-71) is obtained by replacing n in the solution (2-66) of (2-65) by v. Therefore, a solution of (2-71) is

$$R = j_v(k_0\sqrt{\varepsilon_\theta}\, r) \qquad (2\text{-}72)$$

2.4 The wave functions $\boldsymbol{\psi}^{\mathrm{TM}}$ and $\boldsymbol{\psi}^{\mathrm{TE}}$

Using the results obtained in sections 2.2 and 2.3, the general solutions for both scalar potentials ψ^{TM} and ψ^{TE} are proposed in this section.

2.4.1 The wave function $\boldsymbol{\psi}^{TM}$
In Section 2.2.1, ψ^{TM} was shown to satisfy (2-25)

(2-25), which repeated here, is

$$\left(\frac{\varepsilon_r}{\varepsilon_\theta}\right)\frac{1}{r^2}\frac{\partial}{\partial r}\left(r^2\frac{\partial \psi^{TM}}{\partial r}\right) + \frac{1}{r^2 \sin \theta}\frac{\partial}{\partial \theta}\left(\sin \theta \frac{\partial \psi^{TM}}{\partial \theta}\right) + \frac{1}{r^2 \sin^2 \theta}\frac{\partial^2 \psi^{TM}}{\partial \phi^2}$$

$$+ k_0^2 \varepsilon_r \psi^{TM} = 0. \tag{2-73}$$

From the development (2-52)–(2-72), it is evident that general solutions of (2-73) for ψ^{TM} are $\psi_{\{e,o\}mn}^{TM(i)}$ given by

$$\psi_{\{e,o\}mn}^{TM(i)} = b_\nu^{(i)}(k_0\sqrt{\varepsilon_\theta}\,r)P_n^m(\cos \theta)\{\cos (m\phi), \sin (m\phi)\} \tag{2-74}$$

where ν is given by (2-70), $b_\nu^{(1)} = j_\nu$, $b_\nu^{(2)} = y_\nu$, $b_\nu^{(3)} = h_\nu^{(1)}$, and $b_\nu^{(4)} = h_\nu^{(2)}$. Here, j_ν and y_ν are, respectively, the spherical Bessel functions of the first and second kinds, $h_\nu^{(1)} = j_\nu + jy_\nu$ and $h_\nu^{(2)} = j_\nu - jy_\nu$. For $(i = 1,2,3,4)$, the spherical Bessel function $b_\nu^{(i)}(x)$ is given by [[22], (D-20)]

$$b_\nu^{(i)}(x) = \sqrt{\frac{\pi}{2x}}\, B_{\nu+1/2}^{(i)}(x) \tag{2-75}$$

where $B_n^{(1)} = J_n$, $B^{(2)} = Y_n$, $B^{(3)} = H_n^{(1)}$, and $B_n^{(4)} = H_n^{(2)}$ and J_n is the cylindrical Bessel function of the first kind of order n, Y_n is the cylindrical Bessel function of the second kind, $H_n^{(1)} = J_n + jY_n$, and $H_n^{(2)} = J_n - jY_n$. Also, $\{\{P_n^m, n = 0,1,2, ...\}, m \leq n\}$ are the associated Legendre polynomials. In (2-74), the subscript $\{e, o\}$ stands for either the subscript e or the subscript o. The ϕ-dependence of $\psi_{emn}^{TM(i)}$ is $\cos (m\phi)$ and the ϕ-dependence of $\psi_{omn}^{TM(i)}$ is $\sin (m\phi)$. The most general TM wave function is ψ^{TM} given by

$$\psi^{TM} = \mu_0 \sum_{i=1}^{4}\sum_{m,n}\left(a_{emn}^{TM(i)}\psi_{emn}^{TM(i)} + a_{omn}^{TM(i)}\psi_{omn}^{TM(i)}\right) \tag{2-76}$$

23

where $a_{emn}^{TM(i)}$ and $a_{omn}^{TM(i)}$ are arbitrary complex constants and $\psi_{emn}^{TM(i)}$ and $\psi_{omn}^{TM(i)}$ are given by (2-74). The factor μ_0 was put in (2-76) because $\boldsymbol{A}$ of (2-14) should be proportional to μ_0.

2.4.2 The wave function $\boldsymbol{\psi}^{\mathbf{TE}}$

The wave function ψ^{TE} satisfies (2-50) which is similar to (2-52) Repeating the development of (2-52)–(2-72), starting from (2-50) instead of (2-52), we observe that the equations for $H(\theta)$ and $\Phi(\phi)$ are the same as those obtained starting from (2-52) but that the equation for $R(r)$ is the equation for the spherical Bessel functions of argument $k_0\sqrt{\varepsilon_\theta}\,r)$ and order n. Therefore, we obtain

$$\psi_{\{e,o\}mn}^{TE(i)} = b_n^{(i)}(k_0\sqrt{\varepsilon_\theta}\,r)P_n^m(\cos\,\theta)\{\cos\,(m\phi),\sin\,(m\phi)\} \qquad (2\text{-}77)$$

where $b_n^{(1)} = j_n$, $b_n^{(2)} = y_n$, $b_n^{(3)} = h_n^{(1)}$, and $b_n^{(4)} = h_n^{(2)}$. Here, j_n and y_n are, respectively, the spherical Bessel functions of the first and second kinds, $h_n^{(1)} = j_n + jy_n$ and $h_n^{(2)} = j_n - jy_n$. Also, $\{\{P_n^m, n = 0,1,2,\dots\}, m \leq n\}$ are the associated Legendre polynomials. In (2-77), the subscript $\{e,o\}$ stands for either the subscript e or the subscript o. The ϕ-dependence of $\psi_{emn}^{TE(i)}$ is $\cos\,(m\phi)$ and the ϕ-dependence of $\psi_{omn}^{TE(i)}$ is $\sin\,(m\phi)$. The most general TE wave function is ψ^{TE} given by

$$\psi^{TE} = \varepsilon_0\varepsilon_\theta \sum_{i=1}^{4}\sum_{m,n}\left(a_{emn}^{TE(i)}\psi_{emn}^{TE(i)} + a_{omn}^{TE(i)}\psi_{omn}^{TE(i)}\right) \qquad (2\text{-}78)$$

24

where $a_{emn}^{\text{TE}(i)}$ and $a_{omn}^{\text{TE}(i)}$ are arbitrary complex constants and $\psi_{emn}^{\text{TE}(i)}$ and $\psi_{omn}^{\text{TE}(i)}$ are given by (2-77). The factor $\varepsilon_0 \varepsilon_\theta$ was put in (2-78) because $\boldsymbol{F}$ of (2-35) should be proportional to $\varepsilon_0 \varepsilon_\theta$.

2.5 The calculation of the E and H field components of the TE and TM waves using the vector potentials A and F

Using the derived scalar potentials ψ^{TM} and ψ^{TE} in the sections 2.4.1 and 2.4.2, the electric and magnetic field components corresponding to TE and TM waves are derived in this section.

2.5.1 The TM field components

Substitution of (2-14) into (2-8) and (2-10) gives

$$\boldsymbol{B}^{\text{TM}} = \nabla \times (\hat{\boldsymbol{r}} A_r) \tag{2-79}$$

$$\boldsymbol{D}^{\text{TM}} = \frac{1}{j\omega\mu_0} \nabla \times \nabla \times (\hat{\boldsymbol{r}} A_r) \tag{2-80}$$

$$A_r = r\psi^{\text{TM}}. \tag{2-81}$$

Expressions are needed for the vectors on the right-hand sides of (2-79) and (2-80). If $\boldsymbol{A}$ was a general vector function given by

$$\boldsymbol{A} = \hat{\boldsymbol{r}} A_r + \hat{\boldsymbol{\theta}} A_\theta + \hat{\boldsymbol{\phi}} A_\phi, \tag{2-82}$$

then [[21], (A-12)]

$$\nabla \times \mathbf{A} = \hat{\mathbf{r}} \frac{1}{r \sin \theta} \left[\frac{\partial}{\partial \theta} (A_\phi \sin \theta) - \frac{\partial A_\theta}{\partial \phi} \right] + \hat{\theta} \frac{1}{r} \left[\frac{1}{\sin \theta} \frac{\partial A_r}{\partial \phi} - \frac{\partial}{\partial r} (r A_\phi) \right]$$

$$+ \hat{\phi} \frac{1}{r} \left[\frac{\partial}{\partial r} (r A_\theta) - \frac{\partial A_r}{\partial \theta} \right]. \tag{2-83}$$

With $\mathbf{A} = \hat{\mathbf{r}} A_r$, (2-83) reduces to

$$\nabla \times (\hat{\mathbf{r}} A_r) = \hat{\theta} \left(\frac{1}{r \sin \theta} \frac{\partial A_r}{\partial \phi} \right) - \hat{\phi} \left(\frac{1}{r} \frac{\partial A_r}{\partial \theta} \right). \tag{2-84}$$

Evaluating $\nabla \times \nabla \times (\hat{\mathbf{r}} A_r)$ by first substituting (2-84) for $\nabla \times (\hat{\mathbf{r}} A_r)$ and then using

(2-83) to do the outside curl operation in $\nabla \times \nabla \times (\hat{\mathbf{r}} A_r)$, we obtain

$$\nabla \times \nabla \times (\hat{\mathbf{r}} A_r) = \hat{\mathbf{r}} \frac{1}{r \sin \theta} \left[\frac{\partial}{\partial \theta} \left(-\frac{\sin \theta}{r} \frac{\partial A_r}{\partial \theta} \right) - \frac{\partial}{\partial \phi} \left(\frac{1}{r \sin \theta} \frac{\partial A_r}{\partial \phi} \right) \right] +$$

$$\hat{\theta} \frac{1}{r} \left[-\frac{\partial}{\partial r} \left(-\frac{\partial A_r}{\partial \theta} \right) \right] + \hat{\phi} \frac{1}{r} \left[\frac{\partial}{\partial r} \left(\frac{1}{\sin \theta} \frac{\partial A_r}{\partial \phi} \right) \right] \tag{2-85}$$

which reduces to

$$\nabla \times \nabla \times (\hat{\mathbf{r}} A_r) = \hat{\mathbf{r}} \frac{1}{r^2 \sin \theta} \left[-\frac{\partial}{\partial \theta} \left(\sin \theta \frac{\partial A_r}{\partial \theta} \right) - \frac{1}{\sin \theta} \frac{\partial^2 A_r}{\partial \phi^2} \right]$$

$$+ \hat{\theta} \frac{1}{r} \frac{\partial^2 A_r}{\partial r \partial \theta} + \hat{\phi} \frac{1}{r \sin \theta} \frac{\partial^2 A_r}{\partial r \partial \phi}. \tag{2-86}$$

Equation (2-86) is equivalent to

$$\nabla \times \nabla \times (\hat{r} A_r)$$

$$= \hat{r} \left[-\frac{1}{r^2} \frac{\partial^2 A_r}{\partial \theta^2} - \frac{1}{r^2 \tan \theta} \frac{\partial A_r}{\partial \theta} - \frac{1}{r^2 \sin^2 \theta} \frac{\partial^2 A_r}{\partial \phi^2} \right] \qquad (2\text{-}87)$$

$$+ \hat{\theta} \left(\frac{1}{r} \frac{\partial^2 A_r}{\partial r \partial \theta} \right) + \hat{\phi} \left(\frac{1}{r \sin \theta} \frac{\partial^2 A_r}{\partial \phi \partial r} \right).$$

In retrospect, the present derivation of (2-87) is hardly necessary because (2-87) is easier to obtain by replacing $r\psi^{\mathrm{TM}}$ in (2-15) by A_r. The term in the square brackets in (2-87) needs to be simplified. Using (2-81) to replace $r\psi^{\mathrm{TM}}$ in (2-21) by A_r, we obtain

$$-\frac{1}{r^2} \frac{\partial^2 A_r}{\partial \theta^2} - \frac{1}{r^2 \tan \theta} \frac{\partial A_r}{\partial \theta} - \frac{1}{r^2 \sin^2 \theta} \frac{\partial^2 A_r}{\partial \phi^2} = \left(\frac{\varepsilon_r}{\varepsilon_\theta} \right) \frac{\partial^2 A_r}{\partial r^2} + k_0^2 \varepsilon_r A_r. \qquad (2\text{-}88)$$

Substitution of (2-88) into (2-87) gives

$$\nabla \times \nabla \times (\hat{r} A_r = \hat{r} \left(\left(\frac{\varepsilon_r}{\varepsilon_\theta} \right) \frac{\partial^2 A_r}{\partial r^2} + k_0^2 \varepsilon_r A_r \right) + \hat{\theta} \left(\frac{1}{r} \frac{\partial^2 A_r}{\partial r \partial \theta} \right)$$

$$+ \hat{\phi} \left(\frac{1}{r \sin \theta} \frac{\partial^2 A_r}{\partial \phi \partial r} \right). \qquad (2\text{-}89)$$

Substitution of (2-84) into (2-79) and substitution of (2-89) into (2-80) give

$$\boldsymbol{B}^{\mathrm{TM}} = \hat{\theta} \left(\frac{1}{r \sin \theta} \frac{\partial A_r}{\partial \phi} \right) - \hat{\phi} \left(\frac{1}{r} \frac{\partial A_r}{\partial \theta} \right) \qquad (2\text{-}90)$$

$$\boldsymbol{D}^{\text{TM}} = \frac{1}{j\omega\mu_0} \{\hat{\boldsymbol{r}} \left(\left(\frac{\varepsilon_r}{\varepsilon_\theta}\right) \frac{\partial^2 A_r}{\partial r^2} + k_0^2 \varepsilon_r A_r \right) + \hat{\boldsymbol{\theta}} \left(\frac{1}{r} \frac{\partial^2 A_r}{\partial r \partial \theta} \right)$$

$$+ \hat{\boldsymbol{\phi}} \left(\frac{1}{r \sin \theta} \frac{\partial^2 A_r}{\partial \phi \partial r} \right) \} \tag{2-91}$$

where A_r is obtained by (2-81) and ψ^{TM} is given by (2-76) where $\psi_{\{e,o\}mn}^{\text{TM}(i)}$ is given by (2-74). Detailed expressions for $\boldsymbol{B}^{\text{TM}}$ and $\boldsymbol{D}^{\text{TM}}$ are obtained by expanding A_r in (2-90) and (2-91). Substitution of (2-76) into (2-81) gives

$$A_r = \mu_0 \sum_{i=1}^{4} \sum_{m,n} \left(a_{emn}^{\text{TM}(i)} A_{r,emn}^{(i)} + a_{omn}^{\text{TM}(i)} A_{r,omn}^{(i)} \right) \tag{2-92}$$

where

$$A_{r,\{e,o\}mn}^{(i)} = r\psi_{\{e,o\}mn}^{\text{TM}(i)} \tag{2-93}$$

and the subscript $\{e,o\}$ stands for either e or o. Substitution of (2-74) into (2-93) gives

$$A_{r,\{e,o\}mn}^{(i)} = \frac{1}{k_0\sqrt{\varepsilon_\theta}} \hat{B}_\nu^{(i)}(k_0\sqrt{\varepsilon_\theta}\, r) P_n^m(\cos\,\theta)\{\cos\,(m\phi), \sin\,(m\phi)\} \tag{2-94}$$

where $\hat{B}_\nu^{(i)}(x)$ is the alternative spherical Bessel function given by [[21], (6-23)]

$$\hat{B}_\nu^{(i)}(x) = xb_\nu^{(i)}(x) \tag{2-95}$$

where $b_\nu^{(i)}$ is the spherical Bessel function given by (2-75). Substitution of (2-75) into (2-95) gives

$$\hat{B}_v^{(i)}(x) = \sqrt{\frac{\pi x}{2}} \, B_{v+1/2}^{(i)}(x) \tag{2-96}$$

where $B_{v+1/2}^{(i)}(x)$ is the cylindrical Bessel function described in the sentence that contains

(2-75). Substitution of (2-92) into (2-90) and (2-91) gives

$$\boldsymbol{B}^{\text{TM}} = \mu_0 \sum_{i=1}^{4} \sum_{m,n} \{ a_{emn}^{\text{TM}(i)} \left(\hat{\theta} \frac{1}{r \sin \theta} \frac{\partial A_{r,emn}^{(i)}}{\partial \phi} - \hat{\phi} \frac{1}{r} \frac{\partial A_{r,emn}^{(i)}}{\partial \theta} \right)$$

$$+ a_{omn}^{\text{TM}(i)} \left(\hat{\theta} \frac{1}{r \sin \theta} \frac{\partial A_{r,omn}^{(i)}}{\partial \phi} - \hat{\phi} \frac{1}{r} \frac{\partial A_{r,omn}^{(i)}}{\partial \theta} \right) \} \tag{2-97}$$

$$\boldsymbol{D}^{\text{TM}} = \frac{1}{j\omega} \sum_{i=1}^{4} \sum_{m,n} \{ a_{emn}^{\text{TM}(i)} (\hat{r} \left(\left(\frac{\varepsilon_r}{\varepsilon_\theta} \right) \frac{\partial^2 A_{r,emn}^{(i)}}{\partial r^2} + k_0^2 \varepsilon_r A_{r,emn}^{(i)} \right)$$

$$+ \hat{\theta} \left(\frac{1}{r} \frac{\partial^2 A_{r,emn}^{(i)}}{\partial r \partial \theta} \right) + \hat{\phi} \left(\frac{1}{r \sin \theta} \frac{\partial^2 A_{r,emn}^{(i)}}{\partial \phi \partial r} \right))$$

$$+ a_{omn}^{\text{TM}(i)} (\hat{r} \left(\left(\frac{\varepsilon_r}{\varepsilon_\theta} \right) \frac{\partial^2 A_{r,omn}^{(i)}}{\partial r^2} + k_0^2 \varepsilon_r A_{r,omn}^{(i)} \right)$$

$$+ \hat{\theta} \left(\frac{1}{r} \frac{\partial^2 A_{r,omn}^{(i)}}{\partial r \partial \theta} \right) + \hat{\phi} \left(\frac{1}{r \sin \theta} \frac{\partial^2 A_{r,omn}^{(i)}}{\partial \phi \partial r} \right)) \}. \tag{2-98}$$

Seeking to simplify the coefficients of $\hat{r}$ in (2-98), we go back to (2-53) where $\psi_{\{e,o\}mn}^{\text{TM}(i)}$

could be $R(r)H(\theta)\Phi(\phi)$. Multiplying (2-61) by $\psi_{\{e,o\}mn}^{\text{TM}(i)}$ and using (2-51), we obtain

$$\left(\frac{\varepsilon_r}{\varepsilon_\theta} \right) \frac{\partial}{\partial r} \left(r^2 \frac{\partial \psi_{\{e,o\}mn}^{TM(i)}}{\partial r} \right) + k_0^2 \varepsilon_r r^2 \psi_{\{e,o\}mn}^{\text{TM}(i)} = n(n+1)\psi_{\{e,o\}mn}^{\text{TM}(i)} \tag{2-99}$$

Replacing ψ^{TM} in (2-24) by $\psi_{\{e,o\}mn}^{\text{TM}(i)}$, we obtain

29

$$\frac{\partial}{\partial r}\left(r^2 \frac{\psi_{\{e,o\}mn}^{TM(i)}}{\partial r}\right) = r\frac{\partial^2}{\partial r^2}\left(r\psi_{\{e,o\}mn}^{TM(i)}\right). \tag{2-100}$$

Substituting (2-100) into (2-99) and then dividing the resulting equation by r, we obtain

$$\left(\frac{\varepsilon_r}{\varepsilon_\theta}\right)\frac{\partial^2 A_{r,\{e,o\}mn}^{(i)}}{\partial r^2} + k_0^2 \varepsilon_r A_{r,\{e,o\}mn}^{(i)} = \frac{n(n+1)}{r^2} A_{r,\{e,o\}mn}^{(i)} \tag{2-101}$$

where $A_{r,\{e,o\}mn}^{(i)}$ is given by (2-93). Substitution of (2-101) into (2-98) gives

$$\boldsymbol{D}^{\text{TM}} = \frac{1}{j\omega} \sum_{i=1}^{4} \sum_{m,n} \{ a_{emn}^{\text{TM}(i)} (\hat{\boldsymbol{r}}\left(\frac{n(n+1)}{r^2} A_{r,emn}^{(i)}\right) + \hat{\theta}\left(\frac{1}{r}\frac{\partial^2 A_{r,emn}^{(i)}}{\partial r\partial\theta}\right)$$

$$+\hat{\phi}\left(\frac{1}{r \sin\theta}\frac{\partial^2 A_{r,emn}^{(i)}}{\partial\phi\partial r}\right)) + a_{omn}^{\text{TM}(i)} (\hat{\boldsymbol{r}}\left(\frac{n(n+1)}{r^2} A_{r,omn}^{(i)}\right)$$

$$+ \hat{\theta}\left(\frac{1}{r}\frac{\partial^2 A_{r,omn}^{(i)}}{\partial r\partial\theta}\right) + \hat{\phi}\left(\frac{1}{r \sin\theta}\frac{\partial^2 A_{r,omn}^{(i)}}{\partial\phi\partial r}\right))\}. \tag{2-102}$$

Using (2-2) and (2-1), respectively, $\mathbf{H}^{\text{TM}}$ and $\mathbf{E}^{\text{TM}}$ can be written as

$$\boldsymbol{H}^{\text{TM}} = \frac{1}{\mu_0} \boldsymbol{B}^{\text{TM}} \tag{2-103}$$

$$\boldsymbol{E}^{\text{TM}} = \frac{1}{\varepsilon_0} (\bar{\bar{\varepsilon}}^{-1} \cdot \boldsymbol{D}^{\text{TM}}). \tag{2-104}$$

Equation (2-102) is recast as

$$\boldsymbol{D}^{\text{TM}} = \hat{\boldsymbol{r}}\left(D_{r,e}^{\text{TM}} + D_{r,o}^{\text{TM}}\right) + \hat{\theta}\left(D_{\theta,e}^{\text{TM}} + D_{\theta,o}^{\text{TM}}\right) + \hat{\phi}\left(D_{\phi,e}^{\text{TM}} + D_{\phi,o}^{\text{TM}}\right) \tag{2-105}$$

where

$$D_{r,\{e,o\}}^{\text{TM}} = \frac{1}{j\omega}\sum_{i=1}^{4}\sum_{m,n}\left(a_{\{e,o\}mn}^{\text{TM}(i)}\frac{n(n+1)}{r^2}A_{r,\{e,o\}mn}^{(i)}\right) \tag{2-106}$$

$$D_{\theta,\{e,o\}}^{\text{TM}} = \frac{1}{j\omega}\sum_{i=1}^{4}\sum_{m,n}\left(a_{\{e,o\}mn}^{\text{TM}(i)}\frac{1}{r}\frac{\partial^2 A_{r,\{e,o\}mn}^{(i)}}{\partial r\partial\theta}\right) \tag{2-107}$$

$$D_{\phi,\{e,o\}}^{\text{TM}} = \frac{1}{j\omega}\sum_{i=1}^{4}\sum_{m,n}\left(a_{\{e,o\}mn}^{\text{TM}(i)}\frac{1}{r\sin\theta}\frac{\partial^2 A_{r,\{e,o\}mn}^{(i)}}{\partial\phi\partial r}\right). \tag{2-108}$$

Use of (2-51) in (2-67) gives

$$n(n+1) = \frac{\nu(\nu+1)\varepsilon_r}{\varepsilon_\theta}. \tag{2-109}$$

Substituting (2-109) into (2-106), we obtain the following alternative expression for $D_{r,\{e,o\}}^{\text{TM}}$.

$$D_{r,\{e,o\}}^{\text{TM}} = \frac{1}{j\omega}\sum_{i=1}^{4}\sum_{m,n}\left(a_{\{e,o\}mn}^{\text{TM}(i)}\frac{\nu(\nu+1)\varepsilon_r}{r^2\varepsilon_\theta}A_{r,\{e,o\}mn}^{(i)}\right). \tag{2-110}$$

Substitution of (2-97) into (2-103) gives

$$\boldsymbol{H}^{\text{TM}} = \sum_{i=1}^{4}\sum_{m,n}\{a_{emn}^{\text{TM}(i)}\left(\hat{\theta}\frac{1}{r\sin\theta}\frac{\partial A_{r,emn}^{(i)}}{\partial\phi}-\hat{\phi}\frac{1}{r}\frac{\partial A_{r,emn}^{(i)}}{\partial\theta}\right)$$
$$+ a_{omn}^{\text{TM}(i)}\left(\hat{\theta}\frac{1}{r\sin\theta}\frac{\partial A_{r,omn}^{(i)}}{\partial\phi}-\hat{\phi}\frac{1}{r}\frac{\partial A_{r,omn}^{(i)}}{\partial\theta}\right)\}. \tag{2-111}$$

Substituting (2-93) into (2-111) gives

$$\boldsymbol{H}^{\mathrm{TM}} = \sum_{i=1}^{4} \sum_{\mathrm{e,o},m,n} \left(a_{\{e,o\}mn}^{\mathrm{TM}(i)} \left(\hat{\theta} \frac{1}{\sin \theta} \frac{\partial \psi_{\{e,o\}mn}^{TM(i)}}{\partial \phi} - \hat{\phi} \frac{\partial \psi_{\{e,o\}mn}^{TM(i)}}{\partial \theta} \right) \right) \qquad (2\text{-}112)$$

where inclusion of $\sum_{\mathrm{e,o}}$ has allowed the separate even and odd expressions in (2-111) to be written as one expression. Substitution of (2-74) into (2-112) gives

$$\boldsymbol{H}^{\mathrm{TM}} = \sum_{i=1}^{4} \sum_{\mathrm{e,o},m,n} \left(a_{\{e,o\}mn}^{\mathrm{TM}(i)} \boldsymbol{M}_{\{e,o\}mn}^{(i)}(k, v) \right) \qquad (2\text{-}113)$$

where

$$\boldsymbol{M}_{\{e,o\}mn}^{(i)}(k, v) = b_v^{(i)}(kr)(\hat{\theta} \frac{m}{\sin \theta} P_n^m(\cos \theta)$$

$$. \{-\sin (m\phi), \cos (m\phi)\} - \hat{\phi} \frac{dP_n^m(\cos \theta)}{d\theta} \{\cos (m\phi), \sin (m\phi)\}) \qquad (2\text{-}114)$$

where

$$k = k_0 \sqrt{\varepsilon_\theta} \qquad (2\text{-}115)$$

and, using (2-51) in (2-70),

$$v = -\frac{1}{2} + \sqrt{\frac{n(n+1)\varepsilon_\theta}{\varepsilon_r} + \frac{1}{4}}. \qquad (2\text{-}116)$$

Using the identity

$$-a + \sqrt{b + a^2} = \frac{\left(-a + \sqrt{b + a^2}\right)\left(a + \sqrt{b + a^2}\right)}{a + \sqrt{b + a^2}} = \frac{b}{a + \sqrt{b + a^2}}, \qquad (2\text{-}117)$$

(2-116) is expressed as

32

$$v = \frac{n(n+1)\varepsilon_\theta}{\varepsilon_r \left(\frac{1}{2} + \sqrt{\frac{n(n+1)\varepsilon_\theta}{\varepsilon_r} + \frac{1}{4}}\right)}.$$ (2-118)

The right-hand side of (2-118) is less susceptible to roundoff error than the right-hand side of (2-116). Substituting (2-3) and (2-105) into (2-104) and then doing the indicated scalar multiplication, we obtain

$$\boldsymbol{E}^{\mathrm{TM}} = \frac{1}{\varepsilon_0}\left(\hat{\boldsymbol{r}}\,\frac{D_{r,e}^{TM} + D_{r,o}^{TM}}{\varepsilon_r} + \hat{\theta}\,\frac{D_{\theta,e}^{TM} + D_{\theta,o}^{TM}}{\varepsilon_\theta} + \hat{\phi}\,\frac{D_{\phi,e}^{TM} + D_{\phi,o}^{TM}}{\varepsilon_\theta}\right).$$ (2-119)

Substitution of (2-110), (2-107), and (2-108) into (2-119) gives

$$\boldsymbol{E}^{\mathrm{TM}} = \frac{1}{j\omega\varepsilon_0\varepsilon_\theta}\sum_{i=1}^{4}\sum_{e,o,m,n}\{a_{\{e,o\}mn}^{\mathrm{TM}(i)}(\hat{\boldsymbol{r}}\,\frac{v(v+1)}{r^2}A_{r,\{e,o\}mn}^{(i)}$$

$$+ \hat{\theta}\frac{1}{r}\frac{\partial^2 A_{r,\{e,o\}mn}^{(i)}}{\partial r\partial\theta} + \hat{\phi}\frac{1}{r\sin\theta}\frac{\partial^2 A_{r,\{e,o\}mn}^{(i)}}{\partial\phi\partial r})\}$$ (2-120)

where inclusion of $\sum_{e,o}$ has allowed each pair even and odd expressions in (2-119) to be written as one expression. Substitution of (2-93) into (2-120) gives

$$\boldsymbol{E}^{\mathrm{TM}} = \frac{1}{j\omega\varepsilon_0\varepsilon_\theta}\sum_{i=1}^{4}\sum_{e,o,m,n}\{a_{\{e,o\}mn}^{\mathrm{TM}(i)}(\hat{\boldsymbol{r}}\,\frac{v(v+1)}{r}\psi_{\{e,o\}mn}^{\mathrm{TM}(i)}$$

$$+ \hat{\theta}\frac{1}{r}\frac{\partial^2}{\partial r\partial\theta}\left(r\psi_{\{e,o\}mn}^{\mathrm{TM}(i)}\right) + \hat{\phi}\frac{1}{r\sin\theta}\frac{\partial^2}{\partial\phi\partial r}\left(r\psi_{\{e,o\}mn}^{\mathrm{TM}(i)}\right))\}.$$ (2-121)

Substitution of (2-74) into (2-121) gives, after use of (2-115),

$$E^{\text{TM}} = -j\sqrt{\frac{\mu_0}{\varepsilon_0 \varepsilon_\theta}} \sum_{i=1}^{4} \sum_{e,o,m,n} \left(a_{\{e,o\}mn}^{\text{TM}(i)} N_{\{e,o\}mn}^{(i)}(k,\nu)\right) \tag{2-122}$$

where

$$N_{\{e,o\}mn}^{(i)}(k,\nu) = \hat{r}\,\frac{\nu(\nu+1)}{kr}\,b_\nu^{(i)}(kr)P_n^m(\cos\,\theta)\{\cos\,(m\phi),\sin\,(m\phi)\}$$

$$+\frac{1}{kr}\frac{d}{dr}\left(rb_\nu^{(i)}(kr)\right)(\hat{\theta}\,\frac{dP_n^m(\cos\,\theta)}{d\theta}\{\cos\,(m\phi),\sin\,(m\phi)\} \tag{2-123}$$

$$+\hat{\phi}\,\frac{m}{\sin\,\theta}\,P_n^m(\cos\,\theta)\{-\sin\,(m\phi),\cos\,(m\phi)\}).$$

2.5.2 The TE field of the vector potential F

Substitution of (2-35)into (2-30) and (2-31) gives

$$\boldsymbol{D}^{\text{TE}} = -\nabla \times (\hat{r}F_r) \tag{2-124}$$

$$\boldsymbol{B}^{\text{TE}} = \frac{1}{j\omega}\nabla \times \left(\bar{\bar{\varepsilon}}^{-1} \cdot (\nabla \times (\hat{r}F_r))\right) \tag{2-125}$$

where

$$F_r = r\psi^{\text{TE}}. \tag{2-126}$$

Expressions are needed for the vectors on the right-hand sides of (2-124) and (2-125). Replacing A_r by F_r in (2-84), we obtain

$$\nabla \times (\hat{r}F_r) = \hat{\theta}\left(\frac{1}{r\,sin\,\theta}\frac{\partial F_r}{\partial \phi}\right) - \hat{\phi}\left(\frac{1}{r}\frac{\partial F_r}{\partial \theta}\right). \tag{2-127}$$

With $\bar{\bar{\varepsilon}}$ given by (2-3) and with $\nabla \times (\hat{r}F_r)$ given by (2-127),

34

$$\bar{\bar{\varepsilon}}^{-1} \cdot (\nabla \times (\hat{r}F_r)) = \hat{\theta} \left(\frac{1}{\varepsilon_0 \varepsilon_\theta r \sin \theta} \frac{\partial F_r}{\partial \phi} \right) - \hat{\phi} \left(\frac{1}{\varepsilon_0 \varepsilon_\theta r} \frac{\partial F_r}{\partial \theta} \right). \tag{2-128}$$

Since the right-hand side of (2-128) is the product of $1/\varepsilon_0 \varepsilon_\theta$ with the right-hand side of (2-84) with A_r replaced by F_r, it follows that $\nabla \times \left(\bar{\bar{\varepsilon}}^{-1} \cdot \left(\nabla \times (\hat{r}F_r) \right) \right)$ is given by the product of $1/(\varepsilon_0 \varepsilon_\theta)$ with the right-hand side of (2-87) with A_r replaced by F_r as follows

$$\nabla \times \left(\bar{\bar{\varepsilon}}^{-1} \cdot \left(\nabla \times (\hat{r}F_r) \right) \right)$$

$$= \hat{r} \left(\frac{1}{\varepsilon_0 \varepsilon_\theta} \right) \left[-\frac{1}{r^2} \frac{\partial^2 F_r}{\partial \theta^2} - \frac{1}{r^2 \tan \theta} \frac{\partial F_r}{\partial \theta} - \frac{1}{r^2 \sin^2 \theta} \frac{\partial^2 F_r}{\partial \phi^2} \right] \tag{2-129}$$

$$+ \hat{\theta} \left(\frac{1}{\varepsilon_0 \varepsilon_\theta r} \frac{\partial^2 F_r}{\partial r \partial \theta} \right) + \hat{\phi} \left(\frac{1}{\varepsilon_0 \varepsilon_\theta r \sin \theta} \frac{\partial^2 F_r}{\partial \phi \partial r} \right).$$

The term in the square brackets in (2-129) needs to be simplified. In (2-49),

$$\frac{\partial}{\partial \theta} \left(\sin \theta \frac{\partial \psi^{TE}}{\partial \theta} \right) = \cos \theta \frac{\partial \psi^{TE}}{\partial \theta} + \sin \theta \frac{\partial^2 \psi^{TE}}{\partial \theta^2}. \tag{2-130}$$

Substitution of (2-130) into (2-49) gives

$$\frac{1}{r} \frac{\partial^2}{\partial r^2} (r \psi^{TE}) + \frac{1}{r^2 \tan \theta} \frac{\partial \psi^{TE}}{\partial \theta} + \frac{1}{r^2} \frac{\partial^2 \psi^{TE}}{\partial \theta^2} + \frac{1}{r^2 \sin^2 \theta} \frac{\partial^2 \psi^{TE}}{\partial \phi^2}$$

$$+ k_0^2 \varepsilon_\theta \psi^{TE} = 0. \tag{2-131}$$

Multiplying (2-131) by r and then rearranging terms, we obtain

$$-\frac{1}{r^2} \frac{\partial^2 F_r}{\partial \theta^2} - \frac{1}{r^2 \tan \theta} \frac{\partial F_r}{\partial \theta} - \frac{1}{r^2 \sin^2 \theta} \frac{\partial^2 F_r}{\partial \phi^2} = \frac{\partial^2 F_r}{\partial r^2} + k_0^2 \varepsilon_\theta F_r \tag{2-132}$$

where F_r is given by (2-126). Substitution of (2-132) into (2-129) gives

35

$$\nabla \times \left(\bar{\bar{\varepsilon}}^{-1} \cdot \left(\nabla \times (\hat{r} F_r) \right) \right)$$

$$= \hat{r} \left(\frac{1}{\varepsilon_0 \varepsilon_\theta} \right) \left(\frac{\partial^2 F_r}{\partial r^2} + k_0^2 \varepsilon_\theta F_r \right) + \hat{\theta} \left(\frac{1}{\varepsilon_0 \varepsilon_\theta r} \frac{\partial^2 F_r}{\partial r \partial \theta} \right) \tag{2-133}$$

$$+ \hat{\phi} \left(\frac{1}{\varepsilon_0 \varepsilon_\theta r \sin \theta} \frac{\partial^2 F_r}{\partial \phi \partial r} \right).$$

Substitution of (2-127) into (2-124) and substitution of (2-133) into (2-125) give

$$\boldsymbol{D}^{\text{TE}} = -\hat{\theta} \left(\frac{1}{r \sin \theta} \frac{\partial F_r}{\partial \phi} \right) + \hat{\phi} \left(\frac{1}{r} \frac{\partial F_r}{\partial \theta} \right) \tag{2-134}$$

$$\boldsymbol{B}^{\text{TE}} = \frac{1}{j \omega \varepsilon_0 \varepsilon_\theta} \{ \hat{r} \left(\frac{\partial^2 F_r}{\partial r^2} + k_0^2 \varepsilon_\theta F_r \right) + \hat{\theta} \left(\frac{1}{r} \frac{\partial^2 F_r}{\partial r \partial \theta} \right) + \hat{\phi} \left(\frac{1}{r \sin \theta} \frac{\partial^2 F_r}{\partial \phi \partial r} \right) \} \tag{2-135}$$

where F_r is given by (2-126) and ψ^{TE} is obtained by (2-78) where $\psi^{\text{TE}(i)}_{\{e,o\}mn}$ is given by (2-77).

Detailed expressions for $\boldsymbol{D}^{\text{TE}}$ and $\boldsymbol{B}^{\text{TE}}$ are now obtained by expanding F_r in (2-134) and (2-135). Substitution of (2-78) into (2-126) gives

$$F_r = \varepsilon_0 \varepsilon_\theta \sum_{i=1}^{4} \sum_{m,n} \left(a^{\text{TE}(i)}_{emn} F^{(i)}_{r,emn} + a^{\text{TE}(i)}_{omn} F^{(i)}_{r,omn} \right) \tag{2-136}$$

where

$$F^{(i)}_{r,\{e,o\}mn} = r \psi^{\text{TE}(i)}_{\{e,o\}mn} \tag{2-137}$$

where the subscript {e,o} stands for either e or o. Either e is chosen on both sides of (2-137) or o is chosen on both sides of (2-137). Substitution of (2-77) into (2-137) gives

$$F_{r,\{e,o\}mn}^{(i)} = \frac{1}{k_0\sqrt{\varepsilon_\theta}}\hat{B}_n^{(i)}(k_0\sqrt{\varepsilon_\theta}r)P_n^m(\cos\theta)\{\cos(m\phi),\sin(m\phi)\} \qquad (2\text{-}138)$$

where $\hat{B}_n^{(i)}$ is the alternative Bessel function given by [(2-21), (6-23)]

$$\hat{B}_n^{(i)}(x) = x b_n^{(i)}(x) \qquad (2\text{-}139)$$

where $b_n^{(i)}$ is the spherical Bessel function given by [(2-21), (D-20)]

$$b_n^{(i)}(x) = \sqrt{\frac{\pi}{2x}}\,B_{n+1/2}^{(i)}(x) \qquad (2\text{-}140)$$

and $B_n^{(i)}(x)$ is the cylindrical Bessel function described in (2-75). Substitution of (2-140) into (2-139) gives

$$\hat{B}_n^{(i)}(x) = \sqrt{\frac{\pi x}{2}}\,B_{n+1/2}^{(i)}(x). \qquad (2\text{-}141)$$

Substitution of (2-136) into (2-134) and (2-135) yields

$$\boldsymbol{D}^{\text{TE}} = \varepsilon_0\varepsilon_\theta \sum_{i=1}^{4}\sum_{m,n}\left\{ a_{emn}^{\text{TE}(i)}\left(-\hat{\theta}\left(\frac{1}{r\sin\theta}\frac{\partial F_{r,emn}^{(i)}}{\partial\phi}\right) + \hat{\phi}\left(\frac{1}{r}\frac{\partial F_{r,emn}^{(i)}}{\partial\theta}\right)\right)\right.$$

$$\left. + a_{omn}^{\text{TE}(i)}\left(-\hat{\theta}\left(\frac{1}{r\sin\theta}\frac{\partial F_{r,omn}^{(i)}}{\partial\phi}\right) + \hat{\phi}\left(\frac{1}{r}\frac{\partial F_{r,omn}^{(i)}}{\partial\theta}\right)\right)\right\} \qquad (2\text{-}142)$$

$$\boldsymbol{B}^{\text{TE}} = \frac{1}{j\omega}\sum_{i=1}^{4}\sum_{m,n}\left\{ a_{emn}^{\text{TE}(i)}\left(\hat{r}\left(\frac{\partial^2 F_{r,emn}^{(i)}}{\partial r^2} + k_0^2\varepsilon_\theta F_{r,emn}^{(i)}\right) + \hat{\theta}\left(\frac{1}{r}\frac{\partial^2 F_{r,emn}^{(i)}}{\partial r\partial\theta}\right) + \right.\right.$$

$$\hat{\phi}\left(\frac{1}{r\sin\theta}\frac{\partial^2 F_{r,emn}^{(i)}}{\partial\phi\partial r}\right)\right) + a_{omn}^{\text{TE}(i)}\left(\hat{r}\left(\frac{\partial^2 F_{r,omn}^{(i)}}{\partial r^2} + k_0^2\varepsilon_\theta F_{r,omn}^{(i)}\right) + \hat{\theta}\left(\frac{1}{r}\frac{\partial^2 F_{r,omn}^{(i)}}{\partial r\partial\theta}\right) +$$

$$\hat{\phi}\left(\frac{1}{r\sin\theta}\frac{\partial^2 F_{r,omn}^{(i)}}{\partial\phi\partial r}\right))\}. \tag{2-143}$$

The coefficients of $\hat{r}$ in (2-143) need to be simplified. When the development (2-52)–(2-72) was repeated, starting from (2-50) for the TE case, we obtained, instead of (2-61),

$$\frac{1}{R}\frac{\partial}{\partial r}\left(r^2\frac{dR}{dr}\right) - n(n+1) + k_0^2\varepsilon_\theta r^2 = 0. \tag{2-144}$$

Multiplying (2-24) by $\psi_{\{e,o\}mn}^{TE(i)}$, we obtain

$$\frac{\partial}{\partial r}\left(r^2\frac{\partial\psi_{\{e,omn\}}^{TE(i)}}{\partial r}\right) + k_0^2\varepsilon_\theta r^2\psi_{\{e,o\}mn}^{TE(i)} = n(n+1)\psi_{\{e,o\}mn}^{TE(i)}. \tag{2-145}$$

Replacing ψ^{TM} in (2-144) by $\psi_{\{e,o\}mn}^{TE(i)}$, we obtain

$$\frac{\partial^2}{\partial r}\left(r^2\frac{\partial\psi_{\{e,o\}mn}^{TE(i)}}{\partial r}\right) = r\frac{\partial^2}{\partial r^2}\left(r\psi_{\{e,o\}mn}^{TE(i)}\right). \tag{2-146}$$

Substituting (2-146) into (2-145) and then dividing the resulting equation by r, we obtain

$$\frac{\partial^2 F_{r,\{e,o\}mn}^{(i)}}{\partial r^2} + k_0^2\varepsilon_\theta F_{r,\{e,o\}mn}^{(i)} = \frac{n(n+1)}{r^2}F_{r,\{e,o\}mn}^{(i)} \tag{2-147}$$

where $F_{r,\{e,o\}mn}^{(i)}$ is given by (2-137). Substitution of (2-147) into (2-143) gives

$$\boldsymbol{B}^{TE} = \frac{1}{j\omega}\sum_{i=1}^{4}\sum_{m,n}\{a_{emn}^{TE(i)}(\hat{r}\left(\frac{n(n+1)}{r^2}F_{r,emn}^{(i)}\right) \tag{2-148}$$

38

$$+\hat{\theta}\left(\frac{1}{r}\frac{\partial^2 F_{r,emn}^{(i)}}{\partial r \partial \theta}\right) + \hat{\phi}\left(\frac{1}{r\sin\theta}\frac{\partial^2 F_{r,emn}^{(i)}}{\partial\phi\partial r}\right)) + a_{omn}^{\mathrm{TE}(i)}(\hat{r}\left(\frac{n(n+1)}{r^2}F_{r,omn}^{(i)}\right)$$

$$+ \hat{\theta}\left(\frac{1}{r}\frac{\partial^2 F_{r,omn}^{(i)}}{\partial r \partial \theta}\right) + \hat{\phi}\left(\frac{1}{r\sin\theta}\frac{\partial^2 F_{r,omn}^{(i)}}{\partial\phi\partial r}\right))\}.$$

Using (2-2) and (2-1), respectively, $\mathbf{H}^{\mathrm{TE}}$ and $\mathbf{E}^{\mathrm{TE}}$ can now be calculated by

$$\boldsymbol{H}^{\mathrm{TE}} = \frac{1}{\mu_0}\boldsymbol{B}^{\mathrm{TE}} \tag{2-149}$$

$$\boldsymbol{E}^{\mathrm{TE}} = (\bar{\bar{\varepsilon}}^{-1}\cdot\boldsymbol{D}^{\mathrm{TE}}). \tag{2-150}$$

Equation (2-142) is recast as

$$\boldsymbol{D}^{\mathrm{TE}} = \hat{\theta}\big(D_{\theta,\mathrm{e}}^{\mathrm{TE}} + D_{\theta,\mathrm{o}}^{\mathrm{TE}}\big) + \hat{\phi}\big(D_{\phi,\mathrm{e}}^{\mathrm{TE}} + D_{\phi,\mathrm{o}}^{\mathrm{TE}}\big) \tag{2-151}$$

where

$$D_{\theta,\{e,o\}}^{\mathrm{TE}} = \varepsilon_0\varepsilon_\theta\sum_{i=1}^{4}\sum_{m,n}\left(a_{\{e,o\}mn}^{\mathrm{TE}(i)}\frac{-1}{r\sin\theta}\frac{\partial F_{r,\{e,o\}mn}^{(i)}}{\partial\phi}\right) \tag{2-152}$$

$$D_{\phi,\{e,o\}}^{\mathrm{TE}} = \varepsilon_0\varepsilon_\theta\sum_{i=1}^{4}\sum_{m,n}\left(a_{\{e,o\}mn}^{\mathrm{TE}(i)}\frac{1}{r}\frac{\partial F_{r,\{e,o\}mn}^{(i)}}{\partial\theta}\right). \tag{2-153}$$

Substitution of (2-148) into (2-149) gives

$$
H^{\mathbf{TE}} = \frac{1}{j\omega\mu_0} \sum_{i=1}^{4} \sum_{m,n} \{ a_{emn}^{\mathrm{TE}(i)} (\hat{r} \left(\frac{n(n+1)}{r^2} F_{r,emn}^{(i)} \right) + \hat{\theta} \left(\frac{1}{r} \frac{\partial^2 F_{r,emn}^{(i)}}{\partial r \partial \theta} \right)
$$

$$
+ \hat{\phi} \left(\frac{1}{r \sin \theta} \frac{\partial^2 F_{r,emn}^{(i)}}{\partial \phi \partial r} \right)) + a_{omn}^{\mathrm{TE}(i)} (\hat{r} \left(\frac{n(n+1)}{r^2} F_{r,omn}^{(i)} \right)
$$

$$
+ \hat{\theta} \left(\frac{1}{r} \frac{\partial^2 F_{r,omn}^{(i)}}{\partial r \partial \theta} \right) + \hat{\phi} \left(\frac{1}{r \sin \theta} \frac{\partial^2 F_{r,omn}^{(i)}}{\partial \phi \partial r} \right)) \}
$$

(2-154)

Substituting (2-137) into (2-154), we obtain

$$
\boldsymbol{H}^{\mathrm{TE}} = \frac{1}{j\omega\mu_0} \sum_{i=1}^{4} \sum_{e,o,m,n} \{ a_{\{e,o\}mn}^{\mathrm{TE}(i)} (\hat{r} \frac{n(n+1)}{r} \psi_{\{e,o\}mn}^{\mathrm{TE}(i)}
$$

$$
+ \hat{\theta} \frac{1}{r} \frac{\partial^2}{\partial r \partial \theta} \left(r \psi_{\{e,o\}mn}^{\mathrm{TE}(i)} \right) + \hat{\phi} \frac{1}{r \sin \theta} \frac{\partial 2}{\partial \phi \partial r} \left(r \psi_{\{e,o\}mn}^{\mathrm{TE}(i)} \right)) \}
$$

(2-155)

where inclusion of $\sum_{e,o}$ has allowed the separate even and odd expressions in (2-154) to be written as one expression. Substitution of (2-77) into (2-155) gives, after use of (2-115),

$$
\boldsymbol{H}^{\mathrm{TE}} = -j \sqrt{\frac{\varepsilon_0 \varepsilon_\theta}{\mu_0}} \sum_{i=1}^{4} \sum_{e,o,m,n} \left(a_{\{e,o\}mn}^{\mathrm{TE}(i)} \boldsymbol{N}_{\{e,o\}mn}^{(i)}(k,n) \right)
$$

(2-156)

where $\boldsymbol{N}_{\{e,o\}mn}^{(i)}(k,n)$ is given by (2-123) with v replaced by n. The same procedure can be applied for calculating $\mathbf{E}^{\mathrm{TE}}$. Substituting (2-3) and (2-151) into (2-150) and then doing the scalar multiplication, we obtain

$$\boldsymbol{E}^{\mathrm{TE}} = \frac{1}{\varepsilon_0 \varepsilon_\theta} \left(\hat{\theta} \big(D_{\theta,\mathrm{e}}^{\mathrm{TE}} + D_{\theta,\mathrm{o}}^{\mathrm{TE}} \big) + \hat{\phi} \big(D_{\phi,\mathrm{e}}^{\mathrm{TE}} + D_{\phi,\mathrm{o}}^{\mathrm{TE}} \big) \right). \tag{2-157}$$

Substitution of (2-152) and (2-153) into (2-157) gives

$$\boldsymbol{E}^{\mathrm{TE}} = -\sum_{i=1}^{4} \sum_{\mathrm{e,o},m,n} \left(a_{\{\mathrm{e,o}\}mn}^{\mathrm{TE}(i)} \left(\hat{\theta}\, \frac{1}{r\sin\theta} \frac{\partial F_{r,\{\mathrm{e,o}\}mn}^{(i)}}{\partial\phi} - \hat{\phi}\, \frac{1}{r} \frac{\partial F_{r,\{\mathrm{e,o}\}mn}^{(i)}}{\partial\theta} \right) \right) \tag{2-158}$$

where inclusion of $\sum_{\mathrm{e,o}}$ has allowed each pair of even and odd expressions in (2-158) to be written as one expression. Substitution of (2-137) into (2-158) gives

$$\boldsymbol{E}^{\mathrm{TE}} = -\sum_{i=1}^{4} \sum_{\mathrm{e,o},m,n} \left(a_{\{\mathrm{e,o}\}mn}^{\mathrm{TE}(i)} \left(\hat{\theta}\, \frac{1}{\sin\theta} \frac{\partial \psi_{\{\mathrm{e,o}\}mn}^{TE(i)}}{\partial\phi} - \hat{\phi}\, \frac{\partial \psi_{\{\mathrm{e,o}\}mn}^{TE(i)}}{\partial\theta} \right) \right). \tag{2-159}$$

Substitution of (2-77) into (2-159) gives

$$\boldsymbol{E}^{\mathrm{TE}} = -\sum_{i=1}^{4} \sum_{\mathrm{e,o},m,n} \left(a_{\{\mathrm{e,o}\}mn}^{\mathrm{TE}(i)} \left(\boldsymbol{M}_{\{\mathrm{e,o}\}mn}^{(i)}(k,n) \right) \right) \tag{2-160}$$

where k is given by (2-115) and $\boldsymbol{M}_{\{\mathrm{e,o}\}mn}^{(i)}(k,n)$ is given by (2-114) with ν replaced by n .

2.6 The derivation of the generalized Mie series coefficients in a radially uniaxial sphere

Consider a radially uniaxial dielectric sphere with radius a immersed in an incident x-polarized time harmonic plane wave traveling in the z-direction as shown in Fig.2.1.

$$\boldsymbol{E}^{\mathrm{i}} = \hat{a}_x e^{-jk_0 z} = \hat{a}_x e^{-jk_0 r\cos\theta} \tag{2-161}$$

$$\mathbf{H}^{\mathrm{i}} = \hat{a}_y \frac{1}{\eta_0} e^{-jk_0 z} \tag{2-162}$$

The sphere is comprised of permeability μ_0, and permittivity tensor of the form.

$$\bar{\bar{\varepsilon}} = \varepsilon_0 \begin{bmatrix} \varepsilon_r & 0 & 0 \\ 0 & \varepsilon_\theta & 0 \\ 0 & 0 & \varepsilon_\theta \end{bmatrix} \tag{2-163}$$

where ε_0 is the permittivity in air and ε_r and ε_θ are the relative electric permittivities parallel and perpendicular to the optic axis, respectively.

Using the spherical to Cartesian coordinate transformation, the radial component of $\mathbf{E}^{\mathrm{i}}$ is given by

$$E_r^{\mathrm{i}} = \sin \theta \cos \phi \ e^{-jk_0 r \cos \theta} \tag{2-164}$$

The partial derivative with respect to θ of [[21], (6-90)] is

$$-jr \sin \theta \ e^{jr \cos \theta} = \sum_{n=0}^{\infty} j^n \ (2n+1) j_n(r) \frac{dP_n(\cos \theta)}{d\theta}. \tag{2-165}$$

Since $\frac{d}{d\theta} P_0(\cos \theta) = 0$, the summation in (2-165) starts at $n = 1$. Substituting the complex conjugate of (2-165) with r replaced by $k_0 r$ into (2-164) gives

$$E_r^{\mathrm{i}} = \frac{\cos \phi}{jk_0 r} \sum_{n=1}^{\infty} j^{-n} \ (2n+1) \hat{j}_n(k_0 r) \frac{dP_n(\cos \theta)}{d\theta}. \tag{2-166}$$

From [[21], (E-25)],

$$\frac{dP_n(\cos\ \theta)}{d\theta} = P_n^1(\cos\ \theta) \tag{2-167}$$

and therefore (2-166) simplifies to

$$E_r^i = \frac{E_0 \cos\ \phi}{jk_0 r} \sum_{n=1}^{\infty} j^{-n}\ (2n+1)j_n(k_0 r)P_n^1(\cos\ \theta). \tag{2-168}$$

The radial component of $\boldsymbol{H}^i$ also obtains by

$$H_r^i = \frac{E_0 \sin\ \phi}{j\eta_0 k_0 r} \sum_{n=1}^{\infty} j^{-n}\ (2n+1)j_n(k_0 r)P_n^1(\cos\ \theta). \tag{2-169}$$
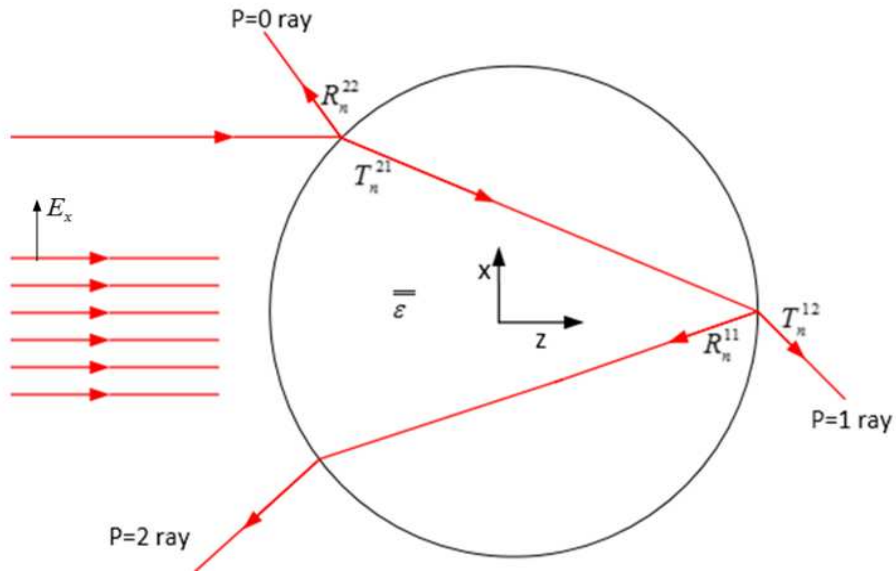
Fig. 2. 1. A plane wave approaching a uniaxial dielectric sphere

As outlined in previous sections, the incident electric and magnetic fields can be expressed as a superposition of TE_r and TM_r fields. The TE_r fields are constructed by letting A=0 and $F = \hat{a}_r F_r$ and the TM_r fields are generated by $A = \hat{a}_r A_r$ and F=0. Using (2-10) and the r-component of (2-89) with $\varepsilon_r = \varepsilon_\theta = 1$, it can be shown that

43

$$E_r^i = \frac{1}{j\omega\mu_0\varepsilon_0}\left(\frac{\partial^2}{\partial r^2} + k_0^2\right)A_r^i \qquad (2\text{-}170)$$

Substituting (2-8) and (2-78) into (2-170), A_r^i is given by $A_r^i = r\hat{a}_r\phi_{TM}^i$ where [2]

From (2-14) , (2-76) with $(i, v, \varepsilon_\theta) = (i, n, \varepsilon_\theta)$, $A = r\phi_{TM}^i$ where

$$\phi_{TM}^i = \mu_0 \sum_{m,n} j_n(k_0 r)P_n^m(\cos\,\theta)\,(a_{emn}^{TM(i)}\cos\,(m\phi) + a_{omn}^{TM(i)}\sin\,(m\phi)) \qquad (2\text{-}171)$$

so that (2-170) becomes

$$E_r^i = \frac{1}{j\omega\varepsilon_0 k_0}\sum_{m,n}((\frac{d^2}{dr^2} + k_0^2)\hat{J}_n(k_0 r))P_n^m(\cos\,\theta)\,(a_{emn}^{TM(i)}\cos\,(m\phi)$$
$$+\,a_{omn}^{TM(i)}\sin\,(m\phi)) \qquad (2\text{-}172)$$

where

$$\hat{J}_n(x) = xj_n(x) \qquad (2\text{-}173)$$

Substitution of (2-168) into (2-172) leads to

$$\left(a_{emn}^{TM(i)}, a_{omn}^{TM(i)}\right) = (a_{e1n}^{TM(i)}, 0) \qquad (2\text{-}174)$$

And

$$\frac{E_0}{jk_0^2 r^2} \sum_{n=1}^{\infty} j^{-n}(2n+1)\hat{J}_n(k_0 r)P_n^1(\cos\theta)$$

$$= \frac{1}{j\omega\varepsilon_0 k_0} \sum_{n=1}^{\infty} a_{e1n}^{TM(i)}((\frac{d^2}{dr^2}+k_0^2)\hat{J}_n(k_0 r))P_n^1(\cos\theta). \tag{2-175}$$

The set of functions $\{P_n^1(\cos\theta), n = 1,3,...\}$ is an orthogonal set so that (2-184) implies that

$$\frac{E_0}{jk_0^2 r^2}j^{-n}(2n+1)\hat{J}_n(k_0 r) = \frac{a_{e1n}^{TM(i)}}{j\omega\varepsilon_0 k_0}((\frac{d^2}{dr^2}+k_0^2)\hat{J}_n(k_0 r))\, P_n^1(\cos\theta) \tag{2-176}$$

with $k_0 = \omega\sqrt{\mu_0\varepsilon_0}$, the solution of (2-185) for $a_{e1n}^{TM(i)}$ is

$$a_{e1n}^{TM(i)} = \sqrt{\frac{\varepsilon_0}{\mu_0}} \frac{E_0 j^{-n}(2n+1)\hat{J}_n(k_0 r)}{r^2((\frac{d^2}{dr^2}+k_0^2)\hat{J}_n(k_0 r))}. \tag{2-177}$$

Now, $\hat{J}_n(k_0 r)$ satisfies (2-147) with $\varepsilon_\theta = 1$ which is

$$\left(\left(\frac{d^2}{dr^2}+k_0^2\right)\hat{J}_n(k_0 r)\right) = \frac{n(n+1)}{r^2}\hat{J}_n(k_0 r). \tag{2-178}$$

Substitution of (2-187) into (2-186) gives

$$a_{e1n}^{TM(i)} = \sqrt{\frac{\varepsilon_0}{\mu_0}} \frac{E_0 j^{-n}(2n+1)}{n(n+1)} \tag{2-179}$$

In view of (2-173), (2-174), and (2-179), (2-171) becomes, upon use of $k_0 = \omega\sqrt{\mu_0\varepsilon_0}$

$$\phi_{TM}^{i} = \frac{\cos\phi}{\omega\eta_0} \sum_{n=1}^{\infty} a_n j_n(k_0 r) P_n^1(\cos\theta) \qquad (2\text{-}180)$$

Where $a_n = \frac{j^{-n}(2n+1)}{n(n+1)}$. A similar procedure can be applied to compute ϕ_{TE}^{i} using

$F_r^i = r\phi_{TE}^i$ where

$$\phi_{TE}^{i} = \frac{\sin\phi}{\omega\eta_0} \sum_{n=1}^{\infty} a_n j_n(k_0 r) P_n^1(\cos\theta) \qquad (2\text{-}181)$$

The scattered fields representing TM$_r$ and TE$_r$ waves are constructed using scalar potentials ϕ_{TM}^{s} and ϕ_{TE}^{s}. The forms of ϕ_{TM}^{s} and ϕ_{TE}^{s} are similar to (2-180)and (2-181) but the radial components are replaced by the Hankel functions of second kind as follows

$$\phi_{TM}^{s} = \frac{\cos\phi}{\omega} \sum_{n=1}^{\infty} b_n h_n^{(2)}(k_0 r) P_n^1(\cos\theta) \qquad (2\text{-}182)$$

$$\phi_{TE}^{s} = \frac{\sin\phi}{\omega\eta_0} \sum_{n=1}^{\infty} c_n h_n^{(2)}(k_0 r) P_n^1(\cos\theta) \qquad (2\text{-}183)$$

where b_n and c_n are well-known generalized Mie series coefficients and are obtained by writing boundary conditions in the interface of the uniaxial dielectric sphere. The Bessel and Hankel functions in (2-180)–(2-183) are alternative spherical Bessel and Hankel functions which are related to regular Bessel and Hankel functions by (2-96).

As suggested in [2] and previous sections, the vector potentials $\hat{a}_r A_r^t$ and $\hat{a}_r F_r^t$ inside the uniaxial sphere are $r\hat{a}_r \phi_{TM}^t$ and $r\hat{a}_r \phi_{TE}^t$ respectively where

$$\phi_{TM}^t = \frac{\cos\phi}{\omega} \sum_{n=1}^{\infty} d_n j_\nu(kr) P_n^1(\cos\theta) \tag{2-184}$$

$$\phi_{TE}^t = \frac{\sin\phi}{\omega\eta_0} \sum_{n=1}^{\infty} e_n j_n(kr) P_n^1(\cos\theta) \tag{2-185}$$

where ν and k are given by (2-115) and (2-116). The spherical components of $\boldsymbol{E}$ and $\boldsymbol{H}$ inside and outside the sphere are now given by

$$E_r^p = \frac{1}{j\omega\mu_0\varepsilon_p} \left(\frac{\partial^2}{\partial r^2} + k_p{}^2 \right) A_r^p \tag{2-186}$$

$$E_\theta^p = \frac{1}{j\omega\mu_0\varepsilon_p r} \frac{\partial^2 A_r^p}{\partial r\partial\theta} - \frac{1}{\varepsilon_p r \sin\theta} \frac{\partial F_r^p}{\partial\phi} \tag{2-187}$$

$$E_\phi^p = \frac{1}{j\omega\mu_0\varepsilon_p r \sin\theta} \frac{\partial^2 A_r^p}{\partial r\partial\phi} + \frac{1}{\varepsilon_p r} \frac{\partial F_r^p}{\partial\theta} \tag{2-188}$$

$$H_r^p = \frac{1}{j\omega\mu_0\varepsilon_p} \left(\frac{\partial^2}{\partial r^2} + k_p{}^2 \right) F_r^p \tag{2-189}$$

$$H_\theta^p = \frac{1}{\mu_0 r \sin\theta} \frac{\partial A_r^p}{\partial\phi} + \frac{1}{j\omega\mu_0\varepsilon_p r} \frac{\partial^2 F_r^p}{\partial r\partial\theta} \tag{2-190}$$

$$H_\phi^p = -\frac{1}{\mu_0 r} \frac{\partial A_r^p}{\partial\theta} + \frac{1}{j\omega\mu_0\varepsilon_p r \sin\theta} \frac{\partial^2 F_r^p}{\partial r\partial\phi} \tag{2-191}$$

where the superscript $p=i$, s, or t and ε_p is $\varepsilon_0\varepsilon_\theta$ and ε_0 for inside and outside the sphere respectively. Note that $k_p = k_0\sqrt{\varepsilon_\theta}$ for inside the sphere and $k_p = k_0$ for outside the sphere. The unknown coefficients b_n, c_n, d_n and e_n, are now determined by satisfying the

boundary conditions which require the continuity of the tangential components of the electric and magnetic fields at the boundary surface of uniaxial sphere

$$E_\theta^i(a) + E_\theta^s(a) = E_\theta^t(a) \tag{2-192}$$

$$E_\phi^i(a) + E_\phi^s(a) = E_\phi^t(a) \tag{2-193}$$

$$H_\theta^i(a) + H_\theta^s(a) = H_\theta^t(a) \tag{2-194}$$

$$H_\phi^i(a) + H_\phi^s(a) = H_\phi^t(a). \tag{2-195}$$

Applying the boundary conditions of (2-192)–(2-195), one can derive the unknown coefficients as follows

$$b_n = \frac{-\sqrt{\varepsilon_\theta}\hat{J}_n'(k_0 a)\hat{J}_\nu(\sqrt{\varepsilon_\theta}k_0 a) + \hat{J}_\nu'(\sqrt{\varepsilon_\theta}k_0 a)\hat{J}_n(k_0 a)}{\sqrt{\varepsilon_\theta}\hat{H}_n^{(2)'}(k_0 a)\hat{J}_\nu(\sqrt{\varepsilon_\theta}k_0 a) - \hat{J}_\nu'(\sqrt{\varepsilon_\theta}k_0 a)\hat{H}_n^{(2)}(k_0 a)} a_n \tag{2-196}$$

$$c_n = \frac{-\hat{J}_n'(k_0 a)\hat{J}_n(\sqrt{\varepsilon_\theta}k_0 a) + \sqrt{\varepsilon_\theta}\hat{J}_n'(\sqrt{\varepsilon_\theta}k_0 a)\hat{J}_n(k_0 a)}{\hat{H}_n^{(2)'}(k_0 a)\hat{J}_n(\sqrt{\varepsilon_\theta}k_0 a) - \sqrt{\varepsilon_\theta}\hat{J}_n'(\sqrt{\varepsilon_\theta}k_0 a)\hat{H}_n^{(2)}(k_0 a)} a_n \tag{2-197}$$

$$d_n = -\frac{j\sqrt{\varepsilon_\theta}}{\sqrt{\varepsilon_\theta}\hat{H}_n^{(2)'}(k_0 a)\hat{J}_\nu(\sqrt{\varepsilon_\theta}k_0 a) - \hat{J}_\nu'(\sqrt{\varepsilon_\theta}k_0 a)\hat{H}_n^{(2)}(k_0 a)} a_n \tag{2-198}$$

$$e_n = -\frac{j}{\hat{H}_n^{(2)'}(k_0 a)\hat{J}_n(\sqrt{\varepsilon_\theta}k_0 a) - \sqrt{\varepsilon_\theta}\hat{J}_n'(\sqrt{\varepsilon_\theta}k_0 a)\hat{H}_n^{(2)}(k_0 a)} a_n \tag{2-199}$$

where each prime in the equations represents the derivative with respect to the argument. The E and H components can now be obtained by applying (2-196)–(2-199) and (2-180)–(2-185) to (2-185)–(2-191).

Chapter 3   The generalized Debye series in a radially uniaxial dielectric sphere

In this chapter, we examine the electromagnetic plane wave scattering by a uniaxial dielectric sphere using the generalized Debye series theory. With the aim of Debye series formulation, the generalized Mie series coefficients are replaced by infinite series of partial wave contributions that are diffracted, reflected and refracted following by p-1 internal reflections in the sphere. In addition to exploring the bistatic Radar Cross Section (RCS) of the positive/negative uniaxial dielectric spheres using Lorenz-Mie theory, the first three terms of the generalized Debye series are investigated and the results are applied to improve our understanding of the scattering mechanism from a uniaxial dielectric sphere.

3.1 Introduction

The majority of materials are anisotropic. Crystals, e.g., calcite, sapphire, and stacked dielectric layers, [25] are among the materials that are naturally and artificially anisotropic. In recent years, the analysis and characterization of anisotropic materials has been a great subject, due to the recent advances in material science, technology and their applications in electromagnetic scattering and microwave engineering [2]. Among those investigations, scattering of electromagnetic waves by uniaxial dielectric spheres has attracted considerable attention due to their cloaking features [26], [27]. Backscattering from a uniaxial dielectric sphere was first studied by Wong et. al. [2] using the generalized Mie series equation. A significant difference between backscattering in uniaxial and isotropic dielectric spheres was reported in his paper. However, as stated in

the paper, there is no general rule for scattering by non-absorbing uniaxial dielectric spheres and therefore further work in this area was required. The Mie series solution, while offering an exact mathematical solution for the scattering problem, fails to provide a physical description of the problem. To overcome this difficulty, the Debye series is used to investigate scattering from an isotropic dielectric sphere [28]. In addition to exploring the bistatic Radar Cross Section (RCS) of a uniaxial dielectric sphere using Lorenz-Mie theory, the generalized Debye series is introduced in the second section. It is shown that the generalized Mie series coefficients b_n and c_n are the decomposition of a series of partial wave contributions that are diffracted, reflected and refracted following by p-1 internal reflections in the sphere [6]. The monostatic and bistatic RCSs are then examined for each term of the Debye series, and compared with the isotropic case.

3.2 Formulation of the generalized Debye series

In this work, we consider a radially uniaxial dielectric sphere with radius a immersed in an incident x-polarized time harmonic plane wave traveling in the z-direction as shown in Fig.3.1.

$$E_i = \hat{a}_x e^{-jk_0 z} = \hat{a}_x e^{-jk_0 r \cos\theta} \tag{3-1}$$

The sphere is comprised of permeability μ_0 and permittivity tensor of the form

$$\bar{\bar{\varepsilon}} = \varepsilon_0 \begin{bmatrix} \epsilon_r & 0 & 0 \\ 0 & \epsilon_\theta & 0 \\ 0 & 0 & \epsilon_\theta \end{bmatrix} \tag{3-2}$$

where ε_0 is the permittivity in air and ε_r and ε_θ are the electric permittivities parallel and perpendicular to the optic axis respectively.

50
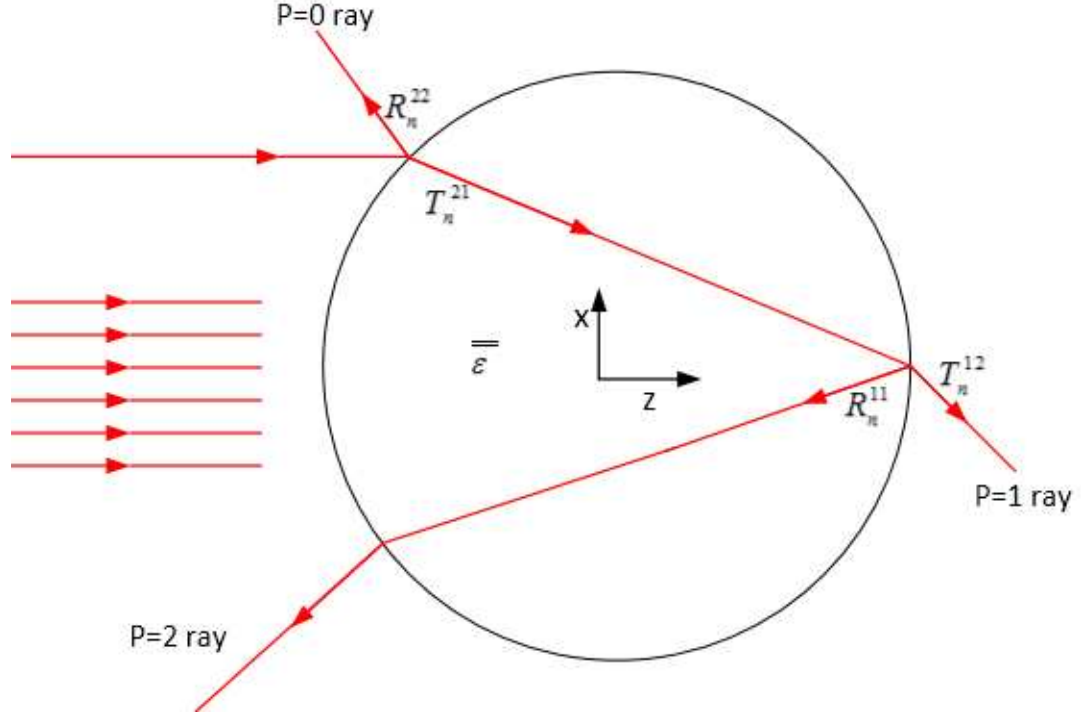
Fig. 3. 1. A plane wave approaching a uniaxial dielectric sphere

The electric and magnetic fields are evaluated by scalar potentials of $\psi(r, \theta, \phi)$ that satisfy (2-26) and (2-50). These equations are repeated here as follows

$$\frac{\varepsilon_r}{\varepsilon_\theta} \frac{1}{r^2} \frac{\partial}{\partial \text{r}} (r^2 \frac{\partial \psi_{TM}}{\partial \text{r}}) + \nabla_t^2 \psi_{TM} + k_0^2 \varepsilon_r \psi_{TM} = 0$$

(3-3)

$$\frac{1}{r^2} \frac{\partial}{\partial r} (r^2 \frac{\partial \psi_{TE}}{\partial \text{r}}) + \nabla_t^2 \psi_{TE} + k_0^2 \varepsilon_\theta \psi_{TE} = 0$$

(3-4)

where $k_0 = \omega/c$ and $\nabla_t^2 = \nabla^2 - \frac{1}{r^2} \frac{\partial}{\partial r} (r^2 \frac{\partial}{\partial r})$. The solutions for the scalar wave equations (3-3) and (3-4) are (2-76) and (2-78) respectively. The magnetic and electric vector potentials are written as $\boldsymbol{A} = r a_r \psi_{TM}$ and $\boldsymbol{F} = r a_r \psi_{TE}$ and therefore

$$\begin{Bmatrix} A_r(r,\theta,\phi) \\ F_r(r,\theta,\phi) \end{Bmatrix} = \sum_{mn} \begin{Bmatrix} A_{mn}\mu_0\hat{B}_v \\ C_{mn}\varepsilon_0\varepsilon_\theta\hat{B}_n \end{Bmatrix} P_n^m(\cos\theta) \begin{Bmatrix} \cos m\phi \\ \sin m\phi \end{Bmatrix} \tag{3-5}$$

where $v = \sqrt{n(n+1)AR + \frac{1}{4}} - \frac{1}{2}$ and $\hat{B}_n$ and $\hat{B}_v$ are the alternative spherical Bessel or

Hankel functions of the first and the second kinds of argument $\sqrt{\varepsilon_\theta}k_0 r$ and are related to

the regular Bessel/Hankel functions by (2-141) and AR is the anisotropy ratio defined by

$AR = \frac{\varepsilon_\theta}{\varepsilon_r}$. In our notation the spherical Hankel functions of the second and first kinds are

employed for outgoing and incoming waves respectively. Consider a single incoming

TM/TE spherical wave with unit amplitude, $A_{mn} = 1/C_{mn} = 1$ incident on the uniaxial

sphere [28],

$$\begin{Bmatrix} F_r(r,\theta,\phi) \\ A_r(r,\theta,\phi) \end{Bmatrix} = \begin{Bmatrix} \mu_0 \\ \varepsilon_0 \end{Bmatrix} \hat{H}_n^{(1)}(k_0 r) P_n^m(\cos\theta) \begin{Bmatrix} \cos m\phi \\ \sin m\phi \end{Bmatrix}. \tag{3-6}$$

When this partial wave hits the boundary interface at $r = a$, the T_n^{21} portion of the

incident wave is transmitted into the sphere and the remaining portion, R_n^{22}, is reflected

back into the air region as shown in Fig. 3.1. The complete TE and TM waves in the two

regions are expressed as

$$\begin{Bmatrix} A_r^1(r,\theta,\phi) \\ F_r^1(r,\theta,\phi) \end{Bmatrix} = \sum_{m,n} \begin{Bmatrix} \mu_0 \\ \varepsilon_0\varepsilon_\theta \end{Bmatrix} T_n^{21\{A\}\atop\{F\}} \begin{Bmatrix} \hat{H}_v^{(1)}(\sqrt{\varepsilon_\theta}k_0 r) \\ \hat{H}_n^{(1)}(\sqrt{\varepsilon_\theta}k_0 r) \end{Bmatrix} f(\theta,\phi) \qquad r \leq a \tag{3-7}$$

$$\begin{Bmatrix} A_r^2(r,\theta,\phi) \\ F_r^2(r,\theta,\phi) \end{Bmatrix} = \sum_{m,n} \begin{Bmatrix} \mu_0 \\ \varepsilon_0 \end{Bmatrix} \left[\hat{H}_n^{(1)}(k_0 r) + R_n^{22\{A\}\atop\{F\}} \hat{H}_n^2(k_0 r) \right] f(\theta,\phi) \; r \geq a \tag{3-8}$$

where $\widehat{H}_v^{(1)}$ and $\widehat{H}_n^{(1)}$ indicate the TM and TE spherical incoming waves respectively and

$f(\theta, \phi) = P_n^m(\cos \theta) \begin{Bmatrix} \cos m\phi \\ \sin m\phi \end{Bmatrix}$. To determine the unknown coefficients T_n^{21} and R_n^{22}, the

tangential electric and magnetic field boundary conditions are applied.

Starting from the TM wave, the tangential electric and magnetic fields can be determined by setting F=0 and substituting the magnetic vector potentials A of (3-7) and (3-8) into (2-187) and (2-181) as follows

$$E_\theta^{1^A} = \frac{1}{j\omega\mu_0\varepsilon_0\varepsilon_\theta} \frac{\partial^2 (\sum_{m,n} \mu_0 T_n^{21^A} \widehat{H}_v^{(1)}(\sqrt{\varepsilon_\theta}k_0 r) f(\theta, \phi))}{\partial r \partial \theta} \tag{3-9}$$

$$H_\theta^{1^A} = \frac{1}{\mu_0 r \sin\theta} \frac{\partial (\sum_{m,n} \mu_0 T_n^{21^A} \widehat{H}_v^{(1)}(\sqrt{\varepsilon_\theta}k_0 r) f(\theta, \phi))}{\partial \phi} \tag{3-10}$$

$$E_\theta^{2^A} = \frac{1}{j\omega\mu_0\varepsilon_0} \frac{\partial^2 (\sum_{m,n} \mu_0 \left[\widehat{H}_n^{(1)}(k_0 r) + R_n^{22^A} \widehat{H}_n^{(2)}(k_0 r) \right] f(\theta, \phi))}{\partial r \partial \theta} \tag{3-11}$$

$$H_\theta^{2^A} = \frac{1}{\mu_0 r \sin\theta} \frac{\partial (\sum_{m,n} \mu_0 \left[\widehat{H}_n^{(1)}(k_0 r) + R_n^{22^A} \widehat{H}_n^{(2)}(k_0 r) \right] f(\theta, \phi))}{\partial \phi}. \tag{3-12}$$

Writing the boundary conditions at the interface of the uniaxial sphere yields

$$E_\theta^{1^A} = E_\theta^{2^A}\big|_{r=a} \tag{3-13}$$

$$H_\theta^{1^A} = H_\theta^{2^A}\big|_{r=a}. \tag{3-14}$$

Substituting (3-9)–(3-12) into (3-13) and (3-14) give

$$\frac{1}{\varepsilon_\theta} \frac{\partial^2 (T_n^{21^A} \widehat{H}_v^{(1)}(\sqrt{\varepsilon_\theta}k_0 a) f(\theta, \phi))}{\partial a \partial \theta}$$

$$= \frac{\partial^2 (\left[\widehat{H}_n^{(1)}(k_0 a) + R_n^{22^A} \widehat{H}_n^{(2)}(k_0 a) \right] f(\theta, \phi))}{\partial a \partial \theta} \tag{3-15}$$

$$\frac{\partial \left(T_n^{21^A} \widehat{H}_v^{(1)}\left(\sqrt{\varepsilon_\theta}k_0 a\right) f(\theta,\phi)\right)}{\partial \phi}$$

$$= \frac{\partial \left(\left[\widehat{H}_n^{(1)}(k_0 a) + R_n^{22^A} \widehat{H}_n^{(2)}(k_0 a)\right] f(\theta,\phi)\right)}{\partial \phi}. \tag{3-16}$$

Equations (3-15) and (3-16) imply that

$$\frac{1}{\sqrt{\varepsilon_\theta}} T_n^{21^A} \widehat{H}_v^{(1)'}\left(\sqrt{\varepsilon_\theta}k_0 a\right) = \left[\widehat{H}_n^{(1)'}(k_0 a) + R_n^{22^A}\widehat{H}_n^{(2)'}(k_0 a)\right] \tag{3-17}$$

$$T_n^{21^A}\widehat{H}_v^{(1)}\left(\sqrt{\varepsilon_\theta}k_0 a\right) = \widehat{H}_n^{(1)}(k_0 a) + R_n^{22^A}\widehat{H}_n^{(2)}(k_0 a) \tag{3-18}$$

where each prime in (3-17) indicates the partial derivative with respect to the argument of

the Hankel function. Multiplying (3-17) by $\widehat{H}_n^{(2)}(k_0 a)$ and (3-18) by $\widehat{H}_n^{(2)'}(k_0 a)$ give

$$\frac{1}{\sqrt{\varepsilon_\theta}} T_n^{21^A}\widehat{H}_v^{(1)'}\left(\sqrt{\varepsilon_\theta}k_0 a\right)\widehat{H}_n^{(2)}(k_0 a)$$

$$= \widehat{H}_n^{(2)}(k_0 a)\left[\widehat{H}_n^{(1)'}(k_0 a) + R_n^{22^A}\widehat{H}_n^{(2)'}(k_0 a)\right] \tag{3-19}$$

$$T_n^{21^A}\widehat{H}_v^{1}\left(\sqrt{\varepsilon_\theta}k_0 a\right)\widehat{H}_n^{2'}(k_0 a) = \widehat{H}_n^{2'}(k_0 a)\left[\widehat{H}_n^{(1)}(k_0 a) + R_n^{22^A}\widehat{H}_n^{(2)}(k_0 a)\right]. \tag{3-20}$$

Subtracting

(3-19) from (3-20) yields

$$T_n^{21^A}\left[\widehat{H}_v^{1}\left(\sqrt{\varepsilon_\theta}k_0 a\right)\widehat{H}_n^{(2)'}(k_0 a) - \frac{1}{\sqrt{\varepsilon_\theta}}\widehat{H}_v^{(1)'}\left(\sqrt{\varepsilon_\theta}k_0 a\right)\widehat{H}_n^{(2)}(k_0 a)\right]$$

$$= \widehat{H}_n^{(2)'}(k_0 a)\widehat{H}_n^{(1)}(k_0 a) - \widehat{H}_n^{(2)}(k_0 a)\widehat{H}_n^{(1)'}(k_0 a). \tag{3-21}$$

Using the Wronskian relationship, the right hand side of (3-21) is simplified to $-2j$ and we find that the transmission coefficient $T_n^{21^A}$ of the TM wave is

$$T_n^{21^A} = \frac{2j\sqrt{\varepsilon_\theta}}{-\sqrt{\varepsilon_\theta}\hat{H}_n^{(2)'}(k_0 a)\hat{H}_\nu^{(1)}\left(\sqrt{\varepsilon_\theta}k_0 a\right) + \hat{H}_\nu^{(1)'}\left(\sqrt{\varepsilon_\theta}k_0 a\right)\hat{H}_n^{(2)}(k_0 a)}. \qquad (3\text{-}22)$$

Substituting (3-22) into (3-17), we find that

$$\frac{\left[-\hat{H}_n^{(2)'}(k_0 a)\hat{H}_n^{(1)}(k_0 a) + \hat{H}_n^{(2)}(k_0 a)\hat{H}_n^{(1)'}(k_0 a)\right]\hat{H}_\nu^{(1)'}\left(\sqrt{\varepsilon_\theta}k_0 a\right)}{-\sqrt{\varepsilon_\theta}\hat{H}_n^{(2)'}(k_0 a)\hat{H}_\nu^{(1)}\left(\sqrt{\varepsilon_\theta}k_0 a\right) + \hat{H}_\nu^{(1)'}\left(\sqrt{\varepsilon_\theta}k_0 a\right)\hat{H}_n^{(2)}(k_0 a)}$$

$$= \left[\hat{H}_n^{(1)'}(k_0 a) + R_n^{22^A}\hat{H}_n^{(2)'}(k_0 a)\right] \qquad (3\text{-}23)$$

which yields

$$R_n^{22^A} = \frac{\sqrt{\varepsilon_\theta}\hat{H}_n^{(1)'}(k_0 a)\hat{H}_\nu^{(1)}\left(\sqrt{\varepsilon_\theta}k_0 a\right) - \hat{H}_\nu^{(1)'}\left(\sqrt{\varepsilon_\theta}k_0 a\right)\hat{H}_n^{(1)}(k_0 a)}{-\sqrt{\varepsilon_\theta}\hat{H}_n^{(2)'}(k_0 a)\hat{H}_\nu^{(1)}\left(\sqrt{\varepsilon_\theta}k_0 a\right) + \hat{H}_\nu^{(1)'}\left(\sqrt{\varepsilon_\theta}k_0 a\right)\hat{H}_n^{(2)}(k_0 a)}. \qquad (3\text{-}24)$$

The same procedure can be applied to calculate the transmission and reflection coefficients corresponding to the *TE* wave. Setting *A=0* and substituting the electric vector potentials *F* of (3-7) and (3-8) into (2-187) and (2-190) yield

$$E_\theta^{1^F} = -\frac{1}{\varepsilon_0\varepsilon_\theta r \sin\theta}\frac{\partial\left[\sum_{m,n}\varepsilon_0\varepsilon_\theta T_n^{21^F}\hat{H}_n^{(1)}\left(\sqrt{\varepsilon_\theta}k_0 r\right)f(\theta,\phi)\right]}{\partial\phi} \qquad (3\text{-}25)$$

$$H_\theta^{1^F} = \frac{1}{j\omega\mu_0\varepsilon_0\varepsilon_\theta r}\frac{\partial^2\left[\sum_{m,n}\varepsilon_0\varepsilon_\theta T_n^{21^F}\hat{H}_n^{(1)}\left(\sqrt{\varepsilon_\theta}k_0 r\right)f(\theta,\phi)\right]}{\partial r\partial\theta} \qquad (3\text{-}26)$$

$$E_\theta^{2^F} = -\frac{1}{\varepsilon_0 r \sin\theta}\frac{\partial\left[\sum_{m,n}\varepsilon_0\left[\hat{H}_n^{(1)}(k_0 r) + R_n^{22^F}\hat{H}_n^{(2)}(k_0 r)\right]f(\theta,\phi)\right]}{\partial\phi} \qquad (3\text{-}27)$$

$$H_\theta^{2^F} = \frac{1}{j\omega\mu_0\varepsilon_0 r} \frac{\partial^2 \left[\sum_{m,n} \varepsilon_0 \left[\widehat{H}_n^{(1)}(k_0 r) + R_n^{22^F} \widehat{H}_n^{(2)}(k_0 r)\right] f(\theta,\phi)\right]}{\partial r \partial \theta}. \tag{3-28}$$

Writing the boundary conditions at the interface of uniaxial sphere yield

$$E_\theta^{1^F} = E_\theta^{2^F}\big|_{r=a} \tag{3-29}$$

$$H_\theta^{1^F} = H_\theta^{2^F}\big|_{r=a}. \tag{3-30}$$

Substituting (3-25)–(3-28) into (3-29) and (3-30) give

$$\frac{\partial \left[T_n^{21^F} \widehat{H}_n^{(1)}(\sqrt{\varepsilon_\theta} k_0 a) f(\theta,\phi)\right]}{\partial \phi}$$
$$= \frac{\partial \left[\left[\widehat{H}_n^{(1)}(k_0 a) + R_n^{22^F} \widehat{H}_n^{(2)}(k_0 a)\right] f(\theta,\phi)\right]}{\partial \phi} \tag{3-31}$$

$$\frac{\partial^2 \left[T_n^{21^F} \widehat{H}_n^{(1)}(\sqrt{\varepsilon_\theta} k_0 a) f(\theta,\phi)\right]}{\partial a \partial \theta}$$
$$= \frac{\partial^2 \left[\left[\widehat{H}_n^{(1)}(k_0 a) + R_n^{22^F} \widehat{H}_n^{(2)}(k_0 a)\right] f(\theta,\phi)\right]}{\partial a \partial \theta} \tag{3-32}$$

Integrating (3-31) over ϕ and (3-32) over θ yield

$$T_n^{21^F} \widehat{H}_n^{(1)}(\sqrt{\varepsilon_\theta} k_0 a) = \widehat{H}_n^{(1)}(k_0 a) + R_n^{22^F} \widehat{H}_n^{(2)}(k_0 a) \tag{3-33}$$

$$\sqrt{\varepsilon_\theta} T_n^{21^F} \widehat{H}_n^{(1)'}(\sqrt{\varepsilon_\theta} k_0 a) = \widehat{H}_n^{(1)'}(k_0 a) + R_n^{22^F} \widehat{H}_n^{(2)'}(k_0 a) \tag{3-34}$$

where each prime in (3-34) indicates the partial derivative with respect to the argument of

the Hankel function. Multiplying (3-33) by $\widehat{H}_n^{(2)'}(k_0 a)$ and (3-34) by $\widehat{H}_n^{(2)}(k_0 a)$ give

$$T_n^{21^F} \widehat{H}_n^{(1)}\left(\sqrt{\varepsilon_\theta}k_0 a\right)\widehat{H}_n^{(2)'}(k_0 a)$$

$$= \widehat{H}_n^{(2)'}(k_0 a)\left[\widehat{H}_n^{(1)}(k_0 a) + R_n^{22^F}\widehat{H}_n^{(2)}(k_0 a)\right] \tag{3-35}$$

$$\sqrt{\varepsilon_\theta}T_n^{21^F} \widehat{H}_n^{(1)'}\left(\sqrt{\varepsilon_\theta}k_0 a\right)\widehat{H}_n^{(2)}(k_0 a)$$

$$= \widehat{H}_n^{(2)}(k_0 a)\left[\widehat{H}_n^{(1)'}(k_0 a) + R_n^{22^F}\widehat{H}_n^{(2)'}(k_0 r)\right]. \tag{3-36}$$

Subtracting (3-35)from (3-36) yields

$$T_n^{21^F}\left[\sqrt{\varepsilon_\theta}\ \widehat{H}_n^{(1)'}\left(\sqrt{\varepsilon_\theta}k_0 a\right)\widehat{H}_n^{(2)}(k_0 a) - \right.$$

$$Hn1\varepsilon\theta k0aHn2'k0a{=}Hn2k0aHn1'k0a{-}Hn2'k0aHn1k0a \tag{3-37}$$

Using the Wronskian relationship, the right hand side of (3-37) is simplified to $2j$ and we find that the transmission coefficient $T_n^{21^F}$ of the TE wave is

$$T_n^{21^F} = \frac{2j}{-\widehat{H}_n^{(2)'}(k_0 a)\,\widehat{H}_n^{(1)}\left(\sqrt{\varepsilon_\theta}k_0 a\right) + \sqrt{\varepsilon_\theta}\ \widehat{H}_n^{(1)'}\left(\sqrt{\varepsilon_\theta}k_0 a\right)\widehat{H}_n^{(2)}(k_0 a)}. \tag{3-38}$$

Substituting of the solution of (3-37) for $T_n^{21^F}$ into (3-33) yields

$$R_n^{22^F} = \frac{\widehat{H}_n^{(1)'}(k_0 a)\widehat{H}_n^{(1)}\left(\sqrt{\varepsilon_\theta}k_0 a\right) - \sqrt{\varepsilon_\theta}\widehat{H}_n^{(1)'}\left(\sqrt{\varepsilon_\theta}k_0 a\right)\widehat{H}_n^{(1)}(k_0 a)}{-\widehat{H}_n^{(2)'}(k_0 a)\widehat{H}_n^{(1)}\left(\sqrt{\varepsilon_\theta}k_0 a\right) + \sqrt{\varepsilon_\theta}\widehat{H}_n^{(1)'}\left(\sqrt{\varepsilon_\theta}k_0 a\right)\widehat{H}_n^{(2)}(k_0 a)} \tag{3-39}$$

The same procedure can be applied for the shadow boundary by assuming an incident outgoing TE/TM wave of unit amplitude hits the boundary interface at r=a in Fig. 3.1. The T_n^{12} portion leaves the sphere, and the remaining portion, R_n^{11} reflects back into it. The complete TE and TM waves in the two regions are

$$
\begin{Bmatrix} A_r^1(r,\theta,\phi) \\ F_r^1(r,\theta,\phi) \end{Bmatrix}
$$

$$
= \sum_{mn} \begin{Bmatrix} \mu_0 \\ \varepsilon_0\varepsilon_\theta \end{Bmatrix} \left[\begin{Bmatrix} \left(\widehat{H}_v^{(2)}\!\left(\sqrt{\varepsilon_\theta}k_0 a\right)\right) \\ \widehat{H}_n^{(2)}\!\left(\sqrt{\varepsilon_\theta}k_0 a\right) \end{Bmatrix} . + R_n^{11^{\{A\}}_{\{F\}}} \begin{Bmatrix} \left(\widehat{H}_v^{(1)}\!\left(\sqrt{\varepsilon_\theta}k_0 a\right)\right) \\ \widehat{H}_n^{(1)}\!\left(\sqrt{\varepsilon_\theta}k_0 a\right) \end{Bmatrix} \right] f(\theta,\phi) \tag{3-40}
$$

for r≤a   and for r≥a   they are given by

$$
\begin{Bmatrix} A_r^2(r,\theta,\phi) \\ F_r^2(r,\theta,\phi) \end{Bmatrix} = \sum_{mn} \begin{Bmatrix} \mu_0 \\ \varepsilon_0 \end{Bmatrix} T_n^{12^{\{A\}}_{\{F\}}} \widehat{H}_n^{(2)}(k_0 r)\, f(\theta,\phi) \tag{3-41}
$$

where $\widehat{H}_n^{(2)}$ and $\widehat{H}_v^{(2)}$ indicate the TE and TM outgoing waves respectively. The two linear equations obtained from boundary condition yields the reflected and refracted amplitude waves. Starting from the TM wave, the tangential electric and magnetic fields can be determined by setting F=0 and substituting the electric vector potentials *A* of (3-31) and

(3-32) into (2-186)–(2-191) as follows

$$
E_\theta^{1\,A}
$$

$$
= \frac{1}{j\omega\mu_0\varepsilon_0\varepsilon_\theta} \frac{d^2\left(\sum_{m,n}\mu_0\left[\left(\widehat{H}_v^{(2)}\!\left(\sqrt{\varepsilon_\theta}k_0 a\right) + R_n^{11^A}\widehat{H}_v^{(1)}\!\left(\sqrt{\varepsilon_\theta}k_0 a\right)\right]f(\theta,\phi)\right)}{dr\,d\theta} \tag{3-42}
$$

$$
H_\theta^{1\,A}
$$

$$
= \frac{1}{\mu_0 r \sin\theta} \frac{d\left(\sum_{m,n}\mu_0\left[\left(\widehat{H}_v^{(2)}\!\left(\sqrt{\varepsilon_\theta}k_0 a\right) + R_n^{11^A}\widehat{H}_v^{(1)}\!\left(\sqrt{\varepsilon_\theta}k_0 a\right)\right]f(\theta,\phi)\right)}{d\phi} \tag{3-43}
$$

$$E_\theta^{2^A} = \frac{1}{j\omega\mu_0\varepsilon_0} \frac{d^2\left(\sum_{mn} \mu_0 T_n^{12^A} \widehat{H}_n^{(2)}(k_0 r) f(\theta,\phi)\right)}{dr d\theta} \tag{3-44}$$

$$H_\theta^{2^A} = \frac{1}{\mu_0 r \sin\theta} \frac{d\left(\sum_{mn} \mu_0 T_n^{12^A} \widehat{H}_n^{(2)}(k_0 r) f(\theta,\phi)\right)}{d\phi} \tag{3-45}$$

Writing the boundary conditions at the shadow boundary of uniaxial sphere yield

$$E_\theta^{1^A} = E_\theta^{2^A}\big|_{r=a} \tag{3-46}$$

$$H_\theta^{1^A} = H_\theta^{2^A}\big|_{r=a} \tag{3-47}$$

Substituting (3-42)–(3-45) into (3-46) and (3-47) give

$$\frac{1}{\varepsilon_\theta} \frac{d^2\left(\left[\left(\widehat{H}_v^{(2)}\left(\sqrt{\varepsilon_\theta}k_0 a\right) + R_n^{11^A}\widehat{H}_v^{(1)}\left(\sqrt{\varepsilon_\theta}k_0 a\right)\right]f(\theta,\phi)\right)}{dr d\theta}$$

$$= \frac{d^2\left(T_n^{12^A}\widehat{H}_n^{(2)}(k_0 r)f(\theta,\phi)\right)}{dr d\theta} \tag{3-48}$$

$$\frac{d\left(\left[\left(\widehat{H}_v^{(2)}\left(\sqrt{\varepsilon_\theta}k_0 a\right) + R_n^{11^A}\widehat{H}_v^{(1)}\left(\sqrt{\varepsilon_\theta}k_0 a\right)\right]f(\theta,\phi)\right)}{d\phi}$$

$$= \frac{d\left(T_n^{12^A}\widehat{H}_n^{(2)}(k_0 r)f(\theta,\phi)\right)}{d\phi} \tag{3-49}$$

Integrating (3-48) over θ and (3-49) over ϕ yield

$$\frac{1}{\sqrt{\varepsilon_\theta}}\left[\left(\widehat{H}_v^{(2)'}\left(\sqrt{\varepsilon_\theta}k_0 a\right) + R_n^{11^A}\widehat{H}_v^{(1)'}\left(\sqrt{\varepsilon_\theta}k_0 a\right)\right] = T_n^{12^A}\widehat{H}_n^{(2)'}(k_0 r) \tag{3-50}$$

$$\left[\left(\widehat{H}_v^{(2)}\left(\sqrt{\varepsilon_\theta}k_0 a\right) + R_n^{11^A}\widehat{H}_v^{(1)}\left(\sqrt{\varepsilon_\theta}k_0 a\right)\right] = T_n^{12^A}\widehat{H}_n^{(2)}(k_0 r) \tag{3-51}$$

where prime in (3-50)–(3-51) indicates the partial derivative with respect to the argument of Hankel functions. Multiplying (3-50) by $\widehat{H}_v^{(1)}\left(\sqrt{\varepsilon_\theta}k_0 a\right)$ and (3-51) by $\widehat{H}_v^{(1)'}\left(\sqrt{\varepsilon_\theta}k_0 a\right)$ give

$$\frac{1}{\sqrt{\varepsilon_\theta}}\left[\left(\widehat{H}_v^{(2)'}\left(\sqrt{\varepsilon_\theta}k_0 a\right) + R_n^{11^A}\widehat{H}_v^{(1)'}\left(\sqrt{\varepsilon_\theta}k_0 a\right)\right]\widehat{H}_v^{(1)}\left(\sqrt{\varepsilon_\theta}k_0 a\right) =$$

$$T_n^{12^A}\widehat{H}_n^{(2)'}(k_0 r)\widehat{H}_v^{(1)}\left(\sqrt{\varepsilon_\theta}k_0 a\right) \tag{3-52}$$

$$\left[\left(\widehat{H}_v^{(2)}\left(\sqrt{\varepsilon_\theta}k_0 a\right) + R_n^{11^A}\widehat{H}_v^{(1)}\left(\sqrt{\varepsilon_\theta}k_0 a\right)\right]\widehat{H}_v^{(1)'}\left(\sqrt{\varepsilon_\theta}k_0 a\right) =$$

$$T_n^{12^A}\widehat{H}_n^{(2)}(k_0 r)\widehat{H}_v^{(1)'}\left(\sqrt{\varepsilon_\theta}k_0 a\right) \tag{3-53}$$

Subtracting (3-52) from (3-53) yields

$$T_n^{12^A}\left[\widehat{H}_n^{(2)}(k_0 r)\widehat{H}_v^{(1)'}\left(\sqrt{\varepsilon_\theta}k_0 a\right) - \sqrt{\varepsilon_\theta}\widehat{H}_n^{(2)'}(k_0 r)\widehat{H}_v^{(1)}\left(\sqrt{\varepsilon_\theta}k_0 a\right)\right] =$$

$$\widehat{H}_v^{(2)}\left(\sqrt{\varepsilon_\theta}k_0 a\right)\widehat{H}_v^{(1)'}\left(\sqrt{\varepsilon_\theta}k_0 a\right) - \widehat{H}_v^{(2)'}\left(\sqrt{\varepsilon_\theta}k_0 a\right)\widehat{H}_v^{(1)}\left(\sqrt{\varepsilon_\theta}k_0 a\right) \tag{3-54}$$

Using Wronskian relationship, the right hand side of (3-54) is simplified to *2j* and we found the transmission coefficient of TM wave $T_n^{12^A}$ is

$$T_n^{12^A} = \frac{2j}{-\sqrt{\varepsilon_\theta}\widehat{H}_n^{(2)'}(k_0 a)\widehat{H}_v^{(1)}\left(\sqrt{\varepsilon_\theta}k_0 r\right) + \widehat{H}_v^{(1)'}\left(\sqrt{\varepsilon_\theta}k_0 a\right)\widehat{H}_n^{(2)}(k_0 a)} \tag{3-55}$$

Substituting (3-55) into (3-52) we found

$$\left[\left(\widehat{H}_v^{(2)'}\left(\sqrt{\varepsilon_\theta}k_0 a\right) + R_n^{11^A}\widehat{H}_v^{(1)'}\left(\sqrt{\varepsilon_\theta}k_0 a\right)\right]$$

$$= \frac{2j\sqrt{\varepsilon_\theta}\widehat{H}_n^{(2)'}(k_0 r)}{-\sqrt{\varepsilon_\theta}\widehat{H}_n^{(2)'}(k_0 a)\widehat{H}_v^{(1)}\left(\sqrt{\varepsilon_\theta}k_0 r\right) + \widehat{H}_v^{(1)'}\left(\sqrt{\varepsilon_\theta}k_0 a\right)\widehat{H}_n^{(2)}(k_0 a)} \tag{3-56}$$

which yields to

$$R_n^{11^A} = \frac{\sqrt{\varepsilon_\theta}\widehat{H}_n^{(2)'}(k_0 a)\widehat{H}_v^{(2)}(\sqrt{\varepsilon_\theta}k_0 a) - \widehat{H}_v^{(2)'}(\sqrt{\varepsilon_\theta}k_0 a)\widehat{H}_n^{(2)}(k_0 a)}{-\sqrt{\varepsilon_\theta}\widehat{H}_n^{(2)'}(k_0 a)\widehat{H}_v^{(1)}(\sqrt{\varepsilon_\theta}k_0 a) + \widehat{H}_v^{(1)'}(\sqrt{\varepsilon_\theta}k_0 a)\widehat{H}_n^{(2)}(k_0 a)} \tag{3-57}$$

The same procedure can be applied to calculate the transmission and reflection coefficients corresponding to *TE* wave. Setting *A=0* and substituting the magnetic vector potentials *F* of (3-40) and (3-41) into (2-186)–(2-191) yields

$$E_\theta^{1^F}$$

$$= -\frac{1}{\varepsilon_0 \varepsilon_\theta r \sin\theta} \frac{d\left[\sum_{mn}\varepsilon_0\varepsilon_\theta\left[\widehat{H}_n^{(2)}(\sqrt{\varepsilon_\theta}k_0 a) + R_n^{11^F}\widehat{H}_n^{(1)}(\sqrt{\varepsilon_\theta}k_0 a)\right]f(\theta,\phi)\right]}{d\phi} \tag{3-58}$$

$$H_\theta^{1^F}$$

$$= \frac{1}{j\omega\mu_0\varepsilon_0\varepsilon_\theta r} \frac{d^2\left[\sum_{mn}\varepsilon_0\varepsilon_\theta\left[\widehat{H}_n^{(2)}(\sqrt{\varepsilon_\theta}k_0 a) + R_n^{11^F}\widehat{H}_n^{(1)}(\sqrt{\varepsilon_\theta}k_0 a)\right]f(\theta,\phi)\right]}{drd\theta} \tag{3-59}$$

$$E_\theta^{2^F} = -\frac{1}{\varepsilon_0 r \sin\theta} \frac{d\left[\sum_{mn}\varepsilon_0 T_n^{12^F}\widehat{H}_n^{(2)}(k_0 r) f(\theta,\phi)\right]}{d\phi} \tag{3-60}$$

$$H_\theta^{2^F} = \frac{1}{j\omega\mu_0\varepsilon_0 r} \frac{d^2\left[\sum_{mn}\varepsilon_0 T_n^{12^F}\widehat{H}_n^{(2)}(k_0 r) f(\theta,\phi)\right]}{drd\theta} \tag{3-61}$$

Writing the boundary conditions at the interface of the uniaxial sphere yield

$$E_\theta^{1^F} = E_\theta^{2^F}|_{r=a} \tag{3-62}$$

$$H_\theta^{1^F} = H_\theta^{2^F}|_{r=a} \tag{3-63}$$

Substituting (3-58)–(3-61) into (3-62)–(3-63) give

$$\frac{d\left[\widehat{H}_n^{(2)}\left(\sqrt{\varepsilon_\theta}k_0 a\right) + R_n^{11^F}\widehat{H}_n^{(1)}\left(\sqrt{\varepsilon_\theta}k_0 a\right)f(\theta,\phi)\right]}{d\phi}$$

$$= \frac{d\left[T_n^{12^F}\widehat{H}_n^{(2)}(k_0 r)f(\theta,\phi)\right]}{d\phi}$$

(3-64)

$$\frac{d^2\left[\widehat{H}_n^{(2)}\left(\sqrt{\varepsilon_\theta}k_0 a\right) + R_n^{11^F}\widehat{H}_n^{(1)}\left(\sqrt{\varepsilon_\theta}k_0 a\right)f(\theta,\phi)\right]}{drd\theta}$$

$$= \frac{d^2\left[T_n^{12^F}\widehat{H}_n^{(2)}(k_0 r)f(\theta,\phi)\right]}{drd\theta}$$

(3-65)

Integrating (3-64) over ϕ and (3-65) over θ yield

$$\widehat{H}_n^{(2)}\left(\sqrt{\varepsilon_\theta}k_0 a\right) + R_n^{11^F}\widehat{H}_n^{(1)}\left(\sqrt{\varepsilon_\theta}k_0 a\right) = T_n^{12^F}\widehat{H}_n^{(2)}(k_0 r)$$

(3-66)

$$\sqrt{\varepsilon_\theta}\left[\widehat{H}_n^{(2)'}\left(\sqrt{\varepsilon_\theta}k_0 a\right) + R_n^{11^F}\widehat{H}_n^{(1)'}\left(\sqrt{\varepsilon_\theta}k_0 a\right)\right] = T_n^{12^F}\widehat{H}_n^{(2)'}(k_0 r)$$

(3-67)

where prime in (3-66) and (3-67) indicates the partial derivative with respect to the argument of Hankel functions. Multiplying (3-66) by $\widehat{H}_n^{(1)'}\left(\sqrt{\varepsilon_\theta}k_0 a\right)$ and (3-67) by $\widehat{H}_n^{(1)}\left(\sqrt{\varepsilon_\theta}k_0 a\right)$ give

$$\widehat{H}_n^{(1)'}\left(\sqrt{\varepsilon_\theta}k_0 a\right)\left[\widehat{H}_n^{(2)}\left(\sqrt{\varepsilon_\theta}k_0 a\right) + R_n^{11^F}\widehat{H}_n^{(1)}\left(\sqrt{\varepsilon_\theta}k_0 a\right)\right]$$

$$= T_n^{12^F}\widehat{H}_n^{(2)}(k_0 r)\widehat{H}_n^{(1)'}\left(\sqrt{\varepsilon_\theta}k_0 a\right)$$

(3-68)

$$\widehat{H}_n^{(1)}\left(\sqrt{\varepsilon_\theta}k_0 a\right)\left[\widehat{H}_n^{(2)'}\left(\sqrt{\varepsilon_\theta}k_0 a\right) + R_n^{11^F}\widehat{H}_n^{(1)'}\left(\sqrt{\varepsilon_\theta}k_0 a\right)\right]$$

$$= \frac{1}{\sqrt{\varepsilon_\theta}}T_n^{12^F}\widehat{H}_n^{(2)'}(k_0 r)\widehat{H}_n^{(1)}\left(\sqrt{\varepsilon_\theta}k_0 a\right)$$

(3-69)

Subtracting (3-68) from (3-69) yields

$$\widehat{H}_n^{(1)}\left(\sqrt{\varepsilon_\theta}k_0a\right)\widehat{H}_n^{(2)'}\left(\sqrt{\varepsilon_\theta}k_0a\right) - \widehat{H}_n^{(1)'}\left(\sqrt{\varepsilon_\theta}k_0a\right)\widehat{H}_n^{(2)}\left(\sqrt{\varepsilon_\theta}k_0a\right) =$$

$$T_n^{12^F}\left[\frac{1}{\sqrt{\varepsilon_\theta}}\widehat{H}_n^{(2)'}(k_0r)\widehat{H}_n^{(1)}\left(\sqrt{\varepsilon_\theta}k_0a\right) - \widehat{H}_n^{(2)}(k_0r)\widehat{H}_n^{(1)'}\left(\sqrt{\varepsilon_\theta}k_0a\right)\right] \tag{3-70}$$

Using Wronskian relationship, the left hand side of (3-70) is simplified to -$2j$ and we found the transmission coefficient of TE wave $T_n^{21^F}$ is

$$T_n^{12^F} = \frac{2j\sqrt{\varepsilon_\theta}}{-\widehat{H}_n^{(2)'}(k_0a)\,\widehat{H}_n^{(1)}\left(\sqrt{\varepsilon_\theta}k_0r\right) + \sqrt{\varepsilon_\theta}\,\widehat{H}_n^{(1)'}\left(\sqrt{\varepsilon_\theta}k_0r\right)\widehat{H}_n^{(2)}(k_0a)} \tag{3-71}$$

The Fresnel coefficients can be expressed as

$$T_n^{21\begin{Bmatrix}A\\F\end{Bmatrix}}$$

$$= \frac{2j\begin{Bmatrix}\sqrt{\varepsilon_\theta}\\1\end{Bmatrix}}{-\begin{Bmatrix}\sqrt{\varepsilon_\theta}\\1\end{Bmatrix}\widehat{H}_n^{(2)'}(k_0a)\begin{Bmatrix}\left(\widehat{H}_v^{(1)}\left(\sqrt{\varepsilon_\theta}k_0a\right)\right)\\\widehat{H}_n^{(1)}\left(\sqrt{\varepsilon_\theta}k_0a\right)\end{Bmatrix} + \begin{Bmatrix}\frac{1}{\sqrt{\varepsilon_\theta}}\end{Bmatrix}\begin{Bmatrix}\widehat{H}_v^{(1)'}\left(\sqrt{\varepsilon_\theta}k_0a\right)\\\widehat{H}_n^{(1)'}\left(\sqrt{\varepsilon_\theta}k_0a\right)\end{Bmatrix}\widehat{H}_n^{(2)}(k_0a)} \tag{3-72}$$

$$R_n^{22\begin{Bmatrix}A\\F\end{Bmatrix}}$$

$$= \frac{\begin{Bmatrix}\sqrt{\varepsilon_\theta}\\1\end{Bmatrix}\widehat{H}_n^{(1)'}(k_0a)\begin{Bmatrix}\widehat{H}_v^{(1)}\left(\sqrt{\varepsilon_\theta}k_0a\right)\\\widehat{H}_n^{(1)}\left(\sqrt{\varepsilon_\theta}k_0a\right)\end{Bmatrix} - \begin{Bmatrix}\frac{1}{\sqrt{\varepsilon_\theta}}\end{Bmatrix}\begin{Bmatrix}\widehat{H}_v^{(1)'}\left(\sqrt{\varepsilon_\theta}k_0a\right)\\\widehat{H}_n^{(1)'}\left(\sqrt{\varepsilon_\theta}k_0a\right)\end{Bmatrix}\widehat{H}_n^{(1)}(k_0a)}{-\begin{Bmatrix}\sqrt{\varepsilon_\theta}\\1\end{Bmatrix}\widehat{H}_n^{(2)'}(k_0a)\begin{Bmatrix}\left(\widehat{H}_v^{(1)}\left(\sqrt{\varepsilon_\theta}k_0a\right)\right)\\\widehat{H}_n^{(1)}\left(\sqrt{\varepsilon_\theta}k_0a\right)\end{Bmatrix} + \begin{Bmatrix}\frac{1}{\sqrt{\varepsilon_\theta}}\end{Bmatrix}\begin{Bmatrix}\widehat{H}_v^{(1)'}\left(\sqrt{\varepsilon_\theta}k_0a\right)\\\widehat{H}_n^{(1)'}\left(\sqrt{\varepsilon_\theta}k_0a\right)\end{Bmatrix}\widehat{H}_n^{(2)}(k_0a)} \tag{3-73}$$

$$T_n^{12\begin{Bmatrix}A\\F\end{Bmatrix}}$$

$$= \frac{2j\begin{Bmatrix}1\\\sqrt{\varepsilon_\theta}\end{Bmatrix}}{-\begin{Bmatrix}\sqrt{\varepsilon_\theta}\\1\end{Bmatrix}\widehat{H}_n^{(2)'}(k_0a)\begin{Bmatrix}\left(\widehat{H}_v^{(1)}\left(\sqrt{\varepsilon_\theta}k_0a\right)\right)\\\widehat{H}_n^{(1)}\left(\sqrt{\varepsilon_\theta}k_0a\right)\end{Bmatrix} + \begin{Bmatrix}\frac{1}{\sqrt{\varepsilon_\theta}}\end{Bmatrix}\begin{Bmatrix}\widehat{H}_v^{(1)'}\left(\sqrt{\varepsilon_\theta}k_0a\right)\\\widehat{H}_n^{(1)'}\left(\sqrt{\varepsilon_\theta}k_0a\right)\end{Bmatrix}\widehat{H}_n^{(2)}(k_0a)} \tag{3-74}$$

63

$$R_n^{11\{A\atop F\}}$$

$$= \frac{\left\{{\sqrt{\varepsilon_\theta}\atop 1}\right\}\widehat{H}_n^{(2)'}(k_0a)\left\{{\widehat{H}_v^{(2)}\left(\sqrt{\varepsilon_\theta}k_0a\right)}\over{\widehat{H}_n^{(2)}\left(\sqrt{\varepsilon_\theta}k_0a\right)}\right\} - \left\{{1\atop \sqrt{\varepsilon_\theta}}\right\}\left\{{\widehat{H}_v^{(2)'}\left(\sqrt{\varepsilon_\theta}k_0a\right)}\over{\widehat{H}_n^{(2)'}\left(\sqrt{\varepsilon_\theta}k_0a\right)}\right\}\widehat{H}_n^{(2)}(k_0a)}{-\left\{{\sqrt{\varepsilon_\theta}\atop 1}\right\}\widehat{H}_n^{(2)'}(k_0a)\left\{{(\widehat{H}_v^{(1)}\left(\sqrt{\varepsilon_\theta}k_0a\right)}\over{\widehat{H}_n^{(1)}\left(\sqrt{\varepsilon_\theta}k_0a\right)}\right\} + \left\{{1\atop \sqrt{\varepsilon_\theta}}\right\}\left\{{\widehat{H}_v^{(1)'}\left(\sqrt{\varepsilon_\theta}k_0a\right)}\over{\widehat{H}_n^{(1)'}\left(\sqrt{\varepsilon_\theta}k_0a\right)}\right\}\widehat{H}_n^{(2)}(k_0a)} \quad (3\text{-}75)$$

To show the equality of Debye and Mie series, we first found the quantity $\left[(1 - Rn22AF)(1 - Rn11AF) - Tn21AFTn12AF\right.$ and then divide it to $1 - Rn11AF$ as follows

$$\left[(1 - R_n^{22\{A\atop F\}})(1 - R_n^{11\{A\atop F\}}) - T_n^{21\{A\atop F\}}T_n^{12\{A\atop F\}}\right]$$

$$= 1 - (R_n^{22} + R_n^{11}) + R_n^{22}R_n^{11\{A\atop F\}} - T_n^{21\{A\atop F\}}T_n^{12} \quad (3\text{-}76)$$

The term $R_n^{22\{A\atop F\}}R_n^{11\{A\atop F\}} - T_n^{21\{A\atop F\}}T_n^{12\{A\atop F\}}$ is written as

$$R_n^{22\{A\atop F\}}R_n^{11\{A\atop F\}} = \frac{\alpha^2\widehat{H}_n^{(1)'}(k_0a)\widehat{H}_n^{(2)'}(k_0a)\left\{{\widehat{H}_v^{(1)}\left(\sqrt{\varepsilon_\theta}k_0a\right)\widehat{H}_v^{(2)}\left(\sqrt{\varepsilon_\theta}k_0a\right)}\over{\widehat{H}_n^{(1)}\left(\sqrt{\varepsilon_\theta}k_0a\right)\widehat{H}_n^{(2)}\left(\sqrt{\varepsilon_\theta}k_0a\right)}\right\}}{D_{\{A\atop F\}}^2}$$

$$- \frac{\alpha\beta\widehat{H}_n^{(1)'}(k_0a)\widehat{H}_n^{(2)}(k_0a)\left\{{\widehat{H}_v^{(1)}\left(\sqrt{\varepsilon_\theta}k_0a\right)\widehat{H}_v^{(2)'}\left(\sqrt{\varepsilon_\theta}k_0a\right)}\over{\widehat{H}_n^{(1)}\left(\sqrt{\varepsilon_\theta}k_0a\right)\widehat{H}_n^{(2)'}\left(\sqrt{\varepsilon_\theta}k_0a\right)}\right\}}{D_{\{A\atop F\}}^2} \quad (3\text{-}77)$$

$$- \frac{\alpha\beta\widehat{H}_n^{(1)}(k_0a)\widehat{H}_n^{(2)'}(k_0a)\left\{{\widehat{H}_v^{1'}\left(\sqrt{\varepsilon_\theta}k_0a\right)\widehat{H}_v^{2}\left(\sqrt{\varepsilon_\theta}k_0a\right)}\over{\widehat{H}_n^{1'}\left(\sqrt{\varepsilon_\theta}k_0a\right)\widehat{H}_n^{2}\left(\sqrt{\varepsilon_\theta}k_0a\right)}\right\}}{D_{\{A\atop F\}}^2}$$

$$+ \frac{\beta^2 \hat{H}_n^{(1)}(k_0 a) \hat{H}_n^{(2)}(k_0 a) \begin{Bmatrix} \hat{H}_v^{(1)'}(\widehat{\sqrt{\varepsilon_\theta}}k_0 a) H_v^{(2)'}(\sqrt{\varepsilon_\theta}k_0 a) \\ \hat{H}_n^{(1)'}(\sqrt{\varepsilon_\theta}k_0 a) \hat{H}_n^{(2)'}(\sqrt{\varepsilon_\theta}k_0 a) \end{Bmatrix}}{D_{\{^A_F\}}^2}$$

$$T_n^{21\{^A_F\}} T_n^{12\{^A_F\}} = \frac{\alpha \left[\hat{H}_n^2(k_0 a) \hat{H}_n^{1'}(k_0 r) - \hat{H}_n^{2'}(k_0 a) \hat{H}_n^1(k_0 r) \right]}{D_{\{^A_F\}}^2} \tag{3-78}$$

$$\times \frac{\beta \left[\begin{Bmatrix} \hat{H}_v^{(2)}(\sqrt{\varepsilon_\theta}k_0 a) \hat{H}_v^{(1)'}(\sqrt{\varepsilon_\theta}k_0 a) \\ \hat{H}_n^{(2)}(\sqrt{\varepsilon_\theta}k_0 a) \hat{H}_n^{(1)'}(\sqrt{\varepsilon_\theta}k_0 a) \end{Bmatrix} - \begin{Bmatrix} \hat{H}_v^{(2)'}(\sqrt{\varepsilon_\theta}k_0 a) \hat{H}_v^{(1)}(\sqrt{\varepsilon_\theta}k_0 a) \\ \hat{H}_n^{(2)'}(\sqrt{\varepsilon_\theta}k_0 a) \hat{H}_n^{(1)}(\sqrt{\varepsilon_\theta}k_0 a) \end{Bmatrix} \right]}{D_{\{^A_F\}}^2}$$

where

$$\alpha = \begin{Bmatrix} \sqrt{\varepsilon_\theta} \\ 1 \end{Bmatrix} \tag{3-79}$$

$$\beta = \begin{Bmatrix} 1 \\ \sqrt{\varepsilon_\theta} \end{Bmatrix} \tag{3-80}$$

and

$$D_{\{^A_F\}} = -\begin{Bmatrix} \sqrt{\varepsilon_\theta} \\ 1 \end{Bmatrix} \hat{H}_n^{(2)'}(k_0 a) \begin{Bmatrix} (\hat{H}_v^{(1)}(\sqrt{\varepsilon_\theta}k_0 a) \\ \hat{H}_n^{(1)}(\sqrt{\varepsilon_\theta}k_0 a) \end{Bmatrix}$$

$$+ \begin{Bmatrix} 1 \\ \sqrt{\varepsilon_\theta} \end{Bmatrix} \begin{Bmatrix} \hat{H}_v^{(1)'}(\sqrt{\varepsilon_\theta}k_0 a) \\ \hat{H}_n^{(1)'}(\sqrt{\varepsilon_\theta}k_0 a) \end{Bmatrix} \hat{H}_n^{(2)}(k_0 a) \tag{3-81}$$

(3-78) can be simplified to

$$T_n^{21\{^A_F\}} T_n^{12\{^A_F\}} = \frac{\alpha\beta \widehat{H}_n^{(2)}(k_0 a)\widehat{H}_n^{(1)'}(k_0 r)\left\{ \begin{matrix} \widehat{H}_v^{(2)}(\sqrt{\varepsilon_\theta}k_0 a)\widehat{H}_v^{(1)'}(\sqrt{\varepsilon_\theta}k_0 a) \\ \widehat{H}_n^{(2)}(\sqrt{\varepsilon_\theta}k_0 a)\widehat{H}_n^{(1)'}(\sqrt{\varepsilon_\theta}k_0 a) \end{matrix} \right\}}{D_{\{^A_F\}}^2}$$

$$- \frac{\alpha\beta \widehat{H}_n^{(2)}(k_0 a)\widehat{H}_n^{(1)'}(k_0 r)\left\{ \begin{matrix} \widehat{H}_v^{(2)'}(\sqrt{\varepsilon_\theta}k_0 a)\widehat{H}_v^{(1)}(\sqrt{\varepsilon_\theta}k_0 a) \\ \widehat{H}_n^{(2)'}(\sqrt{\varepsilon_\theta}k_0 a)\widehat{H}_n^{(1)}(\sqrt{\varepsilon_\theta}k_0 a) \end{matrix} \right\}}{D_{\{^A_F\}}^2}$$

$$- \frac{\alpha\beta \widehat{H}_n^{(2)'}(k_0 a)\widehat{H}_n^{(1)}(k_0 r)\left\{ \begin{matrix} \widehat{H}_v^{(2)}(\sqrt{\varepsilon_\theta}k_0 a)\widehat{H}_v^{(1)'}(\sqrt{\varepsilon_\theta}k_0 a) \\ \widehat{H}_n^{(2)}(\sqrt{\varepsilon_\theta}k_0 a)\widehat{H}_n^{(1)'}(\sqrt{\varepsilon_\theta}k_0 a) \end{matrix} \right\}}{D_{\{^A_F\}}^2} \qquad (3\text{-}82)$$

$$+ \frac{\alpha\beta \widehat{H}_n^{(2)'}(k_0 a)\widehat{H}_n^{(1)}(k_0 r)\left\{ \begin{matrix} \widehat{H}_v^{(2)'}(\sqrt{\varepsilon_\theta}k_0 a)\widehat{H}_v^{(1)}(\sqrt{\varepsilon_\theta}k_0 a) \\ \widehat{H}_n^{(2)'}(\sqrt{\varepsilon_\theta}k_0 a)\widehat{H}_n^{(1)}(\sqrt{\varepsilon_\theta}k_0 a) \end{matrix} \right\}}{D_{\{^A_F\}}^2}$$

Subtracting (3-82) from (3-77) yields

$$R_n^{22\{A\atop F\}} R_n^{11\{A\atop F\}} - T_n^{21\{A\atop F\}} T_n^{12\{A\atop F\}}$$

$$= \frac{\alpha^2 \widehat{H}_n^{(1)'}(k_0 a) \widehat{H}_n^{(2)'}(k_0 a) \begin{Bmatrix} \widehat{H}_v^{(1)}\left(\sqrt{\varepsilon_\theta} k_0 a\right) \widehat{H}_v^{(2)}\left(\sqrt{\varepsilon_\theta} k_0 a\right) \\ \widehat{H}_n^{(1)}\left(\sqrt{\varepsilon_\theta} k_0 a\right) \widehat{H}_n^{(2)}\left(\sqrt{\varepsilon_\theta} k_0 a\right) \end{Bmatrix}}{D_{\{A\atop F\}}^2}$$

$$- \frac{\alpha\beta \widehat{H}_n^{(2)}(k_0 a) \widehat{H}_n^{(1)'}(k_0 r) \begin{Bmatrix} \widehat{H}_v^{(2)}\left(\sqrt{\varepsilon_\theta} k_0 a\right) \widehat{H}_v^{(1)'}\left(\sqrt{\varepsilon_\theta} k_0 a\right) \\ \widehat{H}_n^{(2)}\left(\sqrt{\varepsilon_\theta} k_0 a\right) \widehat{H}_n^{(1)'}\left(\sqrt{\varepsilon_\theta} k_0 a\right) \end{Bmatrix}}{D_{\{A\atop F\}}^2}$$

$$- \frac{\alpha\beta \widehat{H}_n^{(2)'}(k_0 a) \widehat{H}_n^{(1)}(k_0 r) \begin{Bmatrix} \widehat{H}_v^{(2)'}\left(\sqrt{\varepsilon_\theta} k_0 a\right) \widehat{H}_v^{(1)}\left(\sqrt{\varepsilon_\theta} k_0 a\right) \\ \widehat{H}_n^{(2)'}\left(\sqrt{\varepsilon_\theta} k_0 a\right) \widehat{H}_n^{(1)}\left(\sqrt{\varepsilon_\theta} k_0 a\right) \end{Bmatrix}}{D_{\{A\atop F\}}^2} \qquad (3\text{-}83)$$

$$+ \frac{\beta^2 \widehat{H}_n^{(1)}(k_0 a) \widehat{H}_n^{(2)}(k_0 a) \begin{Bmatrix} \widehat{H}_v^{(1)'}\widehat{\left(\sqrt{\varepsilon_\theta} k_0 a\right)} H_v^{(2)'}\left(\sqrt{\varepsilon_\theta} k_0 a\right) \\ \widehat{H}_n^{(1)'}\left(\sqrt{\varepsilon_\theta} k_0 a\right) \widehat{H}_n^{(2)'}\left(\sqrt{\varepsilon_\theta} k_0 a\right) \end{Bmatrix}}{D_{\{A\atop F\}}^2}$$

(3-83) is simplified to

$$R_n^{22\{A\atop F\}} R_n^{11\{A\atop F\}} - T_n^{21\{A\atop F\}} T_n^{12\{A\atop F\}}$$

$$= \frac{\left[D_{\{A\atop F\}}\right]\left[-\alpha \widehat{H}_n^{(1)'}(k_0 a)\begin{Bmatrix} \widehat{H}_v^{(2)}\left(\sqrt{\varepsilon_\theta} k_0 a\right) \\ \widehat{H}_n^{(2)}\left(\sqrt{\varepsilon_\theta} k_0 a\right) \end{Bmatrix} + \beta \widehat{H}_n^{(1)}(k_0 a)\begin{Bmatrix} \widehat{H}_v^{(2)'}\left(\sqrt{\varepsilon_\theta} k_0 a\right) \\ \widehat{H}_n^{(2)'}\left(\sqrt{\varepsilon_\theta} k_0 a\right) \end{Bmatrix}\right]}{D_{\{A\atop F\}}^2} \quad (3\text{-}84)$$

which can also be expressed as

67

$$R_n^{22\{^{\{A\}}_{\{F\}}\}} R_n^{11\{^{\{A\}}_{\{F\}}\}} - T_n^{21\{^{\{A\}}_{\{F\}}\}} T_n^{12\{^{\{A\}}_{\{F\}}\}}$$

$$= \frac{-\alpha \widehat{H}_n^{(1)'}(k_0 a)\left\{\dfrac{\widehat{H}_v^{(2)}\left(\sqrt{\varepsilon_\theta}k_0 a\right)}{\widehat{H}_n^{(2)}\left(\sqrt{\varepsilon_\theta}k_0 a\right)}\right\} + \beta \widehat{H}_n^{(1)}(k_0 a)\left\{\dfrac{\widehat{H}_v^{(2)'}\left(\sqrt{\varepsilon_\theta}k_0 a\right)}{\widehat{H}_n^{(2)'}\left(\sqrt{\varepsilon_\theta}k_0 a\right)}\right\}}{D_{\{^{\{A\}}_{\{F\}}\}}} \qquad (3\text{-}85)$$

The term $1 - \left(R_n^{22\{^{\{A\}}_{\{F\}}\}} + R_n^{11\{^{\{A\}}_{\{F\}}\}} \right)$ is given by

$$1 - \left(R_n^{22\{^{\{A\}}_{\{F\}}\}} + R_n^{11\{^{\{A\}}_{\{F\}}\}} \right)$$

$$= \frac{D - \alpha\left[\widehat{H}_n^{(1)'}(k_0 a)\left\{\dfrac{\widehat{H}_v^{(1)}\left(\sqrt{\varepsilon_\theta}k_0 a\right)}{\widehat{H}_n^{(1)}\left(\sqrt{\varepsilon_\theta}k_0 a\right)}\right\} + \widehat{H}_n^{(2)'}(k_0 a)\left\{\dfrac{\widehat{H}_v^{(2)}\left(\sqrt{\varepsilon_\theta}k_0 a\right)}{\widehat{H}_n^{(2)}\left(\sqrt{\varepsilon_\theta}k_0 a\right)}\right\}\right]}{D_{\{^{\{A\}}_{\{F\}}\}}}$$

$$- \frac{-\beta\left[\widehat{H}_n^{(1)}(k_0 a)\left\{\dfrac{\widehat{H}_v^{(1)'}\left(\sqrt{\varepsilon_\theta}k_0 a\right)}{\widehat{H}_n^{(1)'}\left(\sqrt{\varepsilon_\theta}k_0 a\right)}\right\} + \widehat{H}_n^{(2)}(k_0 a)\left\{\dfrac{\widehat{H}_v^{(2)'}\left(\sqrt{\varepsilon_\theta}k_0 a\right)}{\widehat{H}_n^{(2)'}\left(\sqrt{\varepsilon_\theta}k_0 a\right)}\right\}\right]}{D_{\{^{\{A\}}_{\{F\}}\}}} \qquad (3\text{-}86)$$

Adding (3-85) and (3-86) yields

$$1 - \left(R_n^{22\{^{\{A\}}_{\{F\}}\}} + R_n^{11\{^{\{A\}}_{\{F\}}\}} \right) + R_n^{22\{^{\{A\}}_{\{F\}}\}} R_n^{11\{^{\{A\}}_{\{F\}}\}} - T_n^{21\{^{\{A\}}_{\{F\}}\}} T_n^{12\{^{\{A\}}_{\{F\}}\}} = \qquad (3\text{-}87)$$

$$
\left[-\alpha \left[\widehat{H}_n^{(1)'}(k_0 a) \left\{ \frac{\widehat{H}_v^{(1)}(\sqrt{\varepsilon_\theta} k_0 a) + \widehat{H}_v^{(2)}(\sqrt{\varepsilon_\theta} k_0 a)}{\widehat{H}_n^{(1)}(\sqrt{\varepsilon_\theta} k_0 a) + \widehat{H}_n^{(2)}(\sqrt{\varepsilon_\theta} k_0 a)} \right\} \right. \right.
$$

$$
\left. \left. + \widehat{H}_n^{(2)'}(k_0 a) \left\{ \frac{\widehat{H}_v^{(1)}(\sqrt{\varepsilon_\theta} k_0 a) + \widehat{H}_v^{(2)}(\sqrt{\varepsilon_\theta} k_0 a)}{\widehat{H}_n^{(1)}(\sqrt{\varepsilon_\theta} k_0 a) + \widehat{H}_n^{(2)}(\sqrt{\varepsilon_\theta} k_0 a)} \right\} \right] \Big/ D_{\{F\}}^{\{A\}} \right]
$$

$$
+ \beta \left[\widehat{H}_n^{(1)}(k_0 a) \left\{ \frac{\widehat{H}_v^{(1)'}(\sqrt{\varepsilon_\theta} k_0 a) + \widehat{H}_v^{(2)'}(\sqrt{\varepsilon_\theta} k_0 a)}{\widehat{H}_n^{(1)'}(\sqrt{\varepsilon_\theta} k_0 a) + \widehat{H}_n^{(2)'}(\sqrt{\varepsilon_\theta} k_0 a)} \right\} \right.
$$

$$
\left. + \widehat{H}_n^{(2)}(k_0 a) \left\{ \frac{\widehat{H}_v^{(1)'}(\sqrt{\varepsilon_\theta} k_0 a) + \widehat{H}_v^{(2)'}(\sqrt{\varepsilon_\theta} k_0 a)}{\widehat{H}_n^{(1)'}(\sqrt{\varepsilon_\theta} k_0 a) + \widehat{H}_n^{(2)'}(\sqrt{\varepsilon_\theta} k_0 a)} \right\} \right] \Big/ D_{\{F\}}^{\{A\}}
$$

which is simplified to

$$
1 - \left(R_n^{22\{A\}}_{\{F\}} + R_n^{11\{A\}}_{\{F\}} \right) + R_n^{22\{A\}}_{\{F\}} R_n^{11\{A\}}_{\{F\}} - T_n^{21\{A\}}_{\{F\}} T_n^{12\{A\}}_{\{F\}}
$$

$$
= \frac{\left[-4\alpha \widehat{J}_n'(k_0 a) \left\{ \frac{\widehat{J}_v(\sqrt{\varepsilon_\theta} k_0 a)}{\widehat{J}_n(\sqrt{\varepsilon_\theta} k_0 a)} \right\} + 4\beta \widehat{J}_n(k_0 a) \left\{ \frac{\widehat{J}_v'(\sqrt{\varepsilon_\theta} k_0 a)}{\widehat{J}_n'(\sqrt{\varepsilon_\theta} k_0 a)} \right\} \right]}{D_{\{F\}}^{\{A\}}} \tag{3-88}
$$

The term $1 - R_n^{11\{A\}}_{\{F\}}$ is expressed as

$$
1 - R_n^{11\{A\}}_{\{F\}}
$$

$$
= \frac{-2\alpha \widehat{H}_n^{(2)'}(k_0 a) \left\{ \frac{\widehat{J}_v(\sqrt{\varepsilon_\theta} k_0 a)}{\widehat{J}_n(\sqrt{\varepsilon_\theta} k_0 a)} \right\} + 2\beta \widehat{H}_n^{(2)}(k_0 a) \left\{ \frac{\widehat{J}_v'(\sqrt{\varepsilon_\theta} k_0 a)}{\widehat{J}_n'(\sqrt{\varepsilon_\theta} k_0 a)} \right\}}{D_{\{F\}}^{\{A\}}} \tag{3-89}
$$

Dividing (3-88) over (3-89) yields

$$\begin{Bmatrix} b_n \\ c_n \end{Bmatrix}$$

$$= \frac{-\begin{Bmatrix} \sqrt{\varepsilon_\theta} \\ 1 \end{Bmatrix}\hat{J}'_n(k_0 a)\begin{Bmatrix} \hat{J}_\nu(\sqrt{\varepsilon_\theta}k_0 a) \\ \hat{J}_n(\sqrt{\varepsilon_\theta}k_0 a) \end{Bmatrix} + \begin{Bmatrix} \frac{1}{\sqrt{\varepsilon_\theta}} \end{Bmatrix}\begin{Bmatrix} \hat{J}_\nu(\sqrt{\varepsilon_\theta}k_0 a) \\ \hat{J}_n(\sqrt{\varepsilon_\theta}k_0 a) \end{Bmatrix}' \hat{J}_n(k_0 a)}{-\begin{Bmatrix} \sqrt{\varepsilon_\theta} \\ 1 \end{Bmatrix}\hat{H}^{(2)'}_n(k_0 a)\begin{Bmatrix} \hat{J}_\nu(\sqrt{\varepsilon_\theta}k_0 a) \\ \hat{J}_n(\sqrt{\varepsilon_\theta}k_0 a) \end{Bmatrix} + \begin{Bmatrix} \frac{1}{\sqrt{\varepsilon_\theta}} \end{Bmatrix}\begin{Bmatrix} \hat{J}_\nu(\sqrt{\varepsilon_\theta}k_0 a) \\ \hat{J}_n(\sqrt{\varepsilon_\theta}k_0 a) \end{Bmatrix}' \hat{H}^{(2)}_n(k_0 a)}$$

(3-90)

$$= \frac{1}{2}\left[1 - R_n^{22\{A\}}_{\{F\}} - \frac{T_n^{21\{A\}}_{\{F\}} T_n^{12\{A\}}_{\{F\}}}{1 - R_n^{11\{A\}}_{\{F\}}} \right]$$

$$= \frac{1}{2}\left[1 - R_n^{22\{A\}}_{\{F\}} - \sum_{P=1}^{\infty} T_n^{21\{A\}}_{\{F\}} \left(R_n^{11\{A\}}_{\{F\}} \right)^{P-1} T_n^{12\{A\}}_{\{F\}} \right]$$

where b_n and c_n are recognized as the well-known generalized Mie series coefficients and are identical to (2-196) and (2-197) respectively. Equation (3-90) not only represents the equality of Mie and Debye series but also indicates that the Debye series is not an approximate solution and involves a summation of infinite reflected, refracted and diffracted waves that are reflected p-1 times in the sphere. The bistatic RCS of the uniaxial dielectric sphere characterized by $\varepsilon_r = 2$, $\varepsilon_\theta = 2.5$ evaluated using Lorenz-Mie theory and the summation of the first eight Debye terms is plotted in Fig. 3.2. The results represent a satisfactory agreement between two methods and it can be shown that by increasing the number of terms in the Debye series, they will be eventually identical.

In Fig. 3.3, one can observe that in spite of weak uniaxiality, a significant impact on bistatic RCS is achieved and depending on the type, positive/negative, and the angle of observation, the scattering intensity is considerably different when compare to the isotropic case. Looking at each individual Debye term in Fig. 3.4 provides a

physical insight as to which transmitted, reflected, or refracted rays most greatly affect the bistatic RCS of the uniaxial dielectric sphere.
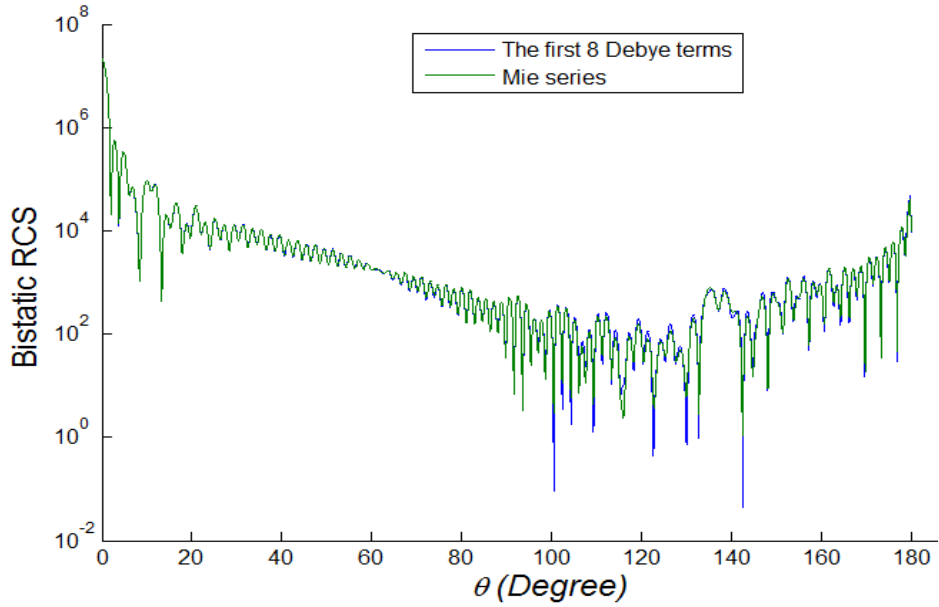

Fig. 3. 2. The bistatic RCS of a uniaxial dielectric sphere calculated using Mie and Debye series, $k_0 a = 100$

A comparison of P-rays, Fig. 3.4, for positive uniaxial and isotropic dielectric spheres reveals that the uniaxiality has minimum impact on p=0 rays, and the bistatic RCS of the both cases are almost identical. Note that p=0 ray, originates from geometrical optics reflection and therefore never penetrate into the sphere.

For the p=1 ray, the intensity is significantly suppressed for the angles smaller than 40°. For the p=2 ray, a considerable improvement is observed on backscattering region and the intensity is roughly strengthened up to 10 times compared to the isotropic sphere. Therefore, by investigating each individual term of Debye series, one can determine the effect of uniaxiality on p-rays and consequently, the observed bistatic RCS differences in Fig. 3.3 can be explained.
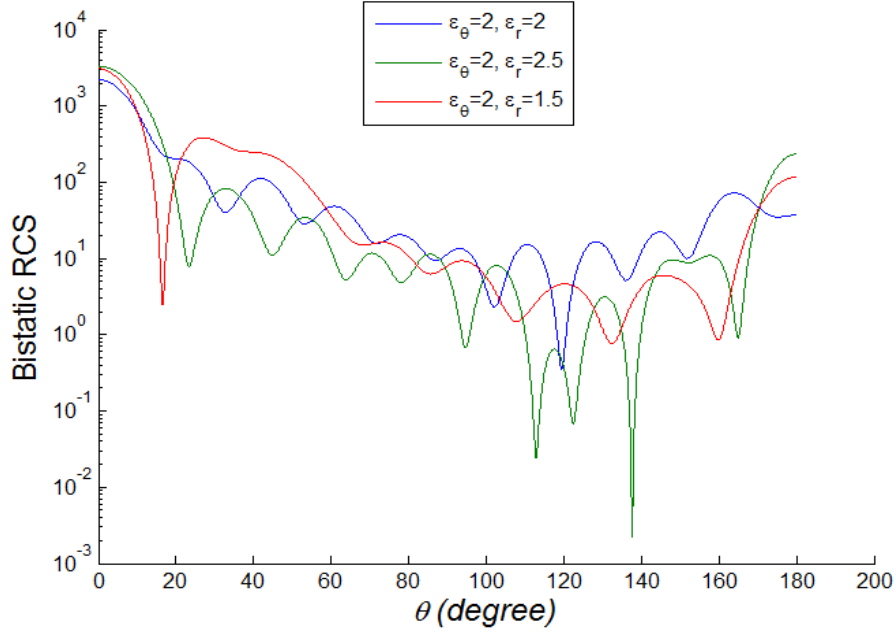
71

Fig. 3. 3. The comparison between bistatic RCS of positive, negative uniaxial and isotropic dielectric spheres, $k_0 a = 10$

The logarithmic polar pattern of the Debye series for the positive uniaxial dielectric sphere is plotted in Fig. 3.5. The results indicate that for $k_0 a = 100$ the beam width corresponding to the p=0 lobe is about 1° and after the p=0 return, p=1 and 4 rays are the next dominant rays in the forward scattering direction respectively. On the other hand, p=2, 6 and 0 rays have the maximum intensity on backscattering direction. Knowing which terms contribute to the back and forward scattering directions, not only provides a physical interpretation of the problem, but also, could be useful in the field of cloaking in which reducing the RCS intensity of the objects became a challenge in recent years.
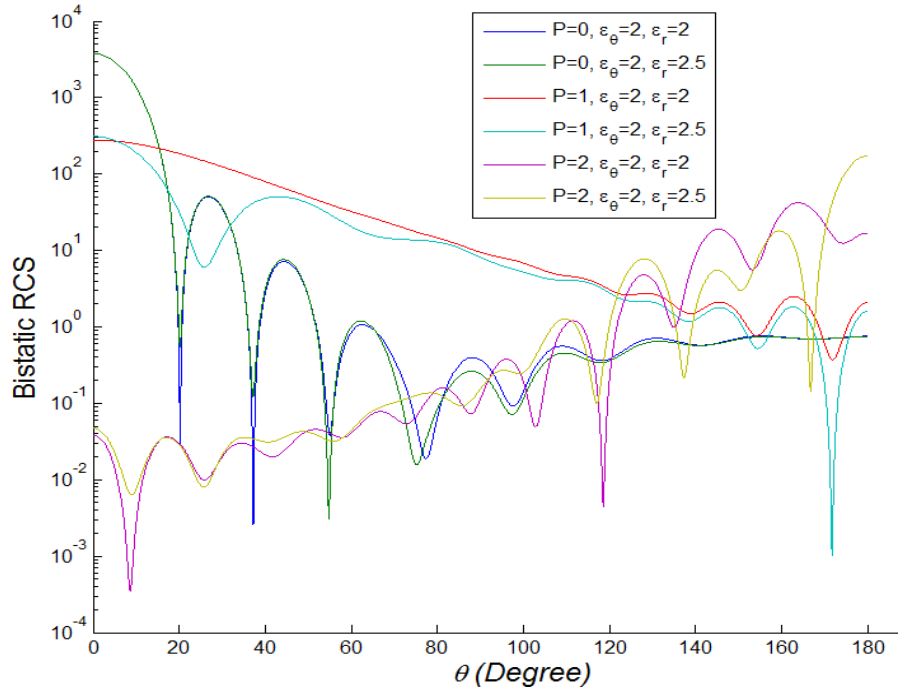
Fig. 3. 4. The comparison of the first three terms of Debye series for positive uniaxial and isotropic dielectric spheres, $k_0 a = 10$
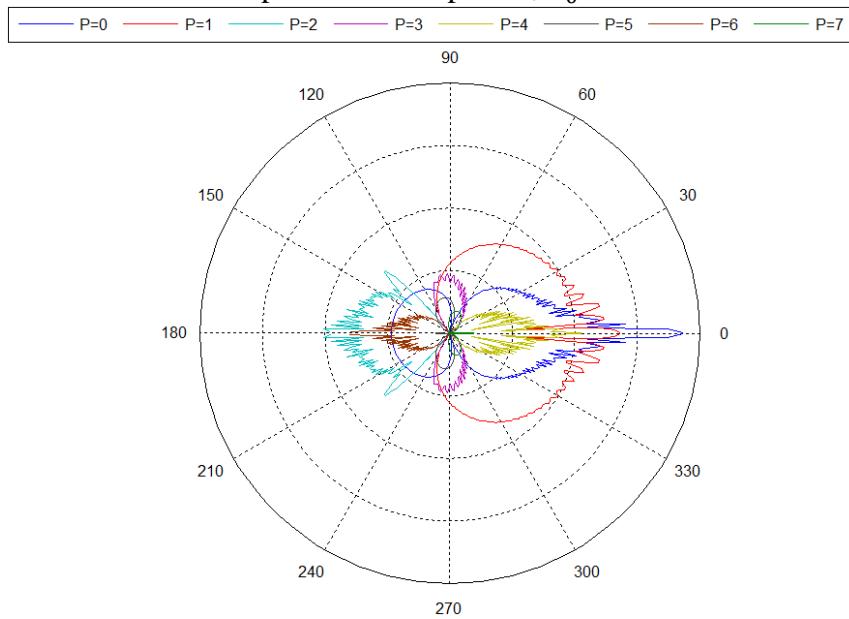

Fig. 3. 5. The logarithmic pattern of the first 8 terms of Debye series for positive uniaxial dielectric sphere, $k_0 a = 100$

3.3 Conclusion

Lorenz-Mie theory offers a general solution for the scattering by uniaxial dielectric spheres, but fails to deliver a physical description of the monostatic/bistatic RCS differences of the problem when compared to the isotropic sphere. To address the problem, this chapter develops the generalized Debye series for a uniaxial dielectric sphere. To validate our calculations, we examined the bistatic RCS of uniaxial sphere using Lorenz-Mie theory and compared the result with the summation of the first eight Debye terms with excellent agreement. By investigating the Debye series of a positive uniaxial dielectric sphere, not only the causes of bistatic RCS differences of the uniaxial and isotropic spheres are identified, but the dominant rays of the back and forward scattering directions are recognized. The results might be of value in the field of cloaking of targets in which uniaxial materials are used to degrade the scattering from objects.

Chapter 4   High frequency scattering from a radially uniaxial dielectric sphere

The high frequency backscattering by a large uniaxial dielectric sphere is presented in this chapter. The term high frequency implies $Ka \gg 1$ where K and a are the propagation constant and radius of the sphere respectively. Using the modified Watson transformation we transform the slowly convergent generalized Mie series summation for a uniaxial dielectric sphere into a rapidly convergent contour integral. The Mie series coefficients are replaced by their equivalent Debye series formulations derived in the preceding chapter. With the aid of Debye's asymptotic formula for the alternative Hankel function, the contour integral is simplified and then computed using the saddle point method. An expression for the high frequency backscattered field is proposed and the monostatic radar cross section (RCS) of a large uniaxial dielectric sphere is computed. The high frequency backscattering of various lossy uniaxial spheres is investigated and the results are then compared with those computed using Lorentz-Mie theory.

4.1   Introduction

Many materials exhibit anisotropic characteristics. Crystals, e.g., calcite, sapphire, and stacked multilayer dielectric materials are among some of the materials that are naturally and artificially anisotropic [25]. In recent years, the analysis and characterization of anisotropic materials has been a great subject due to the recent advances in material science and technology and their applications in electromagnetic scattering and microwave engineering [22]. Among those investigations, the scattering from anisotropic dielectric or coated dielectric sphere has attracted significant attention due to their

cloaking features [29], [27] and [30]. The exact solution of the backscattered field by a radially uniaxial dielectric sphere was first studied by Wong and Chen in [2]. After modifying spherical potential wave functions in a radially uniaxial medium, they derived the generalized Mie coefficient by applying the boundary conditions at the air-uniaxial interface. However, the Mie solution for the isotropic dielectric or coated dielectric sphere suffers from slow convergence at high frequencies as reported by many researchers [31], [32]. To overcome this difficulty, the Watson method [33] was applied to transform the slowly converging Mie series summation into a rapidly converging contour integral and high frequency approximation was derived. High frequency solution of EM backscattering is of great interest in time domain scattering calculation where it is used to approximate the improper Bromwich integral, allowing a significant reduction of the computation time [10].

High frequency scattering of perfectly conducting, dielectric, and coated dielectric spheres is well understood. Electromagnetic scattering by a large perfectly conducting sphere was first studied by Senior and Goodrich [34]. Inada and Plonus [11] found the geometric optics and diffracted field contributions from the isotropic dielectric sphere by applying the Debye series and Watson transformation methods to the Mie series solution. Weston and Hemenger [35] obtained the asymptotic solution for the backscattered field from the coated dielectric sphere by approximating the dielectric portion with an equivalent impedance boundary. A high-frequency analysis of EM scattering from a conducting sphere coated with a composite material was derived by Kim using the Debye series and Watson transformation methods [36].

Although the majority of dielectric materials are anisotropic, to the best of author's

knowledge the asymptotic solution for the backscattered field from a radially uniaxial dielectric sphere has not yet been investigated. In Section 4.2, the generalized Mie series is briefly studied and the modified Watson transformation is used to transform the slowly converging Mie series summation into a rapidly converging contour integral. In Section 4.3, the generalized Debye series for the uniaxial dielectric sphere is introduced and the Mie series coefficients are replaced by their equivalent Debye series formulations. Applying Debye's asymptotic formula for the alternative spherical Hankel function, the Debye series reduces to a form that can be computed using the saddle point method. An approximate formula for high frequency backscattering from the uniaxial dielectric sphere is proposed in Section 4.4 and the results are compared with those computed using the Lorentz-Mie theory.

4.2 Mie series and Watson transformation

Consider a radially uniaxial dielectric sphere with radius a immersed in an incident x-polarized time harmonic plane wave as shown in Fig. 4.1, traveling in the z-direction where the incident wave is defined by

$$E_i = \hat{a}_x e^{-jk_0 z} = \hat{a}_x e^{-jk_0 r \cos\theta}. \tag{4-1}$$

The sphere is comprised of permeability μ_0, and permittivity tensor of the form

$$\bar{\bar{\varepsilon}} = \varepsilon_0 \begin{bmatrix} \epsilon_r & 0 & 0 \\ 0 & \epsilon_\theta & 0 \\ 0 & 0 & \epsilon_\theta \end{bmatrix} \tag{4-2}$$

where ε_0 is the permittivity in air and ε_r and ε_θ are the electric relative permittivities parallel and perpendicular to the optic axis respectively.

77
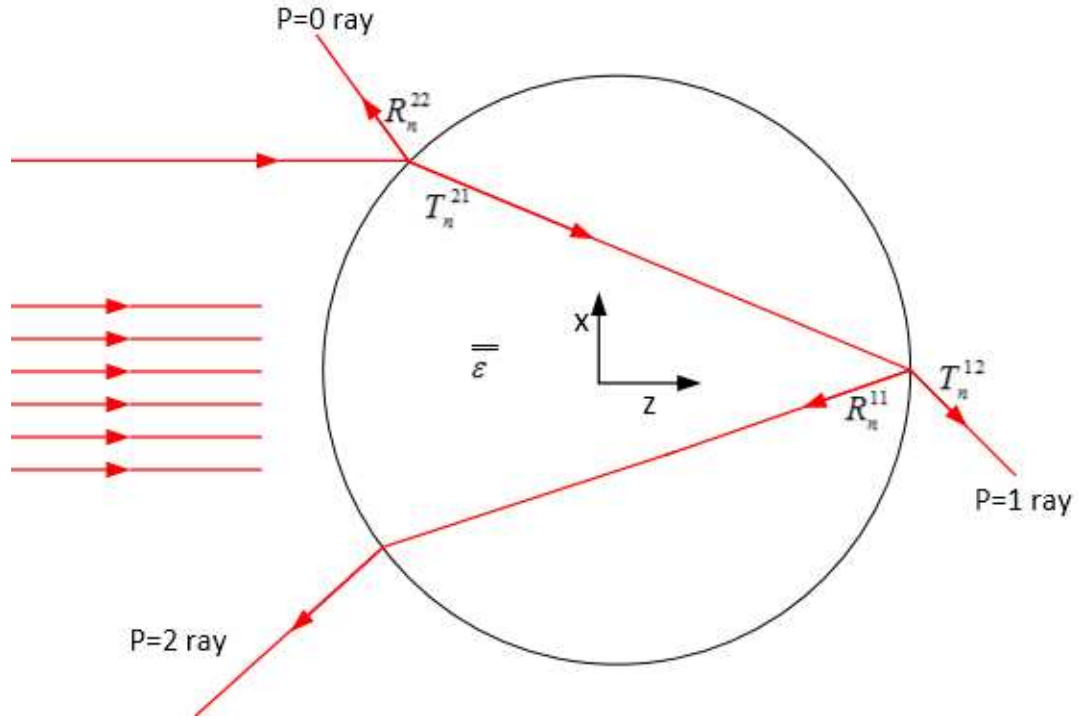
Fig. 4. 1. A plane wave approaching a uniaxial dielectric sphere

Following the backscattering solution of a radially uniaxial dielectric sphere in the presence of a plane electromagnetic wave reported in [2], the electric and magnetic vector potentials A_r^s and F_r^s given by the right-hand sides of (2-173) and (2-174), respectively:

$$A_r^s = \frac{\cos \phi}{\omega} \sum_{n=1}^{\infty} b_n \hat{H}_n^2(k_0 r) P_n^1(\cos \theta) \tag{4-3}$$

$$F_r^s = \frac{\sin \phi}{\omega \eta_0} \sum_{n=1}^{\infty} c_n \hat{H}_n^2(k_0 r) P_n^1(\cos \theta). \tag{4-4}$$

Substituting (4-3) and (4-4) into (2-177)–(2-179) with the superscript p replaced by s, with ε_θ replaced by ε_0, and with k_p replaced by k_0 gives

$$E_r^s = \frac{1}{j\omega\mu_0\varepsilon_0}\left(\frac{\partial}{\partial r^2} + k_0^2\right)\left(\frac{\cos\phi}{\omega}\sum_{n=1}^{\infty} b_n\widehat{H}_n^2(k_0 r)P_n^1(\cos\theta)\right)$$
(4-5)

$$E_\theta^s = \frac{1}{j\omega\mu_0\varepsilon_0 r}\frac{\partial^2}{\partial r\partial\theta}\left(\frac{\cos\phi}{\omega}\sum_{n=1}^{\infty} b_n\widehat{H}_n^2(k_0 r)P_n^1(\cos\theta)\right)$$

$$-\frac{1}{\varepsilon_0 r\sin\theta}\frac{\partial}{\partial\phi}\left(\frac{\sin\phi}{\omega\eta_0}\sum_{n=1}^{\infty} c_n\widehat{H}_n^2(k_0 r)P_n^1(\cos\theta)\right)$$
(4-6)

$$E_\phi^s = \frac{1}{j\omega\mu_0\varepsilon_0 r\sin\theta}\frac{\partial^2}{\partial r\partial\phi}\left(\frac{\cos\phi}{\omega}\sum_{n=1}^{\infty} b_n\widehat{H}_n^2(k_0 r)P_n^1(\cos\theta)\right)$$

$$+\frac{1}{\varepsilon_0 r}\frac{\partial}{\partial\theta}\left(\frac{\sin\phi}{\omega\eta_0}\sum_{n=1}^{\infty} c_n\widehat{H}_n^2(k_0 r)P_n^1(\cos\theta)\right)$$
(4-7)

Because $\frac{d}{d\theta}P_n^1(\cos\theta) = -\sin\theta\,P_n^{1'}(\cos\theta)$, the relationship [21, p.295] Implies that

$$\sin\theta\,P_n^{1'}(\cos\theta) \xrightarrow{\theta\to\pi} \frac{(-1)^n}{2}n(n+1)$$
(4-8)

Also [21, p. 245]

$$\frac{P_n^1(\cos\theta)}{\sin\theta} \xrightarrow{\theta\to\pi} \frac{(-1)^n}{2}n(n+1)$$
(4-9)

Substituting (4-8) and (4-9) into (4-6) and (4-7) gives the back scattering fields

$$E_\theta^s = \frac{1}{j\omega\mu_0\varepsilon_0 r}\left(\frac{\cos\phi}{\omega}\sum_{n=1}^{\infty} b_n \frac{d}{dr}\widehat{H}_n^2(k_0 r)\frac{(-1)^n}{2}n(n+1)\right)$$

$$-\frac{1}{\varepsilon_0 r}\left(\frac{\cos\phi}{\omega\eta_0}\sum_{n=1}^{\infty} c_n\widehat{H}_n^2(k_0 r)\frac{(-1)^n}{2}n(n+1)\right) \tag{4-10}$$

$$E_\phi^s = \frac{-1}{j\omega\mu_0\varepsilon_0 r}\left(\frac{\sin\phi}{\omega}\sum_{n=1}^{\infty} b_n \frac{d}{dr}\widehat{H}_n^2(k_0 r)\frac{(-1)^n}{2}n(n+1)\right)$$

$$-\frac{1}{\varepsilon_0 r}\left(\frac{\sin\phi}{\omega\eta_0}\sum_{n=1}^{\infty} c_n\widehat{H}_n^2(k_0 r)\frac{(-1)^n}{2}n(n+1)\right). \tag{4-11}$$

In the field [21, (D-24) and (6-24)],

$$\widehat{H}_n^2(k_0 r) = j^{n+1}e^{-jk_0 r} \tag{4-12}$$

$$\frac{d}{dr}\widehat{H}_n^2(k_0 r) = j^n k_0 e^{-jk_0 r} \tag{4-13}$$

$$\left(\frac{d}{dr^2} + k_0{}^2\right)\widehat{H}_n^2(k_0 r) = \left(-k_0{}^2 + k_0{}^2\right)j^{n+1}e^{-jk_0 r} = 0 \tag{4-14}$$

so that (4-5), (4-10), and (4-11) become

$$E_r^s = 0 \tag{4-15}$$

80

$$E_\theta^s = \frac{\cos\phi\, e^{-jk_0 r}}{jk_0 r} \sum_{n=1}^{\infty} (b_n - c_n) \frac{(-1)^{n+1}}{2} j^n n(n+1) \tag{4-16}$$

$$E_\phi^s = \frac{\sin\phi\, e^{-jk_0 r}}{jk_0 r} \sum_{n=1}^{\infty} (b_n - c_n) \frac{(-1)^{n+1}}{2} j^n n(n+1). \tag{4-17}$$

The previous equations are recast as

$$E = \frac{e^{-jk_0 r}}{jk_0 r} S(\pi)(\cos\phi\, \hat{a}_\theta + \sin\phi\, \hat{a}_\phi) \tag{4-18}$$

$$S(\pi) = \sum_{n=1}^{\infty} (-1)^{n+1}\left(n+\frac{1}{2}\right)\left(\frac{b_n - c_n}{a_n}\right) \tag{4-19}$$

where $a_n = \frac{j^{-n}(2n+1)}{n(n+1)}$ and b_n and c_n are the well-known generalized Mie series

coefficients which are defined as follows

$$
\begin{Bmatrix} b_n \\ c_n \end{Bmatrix}
$$

$$= \frac{-\begin{Bmatrix} \sqrt{\varepsilon_\theta} \\ 1 \end{Bmatrix} \hat{J}_n'(k_0 a) \begin{Bmatrix} \hat{J}_\nu(\sqrt{\varepsilon_\theta}k_0 a) \\ \hat{J}_n(\sqrt{\varepsilon_\theta}k_0 a) \end{Bmatrix} + \begin{Bmatrix} 1 \\ \sqrt{\varepsilon_\theta} \end{Bmatrix} \begin{Bmatrix} \hat{J}_\nu(\sqrt{\varepsilon_\theta}k_0 a) \\ \hat{J}_n(\sqrt{\varepsilon_\theta}k_0 a) \end{Bmatrix}' \hat{J}_n(k_0 a)}{\begin{Bmatrix} \sqrt{\varepsilon_\theta} \\ 1 \end{Bmatrix} \hat{H}_n^{(2)'}(k_0 a) \begin{Bmatrix} \hat{J}_\nu(\sqrt{\varepsilon_\theta}k_0 a) \\ \hat{J}_n(\sqrt{\varepsilon_\theta}k_0 a) \end{Bmatrix} - \begin{Bmatrix} 1 \\ \sqrt{\varepsilon_\theta} \end{Bmatrix} \begin{Bmatrix} \hat{J}_\nu(\sqrt{\varepsilon_\theta}k_0 a) \\ \hat{J}_n(\sqrt{\varepsilon_\theta}k_0 a) \end{Bmatrix}' \hat{H}_n^{(2)}(k_0 a)} a_n \tag{4-20}$$

where $\nu = \sqrt{n(n+1)AR + \frac{1}{4}} - \frac{1}{2}$ and anisotropic ratio $AR = \frac{\varepsilon_\theta}{\varepsilon_r}$. To overcome the

difficulties associated with slowly converging Mie series, we employ Watson

transformation in (4-19). In order to use this method, (4-19) is first modified to sum up

from n=0. Then the n=0 term is subtracted again from eigen function series solution as

81

follows:

$$S(\pi) = \frac{1}{2a_0}(b_0 - c_0) + \sum_{n=0}^{\infty}(-1)^{n+1}(n+\frac{1}{2})(\frac{b_n - c_n}{a_n})$$

(4-21)

Because $b_0 - c_0$ contains the factor a_0, the singularity of $\frac{b_0 - c_0}{a_0}$ caused by a_n not being

defined at n=0 is removable.

Applying the Watson transformation to the infinite series in (4-21), we obtain

$$S(\pi) = \frac{1}{2a_0}(b_0 - c_0) - \int_C \frac{js(b_n - c_n)}{2a_n\cos(\pi s)}ds$$

(4-22)

where $n = s - 1/2$ and contour C encloses the positive real axis of the complex s plane

as shown in Fig. 4.2. The poles of $\frac{b_n - c_n}{a_n}$ lie in the fourth quadrant of the complex s plane,

shaded regions in Fig. 4.2.

Because the closed contour in Fig. 4.2 consisting of C_1, C, and C_3, does not encircle any

poles of $\frac{js(b_n - c_n)}{2a_n\cos(\pi s)}$, the integral of $\frac{js(b_n - c_n)}{2a_n\cos(\pi s)}$ around this closed contour is zero so that

$$-\int_C \frac{js(b_n - c_n)}{2a_n\cos(\pi s)}ds$$

$$= \int_{C_1} \frac{js(b_s - c_s)}{2\cos(\pi s)}ds + \int_{C_2} \frac{js(b_s - c_s)}{2\cos(\pi s)}ds$$

(4- 23)

$$+ \int_{C_3} \frac{js(b_s - c_s)}{2\cos(\pi s)}ds.$$

82

The integral over C_2 vanishes and the integral over the part of C_3 over the arc of the half circle in the fourth quadrant vanishes [37]–[39] so that the integral over C_3 reduces to $2\pi j \sum Residues\ due\ to\ the\ poles\ of\ the\ integrand\ in\ the\ fourth\ quadrant$.

Therefore, (4-25) reduces to

$$-\int_c \frac{js(b_n - c_n)}{2a_n \cos(\pi s)} ds = \int_{c_1} \frac{js(b_s - c_s)}{2 \cos(\pi s)} ds$$

(4- 24)

$$+2\pi j \sum Residues\ due\ to\ the\ poles\ of\ the\ integrand\ in\ the\ fourth\ quadrant$$

Substituting of (4- 24) into (4-22) gives

$$S(\pi) = \frac{1}{2a_0}(b_0 - c_0) + \int_{c_1} \frac{js(b_n - c_n)}{2a_n \cos(\pi s)} ds$$

(4-25)

$$+ 2\pi j \sum Residues\ due\ to\ the\ poles\ of\ the\ integrand$$

The asymptotic high frequency solution for the n=0 term and line integral of path C_1 gives the geometric optics solution for the far backscattered field. The residue series represents the creeping wave contribution to the backscattering field.

In the next section, the general Debye series solution is applied to simplify and then calculate the n=0 term along with the line integral associated with path C_1.
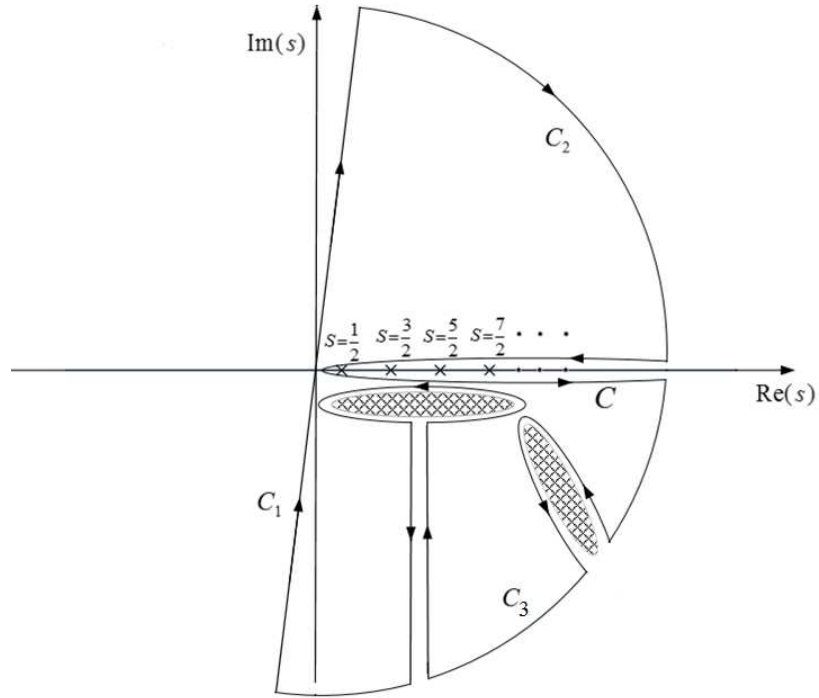
Fig. 4. 2. The contour C, C_1, C_2, and C_3 in the complex s-plane. C_1 is the straight line close to the imaginary axis. C_2 is in the first quadrant, C_3 is in the fourth quadrant. $C+C_1+C_2+C_3$ is a closed contour.

4.3 The formulation of geometric optics backscattering from the uniaxial sphere

As illustrated in the previous chapter, the p=0 term in Debye series solution represents the contribution due to the reflection from the surface of the sphere and the remaining p-waves are the contributions arising from P-1 reflection in the sphere [28].

Using (3-89), we obtain

$$\frac{b_n - c_n}{a_n} = \Gamma_o + \Gamma_p$$

(4-26)

where

$$\Gamma_o = \frac{1}{2}[R_n^{22^A} - R_n^{22^F}] \tag{4-27}$$

$$\Gamma_p = -\frac{1}{2}[\Gamma_p^{n^A} - \Gamma_p^{n^F}] = -\frac{1}{2}\left[\left(\frac{T_n^{21^A} T_n^{12^A}}{1 - R_n^{11^A}}\right) - \left(\frac{T_n^{21^F} T_n^{12^F}}{1 - R_n^{11^F}}\right)\right] \tag{4-28}$$

Substituting (4- 24) into the integrand of the integral along the path C_1 in (4- 23), we

obtain

$$\int_{C_1} \frac{js(b_s - c_s)}{2\cos(\pi s)} ds = I_O + I_p \tag{4-29}$$

Where

$$I_O = \int_{C_1} \frac{js\Gamma_o}{2\cos(\pi s)} ds \tag{4-30}$$

$$I_p = \int_{C_1} \frac{js\Gamma_p}{2\cos(\pi s)} ds \tag{4-31}$$

where the Γ_o corresponds to the portion of the incident wave that reflects back at the front

surface of the sphere and Γ_p represents the portion of the incident wave that enters the

sphere and after number of reflections, it reemerges out from sphere. Using the Debye

asymptotic formulas for the Hankel functions given in [40]–[42] for large argument x and

index $v \ll x$,

$$H_s^{(1)}(x) = \left(\tfrac{1}{2}\pi x \sin\tau\right)^{-\frac{1}{2}} e^{jx(\sin\tau-\tau\cos\tau)-j\frac{\pi}{4}}\left(1 + \frac{j}{8x} + O(x^{-2})\right) \tag{4-32}$$

$$H_s^{(2)}(x) = \left(\tfrac{1}{2}\pi x \sin\tau\right)^{-\frac{1}{2}} e^{-jx(\sin\tau-\tau\cos\tau)+j\frac{\pi}{4}}\left(1 - \frac{j}{8x} + O(x^{-2})\right) \tag{4-33}$$

$$H_s^{(1)'}(x) = j\sin\tau\left(\tfrac{1}{2}\pi x \sin\tau\right)^{-\frac{1}{2}} e^{jx(\sin\tau-\tau\cos\tau)-j\frac{\pi}{4}}\left(1 - \frac{j9}{24x} + O(x^{-2})\right) \tag{4-34}$$

$$H_s^{(2)'}(x) = -j\sin\tau\left(\tfrac{1}{2}\pi x \sin\tau\right)^{-\frac{1}{2}} e^{-jx(\sin\tau-\tau\cos\tau)+j\frac{\pi}{4}}\left(1 + \frac{j9}{24x} \right.$$
$$\left. + O(x^{-2})\right) \tag{4-35}$$

where $s = n + 1/2$ or $s = v + 1/2$ where $n = 0,1,2, \dots$ and

$$v = -\frac{1}{2} + \sqrt{n(n+1)(AR) + \frac{1}{4}} \tag{4-36}$$

$$\cos\tau = \frac{s}{x}. \tag{4-37}$$

And also using (4-33)–(4-36), we obtain

$$\frac{\widehat{H}_{s-1/2}^{(2)'}(k_0 a)}{\widehat{H}_{s-1/2}^{2}(k_0 a)} = -j\sin(\tau) \tag{4-38}$$

$$\frac{\widehat{H}_{s-1/2}^{(1)'}(k_0 a)}{\widehat{H}_{s-1/2}^{(1)}(k_0 a)} = jsin(\tau) \tag{4-39}$$

With $s = n + 1/2$ and K_0A replaced by $\sqrt{\text{E}_\Theta}\text{K}_0\text{A}$, (4-38) and (4-39) become

$$\frac{\widehat{H}_n^{(2)'}\left(\sqrt{\varepsilon_\theta}k_0 a\right)}{\widehat{H}_n^{(2)}\left(\sqrt{\varepsilon_\theta}k_0 a\right)} = -jsin(\tau_n) \tag{4-40}$$

$$\frac{\widehat{H}_n^{(1)'}\left(\sqrt{\text{E}_\Theta}\text{K}_0\text{A}\right)}{\widehat{H}_n^{(1)}\left(\sqrt{\text{E}_\Theta}\text{K}_0\text{A}\right)} = jsin(\tau_n) \tag{4-41}$$

where

$$\cos\tau_n = \frac{n + \dfrac{1}{2}}{\sqrt{\varepsilon_\theta}k_0 a} \tag{4-42}$$

$$\frac{\widetilde{H}_v^{(2)'}\left(\sqrt{\varepsilon_\theta}k_0 a\right)}{\widetilde{H}_v^{(2)}\left(\sqrt{\varepsilon_\theta}k_0 a\right)} = -jsin(\tau_v) \tag{4-43}$$

$$\frac{\widetilde{H}_v^{(1)'}\left(\sqrt{\varepsilon_\theta}k_0 a\right)}{\widetilde{H}_v^{(1)}\left(\sqrt{\varepsilon_\theta}k_0 a\right)} = jsin(\tau_v) \tag{4-44}$$

where

$$\cos\tau_v = \frac{v + \dfrac{1}{2}}{\sqrt{\varepsilon_\theta}k_0 a} \tag{4-45}$$

Using [21, (D-21)], (4-32) and (4-33), we obtain

$$
\frac{\widehat{H}^{(1)}_{s-1/2}(x)}{\widehat{H}^{(2)}_{s-1/2}(x)} = e^{2jx(\sin\tau - \tau\cos\tau) - j\frac{\pi}{2}}\left(1 - \frac{j}{4x} + O(x^{-2})\right)
\tag{4-46}
$$

$$
\frac{\widehat{H}^{(2)}_{s-1/2}(x)}{\widehat{H}^{(1)}_{s-1/2}(x)} = e^{-2jx(\sin\tau - \tau\cos\tau) + j\frac{\pi}{2}}\left(1 + \frac{j}{4x} + O(x^{-2})\right)
\tag{4-47}
$$

The reflection and transmission coefficients of (3-72)–(3-75) can be expressed as follows:

Multiplying and dividing the numerator and denominator of (3-73) by $\left\{\begin{array}{c}\frac{1}{\widehat{H}^{(1)}_{v}(\sqrt{\varepsilon_\theta}k_0 a)} \\ \frac{1}{\widehat{H}^{(1)}_{n}(\sqrt{\varepsilon_\theta}k_0 a)}\end{array}\right\}$ and

then factoring $\widehat{H}^{(1)}_{n}(k_0 a)$ out of the resulting numerator and factoring $\widehat{H}^{(2)}_{n}(k_0 a)$ our of the resulting denominator yield

$$
R^{22\{A\}}_{n\,\{F\}} = \frac{\left(\left(\left\{\begin{array}{c}\sqrt{\varepsilon_\theta}\\1\end{array}\right\}\frac{\widehat{H}^{(1)'}_{n}(k_0 a)}{\widehat{H}^{(1)}_{n}(k_0 a)} - \left\{\begin{array}{c}1\\\sqrt{\varepsilon_\theta}\end{array}\right\}\left(\begin{array}{c}\frac{\widehat{H}^{(1)'}_{v}(\sqrt{\varepsilon_\theta}k_0 a)}{\widehat{H}^{(1)}_{v}(\sqrt{\varepsilon_\theta}k_0 a)}\\\frac{\widehat{H}^{(1)'}_{n}(\sqrt{\varepsilon_\theta}k_0 a)}{\widehat{H}^{(1)}_{n}(\sqrt{\varepsilon_\theta}k_0 a)}\end{array}\right)\right)\widehat{H}^{(1)}_{n}(k_0 a)\right)}{\left(-\left\{\begin{array}{c}\sqrt{\varepsilon_\theta}\\1\end{array}\right\}\frac{\widehat{H}^{(2)'}_{n}(k_0 a)}{\widehat{H}^{(2)}_{n}(k_0 a)} + \left\{\begin{array}{c}1\\\sqrt{\varepsilon_\theta}\end{array}\right\}\left(\begin{array}{c}\frac{\widehat{H}^{(1)'}_{v}(\sqrt{\varepsilon_\theta}k_0 a)}{\widehat{H}^{(1)}_{v}(\sqrt{\varepsilon_\theta}k_0 a)}\\\frac{\widehat{H}^{(1)'}_{n}(\sqrt{\varepsilon_\theta}k_0 a)}{\widehat{H}^{(1)}_{n}(\sqrt{\varepsilon_\theta}k_0 a)}\end{array}\right)\right)\widehat{H}^{(2)}_{n}(k_0 a)}.
\tag{4-48}
$$

Multiplying the numerator and denominator of (3-74) by $\dfrac{1}{\widehat{H}^{(2)}_{n}(k_0 a)}$ and then factoring

$\begin{Bmatrix}\widehat{H}_v^{(2)}(\sqrt{\varepsilon_\theta}k_0a)\\\widehat{H}_n^{(2)}(\sqrt{\varepsilon_\theta}k_0a)\end{Bmatrix}$ out of the resulting numerator and factoring $\begin{Bmatrix}\widehat{H}_v^{(1)}(\sqrt{\varepsilon_\theta}k_0a)\\\widehat{H}_n^{(1)}(\sqrt{\varepsilon_\theta}k_0a)\end{Bmatrix}$ out of the

resulting denominator yield

$R_n^{11\{^{A}_{F}\}}$

$$= \frac{\left(\left(\left\{\begin{matrix}\sqrt{\varepsilon_\theta}\\1\end{matrix}\right\}\dfrac{\widehat{H}_n^{(2)'}(k_0a)}{\widehat{H}_n^{(2)}(k_0a)} - \left\{\begin{matrix}1\\\sqrt{\varepsilon_\theta}\end{matrix}\right\}\begin{Bmatrix}\dfrac{\widehat{H}_v^{(2)'}(\sqrt{\varepsilon_\theta}k_0a)}{\widehat{H}_v^{(2)}(\sqrt{\varepsilon_\theta}k_0a)}\\\dfrac{\widehat{H}_n^{(2)'}(\sqrt{\varepsilon_\theta}k_0a)}{\widehat{H}_n^{(2)}(\sqrt{\varepsilon_\theta}k_0a)}\end{Bmatrix}\right)\begin{Bmatrix}\widehat{H}_v^{(2)}(\sqrt{\varepsilon_\theta}k_0a)\\\widehat{H}_n^{(2)}(\sqrt{\varepsilon_\theta}k_0a)\end{Bmatrix}\right)}{\left(\left(-\left\{\begin{matrix}\sqrt{\varepsilon_\theta}\\1\end{matrix}\right\}\dfrac{\widehat{H}_n^{(2)'}(k_0a)}{\widehat{H}_n^{(2)}(k_0a)} + \left\{\begin{matrix}1\\\sqrt{\varepsilon_\theta}\end{matrix}\right\}\begin{Bmatrix}\dfrac{\widehat{H}_v^{(1)'}(\sqrt{\varepsilon_\theta}k_0a)}{\widehat{H}_v^{(1)}(\sqrt{\varepsilon_\theta}k_0a)}\\\dfrac{\widehat{H}_n^{(1)'}(\sqrt{\varepsilon_\theta}k_0a)}{\widehat{H}_n^{(1)}(\sqrt{\varepsilon_\theta}k_0a)}\end{Bmatrix}\right)\begin{Bmatrix}\widehat{H}_v^{(1)}(\sqrt{\varepsilon_\theta}k_0a)\\\widehat{H}_n^{(1)}(\sqrt{\varepsilon_\theta}k_0a)\end{Bmatrix}\right)}$$ (4-49)

Using (3-21) and (3-37), we obtain

$T_n^{21\{^{A}_{F}\}}$

$$= \frac{-\left\{\begin{matrix}\sqrt{\varepsilon_\theta}\\1\end{matrix}\right\}(\widehat{H}_n^{(2)'}(k_0a)\widehat{H}_n^{(1)}(k_0a) + \widehat{H}_n^{(2)}(k_0a)\widehat{H}_n^{(1)'}(k_0a))}{-\left\{\begin{matrix}\sqrt{\varepsilon_\theta}\\1\end{matrix}\right\}\widehat{H}_n^{(2)'}(k_0a)\begin{Bmatrix}\widehat{H}_v^{(1)}(\sqrt{\varepsilon_\theta}k_0a)\\\widehat{H}_n^{(1)}(\sqrt{\varepsilon_\theta}k_0a)\end{Bmatrix} + \left\{\begin{matrix}1\\\sqrt{\varepsilon_\theta}\end{matrix}\right\}\begin{Bmatrix}\widehat{H}_v^{(1)'}(\sqrt{\varepsilon_\theta}k_0a)\\\widehat{H}_n^{(1)'}(\sqrt{\varepsilon_\theta}k_0a)\end{Bmatrix}\widehat{H}_n^{(2)}(k_0a)}.$$ (4-50)

Deriving the numerator and denominator of (4-44) by $\widehat{H}_n^{(2)}(k_0a)$ and then factoring

$\widehat{H}_n^{(1)}(k_0a)$ out of resulting numerator and factoring $\begin{Bmatrix}\widehat{H}_v^{(1)}(\sqrt{\varepsilon_\theta}k_0a)\\\widehat{H}_n^{(1)}(\sqrt{\varepsilon_\theta}k_0a)\end{Bmatrix}$ yield

$$T_n^{21\{A\atop F\}}$$

$$= \frac{\left\{\sqrt{\varepsilon_\theta} \atop 1\right\} \widehat{H}_n^{(1)}(k_0 a)\left(-\dfrac{\widehat{H}_n^{(2)'}(k_0 a)}{\widehat{H}_n^{(2)}(k_0 a)} + \dfrac{\widehat{H}_n^{(1)'}(k_0 a)}{\widehat{H}_n^{(1)}(k_0 a)}\right)}{\left(-\left\{\sqrt{\varepsilon_\theta} \atop 1\right\}\dfrac{\widehat{H}_n^{(2)'}(k_0 a)}{\widehat{H}_n^{(2)}(k_0 a)} + \left\{1 \atop \sqrt{\varepsilon_\theta}\right\}\left\{\dfrac{\widehat{H}_v^{(1)'}(\sqrt{\varepsilon_\theta}k_0 a)}{\widehat{H}_v^{(1)}(\sqrt{\varepsilon_\theta}k_0 a)} \atop \dfrac{\widehat{H}_n^{(1)'}(\sqrt{\varepsilon_\theta}k_0 a)}{\widehat{H}_n^{(1)}(\sqrt{\varepsilon_\theta}k_0 a)}\right\}\right)\left\{\widehat{H}_v^{(1)}(\sqrt{\varepsilon_\theta}k_0 a) \atop \widehat{H}_n^{(1)}(\sqrt{\varepsilon_\theta}k_0 a)\right\}} \qquad (4\text{-}51)$$

Using (3-54) and (3-70) we obtain

$$T_n^{12\{A\atop F\}}$$

$$= \frac{\left\{1 \atop \sqrt{\varepsilon_\theta}\right\}\left\{\widehat{H}_v^{(2)}(\sqrt{\varepsilon_\theta}k_0 a)\widehat{H}_v^{(1)'}(\sqrt{\varepsilon_\theta}k_0 a) - \widehat{H}_v^{(2)'}(\sqrt{\varepsilon_\theta}k_0 a)\widehat{H}_v^{(1)}(\sqrt{\varepsilon_\theta}k_0 a) \atop \widehat{H}_n^{(2)}(\sqrt{\varepsilon_\theta}k_0 a)\widehat{H}_n^{(1)'}(\sqrt{\varepsilon_\theta}k_0 a) - \widehat{H}_n^{(2)'}(\sqrt{\varepsilon_\theta}k_0 a)\widehat{H}_n^{(1)}(\sqrt{\varepsilon_\theta}k_0 a)\right\}}{-\left\{\sqrt{\varepsilon_\theta} \atop 1\right\}\widehat{H}_n^{(2)'}(k_0 a)\left\{\widehat{H}_v^{(1)}(\sqrt{\varepsilon_\theta}k_0 a) \atop \widehat{H}_n^{(1)}(\sqrt{\varepsilon_\theta}k_0 a)\right\} + \left\{1 \atop \sqrt{\varepsilon_\theta}\right\}\left\{\widehat{H}_v^{(1)'}(\sqrt{\varepsilon_\theta}k_0 a) \atop \widehat{H}_n^{(1)'}(\sqrt{\varepsilon_\theta}k_0 a)\right\}\widehat{H}_n^{(2)}(k_0 a)} . \qquad (4\text{-}52)$$

Multiplying the numerator and denominator of (4-52) by $\left\{\dfrac{1}{\widehat{H}_v^{(1)}(\sqrt{\varepsilon_\theta}k_0 a)\widehat{H}_v^{(2)}(\sqrt{\varepsilon_\theta}k_0 a)} \atop \dfrac{1}{\widehat{H}_n^{(1)}(\sqrt{\varepsilon_\theta}k_0 a)\widehat{H}_n^{(2)}(\sqrt{\varepsilon_\theta}k_0 a)}\right\}$ and

then factoring $\left\{\dfrac{\widehat{H}_n^{(2)}(k_0 a)}{\widehat{H}_v^{(2)}(\sqrt{\varepsilon_\theta}k_0 a)} \atop \dfrac{\widehat{H}_n^{(2)}(k_0 a)}{\widehat{H}_v^{(2)}(\sqrt{\varepsilon_\theta}k_0 a)}\right\}$ out of the resulting denominator yeild

$$T_n^{12\{{}^A_F\}} = \frac{\left\{{}^{1}_{\sqrt{\varepsilon_\theta}}\right\}\left\{\dfrac{\widehat{H}_v^{(1)'}\left(\sqrt{\varepsilon_\theta}k_0 a\right)}{\widehat{H}_v^{(1)}\left(\sqrt{\varepsilon_\theta}k_0 a\right)} - \dfrac{\widehat{H}_v^{(2)'}\left(\sqrt{\varepsilon_\theta}k_0 a\right)}{\widehat{H}_v^{(2)}\left(\sqrt{\varepsilon_\theta}k_0 a\right)} \\ \dfrac{\widehat{H}_n^{(1)'}\left(\sqrt{\varepsilon_\theta}k_0 a\right)}{\widehat{H}_n^{(1)}\left(\sqrt{\varepsilon_\theta}k_0 a\right)} - \dfrac{\widehat{H}_n^{(2)'}\left(\sqrt{\varepsilon_\theta}k_0 a\right)}{\widehat{H}_n^{(2)}\left(\sqrt{\varepsilon_\theta}k_0 a\right)}\right\}}{-\left\{{}^{\sqrt{\varepsilon_\theta}}_{1}\right\}\dfrac{\widehat{H}_n^{(2)'}(k_0 a)}{\widehat{H}_n^{(2)}(k_0 a)} + \left\{{}^{1}_{\sqrt{\varepsilon_\theta}}\right\}\left\{\dfrac{\widehat{H}_v^{(1)'}\left(\sqrt{\varepsilon_\theta}k_0 a\right)}{\widehat{H}_v^{(1)}\left(\sqrt{\varepsilon_\theta}k_0 a\right)} \\ \dfrac{\widehat{H}_n^{(1)'}\left(\sqrt{\varepsilon_\theta}k_0 a\right)}{\widehat{H}_n^{(1)}\left(\sqrt{\varepsilon_\theta}k_0 a\right)}\right\}}$$

$$\cdot\frac{\left\{{}^{\widehat{H}_v^{(2)}\left(\sqrt{\varepsilon_\theta}k_0 a\right)}_{\widehat{H}_n^{(2)}\left(\sqrt{\varepsilon_\theta}k_0 a\right)}\right\}}{\widehat{H}_n^{(2)}(k_0 a)} \tag{4-53}$$

Substituting (4-38)–(4-41), (4-43), (4-44), (4-46) and (4-47)into (4-48), (4-49), (4-51)

and (4-52) give

$$\left\{{}^{R_n^{22^A}}_{R_n^{22^F}}\right\} = \left\{\begin{matrix}\dfrac{N\sin\tau - \sin(\tau_v)}{N\sin\tau + \sin(\tau_v)} \\ \dfrac{\sin\tau - N\sin(\tau_n)}{\sin\tau + N\sin(\tau_n)}\end{matrix}\right\} e^{2jk_0 a(\sin(\tau)-\tau\cos\tau)-j\frac{\pi}{2}}$$

$$\cdot\left(1 - \frac{j}{4k_0 a} + O((k_0 a)^{-2})\right) \tag{4-54}$$

$$\left\{{}^{R_n^{11^A}}_{R_n^{11^F}}\right\} \simeq \left\{\begin{matrix}\dfrac{\sin\tau_v - N\sin\tau}{\sin\tau_v + N\sin(\tau)} \\ \cdot e^{2jNk_0 a(\sin(\tau_v)-\tau_v\cos\tau_v)-j\frac{\pi}{2}} \\ \dfrac{-\sin\tau + N\sin\tau_n}{N\sin\tau_n + \sin\tau} \\ \cdot e^{2jNk_0 a(\sin(\tau_n)-\tau_n\cos\tau_n)-j\frac{\pi}{2}}\end{matrix}\right\} \tag{4-55}$$

$$\begin{Bmatrix} T_n^{21^A} \\ T_n^{21^F} \end{Bmatrix} = \begin{Bmatrix} \dfrac{2N \sin \tau}{N \sin \tau + \sin \tau_v} \\ \dfrac{2 \sin \tau}{\sin \tau + N \sin \tau_N} \end{Bmatrix} \dfrac{\widehat{H}_n^{(1)}(k_0 a)}{\begin{Bmatrix} \widehat{H}_v^{(1)}(Nk_0 a) \\ \widehat{H}_n^{(1)}(Nk_0 a) \end{Bmatrix}} \tag{4-56}$$

$$\begin{Bmatrix} T_n^{12^A} \\ T_n^{12^F} \end{Bmatrix} = \begin{Bmatrix} \dfrac{2 \sin \tau_v}{N \sin \tau + \sin \tau_v} \\ \dfrac{2N \sin \tau_N}{\sin \tau + N \sin \tau_N} \end{Bmatrix} \dfrac{\begin{Bmatrix} \widehat{H}_v^{(2)}(Nk_0 a) \\ \widehat{H}_n^{(2)}(Nk_0 a) \end{Bmatrix}}{\widehat{H}_n^{(2)}(k_0 a)} \tag{4-57}$$

where $N = \sqrt{\varepsilon_\theta}$. Combining (4-27) and (4-54), I_O of (4-30) can be written as

$$I_O = \int_{-\infty}^{-\infty} \dfrac{js[\dfrac{N \sin \tau - \sin(\tau_v)}{N \sin \tau + \sin(\tau_v)} - \dfrac{\sin \tau - N\sin(\tau_n)}{\sin \tau + N \sin(\tau_n)}]w(\tau)f_1(k_0 a)}{4 \cos(\pi s)} ds \tag{4-58}$$

Equation (4-28) is expressed as

$$\Gamma_p = \frac{1}{2}(\Gamma_p^{s^A} - \Gamma_p^{s^F}) \tag{4-59}$$

Where

$$\Gamma_p^{s^A} = T_n^{21^A} T_n^{12^A}(1 - R_n^{11^A})^{-1} \tag{4-60}$$

$$\Gamma_p^{s^F} = T_n^{21^F} T_n^{12^F}(1 - R_n^{11^F})^{-1} \tag{4-61}$$

Substituting of (4- 59) into (4-31) gives

92

$$I_p = \int\limits_{-\infty}^{-\infty} \frac{-js[\Gamma_p^{s^A} - \Gamma_p^{s^F}]}{4\cos(\pi s)} ds$$

(4-62)

Where $f_1(k_0 a) = 1 - \frac{j}{4k_0 a} + O((k_0 a)^{-2})$, and $w(\tau) = e^{2jk_0 a(\sin(\tau) - \tau\cos\tau) - j\frac{\pi}{2}}$ and

Substituting (4-55)–(4-57) into (4- 60) and (4- 61) gives

$$\Gamma_p^{s^A} = \frac{4N\sin\tau\sin\tau_v}{(N\sin\tau + \sin\tau_v)^2} jP(\tau_v)\left[1 \right.$$

$$\left. - \frac{\sin\tau_v - N\sin\tau}{\sin\tau_v + N\sin(\tau)} j\, P(\tau_v)\right]^{-1} w(\tau)f_1(k_0 a)$$

(4-63)

$$\Gamma_p^{s^F} = \frac{4N\sin\tau\sin\tau_n}{(\sin\tau + N\sin\tau_n)^2} jP(\tau_n)\left[1 \right.$$

$$\left. - \frac{-\sin\tau + N\sin\tau_n}{N\sin\tau_n + \sin\tau} jP(\tau_N)\right]^{-1} w(\tau)f_1(k_0 a)$$

(4-64)

where $P(x) = e^{-2jNk_0 a(\sin(x) - x\cos x)}$. Expressing $\cos\pi s = \frac{1 + e^{j2s\pi}}{2e^{js\pi}}$ and $\varphi = 2k_0 a(\sin(\tau) - \tau\cos\tau) + s\pi$, the integrals in (4-58) and (4-62) are expressed in a form that can be computed using the saddle point method. The conditions $\varphi' = 0|_{s=0}$ and $\varphi'' = \frac{2}{k_0 a}\Big|_{s=0}$ yield the saddle point of s=0 and after applying the saddle point technique, we obtain

$$I_O = \left[\frac{N - \sqrt{1 + \frac{AR - 1}{4(Nk_0 a)^2}}}{N + \sqrt{1 + \frac{AR - 1}{4(Nk_0 a)^2}}} + \frac{N - 1}{N + 1}\right]\frac{e^{j2k_0 a}}{2} f_1(k_0 a) \int_{-\infty}^{+\infty} \frac{se^{\frac{js^2}{k_0 a}}}{1 + e^{j2\pi s}} ds$$

(4-65)

$$I_p = \frac{1}{2}\left(\Gamma_p^{0^A} - \Gamma_p^{0^F}\right)e^{j2k_0a}f(k_0a)\int_{-\infty}^{+\infty}\frac{se^{\frac{js^2}{k_0a}}}{1 + e^{j2\pi s}}\,ds \tag{4-66}$$

$$\Gamma_p^{0^A} = \frac{4N\sqrt{1 + \dfrac{AR - 1}{4(Nk_0a)^2}}}{\left(N + \sqrt{1 + \dfrac{AR - 1}{4(Nk_0a)^2}}\right)^2}$$

$$\cdot \frac{je^{-2jk_0a\left(\sqrt{N^2 + \frac{AR-1}{4(k_0a)^2}} - \frac{\sqrt{1-AR}}{2k_0a}\cos^{-1}\frac{\sqrt{1-AR}}{2Nk_0a}\right)}}{1 - j\dfrac{\sqrt{1 + \dfrac{AR - 1}{4(Nk_0a)^2}} - N}{\sqrt{1 + \dfrac{AR - 1}{4(Nk_0a)^2}} + N}e^{-2jk_0a\left(\sqrt{N^2 + \frac{AR-1}{4(k_0a)^2}} - \frac{\sqrt{1-AR}}{2k_0a}\cos^{-1}\frac{\sqrt{1-AR}}{2Nk_0a}\right)}} \tag{4-67}$$

$$\Gamma_p^{0^F} = \frac{4N}{(N + 1)^2}\frac{je^{-2jNk_0a}}{1 - j\dfrac{N - 1}{N + 1}e^{-2jNk_0a}} \tag{4-68}$$

The solution of the integrals in (4-65) and (4-66) is obtained using Scott's method [43]. Setting $u = -2js\pi$ and $\delta = \dfrac{j}{4\pi^2 k_0a}$ the integral can be expressed as follows [11]:

$$\int \frac{ue^{-\delta u^2}}{1 + e^{-u}}\,du = -j2\pi^2 k_0a - \frac{\pi^2}{6} - \frac{j7\pi^2}{240k_0a} + O\left((k_0a)^{-2}\right) \tag{4-69}$$

Substituting (4-69) into (4-65)–(4-66) gives

$$I_O = \frac{jk_0a}{4}\left[\frac{N - \sqrt{1 + \dfrac{AR - 1}{4(k_0a)^2}}}{N + \sqrt{1 + \dfrac{AR - 1}{4(k_0a)^2}}} + \frac{N - 1}{N + 1}\right]e^{j2k_0a}g(k_0a) \tag{4-70}$$

$$I_p = \frac{jk_0a}{4}\left[\Gamma_p^{0^A} - \Gamma_p^{0^F}\right]e^{j2k_0a}g(k_0a) \tag{4-71}$$

94

where $g(k_0a) = 1 - \frac{j}{3k_0a} + O((k_0a)^{-2})$. Setting $AR=1$, (4-70) and (4-71) reduce to front and rear axial returns reported in [11].

The $n = 0$ term of (4-25) can be treated in the same procedure. Replacing terms a_0 and b_0 by their equivalent Debye series, the equation can be approximated using Debye asymptotic formulas, and after some tedious but straightforward algebra we obtained

$$\frac{1}{2}(b_0 - c_0) = -\frac{j}{4}e^{j2k_0a}f(k_0a)\left[\frac{N - \sqrt{1 + \frac{AR - 1}{4(Nk_0a)^2}}}{N + \sqrt{1 + \frac{AR - 1}{4(Nk_0a)^2}}} + \frac{N - 1}{N + 1} + \left[\Gamma_p^{0^A} - \Gamma_p^{0^A}\right]\right]$$

(4-72)

Substituting (4-70)–(4-72) into (4-25), the backscattered fields are expressed as

$$E_O^S =$$

$$\frac{-e^{-jkr}}{4k_0r}\left[\frac{N - \sqrt{1 + \frac{AR-1}{4(Nk_0a)^2}}}{N + \sqrt{1 + \frac{AR-1}{4(Nk_0a)^2}}} + \frac{N-1}{N+1}\right][(k_0a)g(k_0a) + f_1(k_0a)]e^{j2k_0a}\left[\cos\phi\,\hat{a}_\theta + \right.$$

(4-73)

$$\sin\phi a\phi$$

$$E_p^S = \frac{-e^{-jkr}}{4k_0r}\left[\Gamma_p^{0^A} - \Gamma_p^{0^F}\right][(k_0a)g(k_0a) + f(k_0a)]e^{j2k_0a}\left[\left[\cos\phi\,\hat{a}_\theta + \right.\right.$$

(4-74)

$$\sin\phi a\phi$$

where E_O^S and E_p^S represent the total front and back axial backscattered fields respectively. For the fixed values of k_0a and ε_θ , (4-73) suggests that

95

increasing/decreasing the anisotropic ratio leads to the backscattering field reduction/enhancement at high frequencies. However increasing $k_0 a$ degrades the uniaxiality effect and for large values of $k_0 a$ the backscattering eventually reduces to isotropic case reported in [11]. To show the accuracy of the proposed equation, we compared the high frequency monostatic RCS of the lossy uniaxial dielectric spheres with those computed using Lorentz-Mie theory. The normalized monostatic RCS of the lossless case characterized by $\varepsilon_\theta = 10$, $\varepsilon_r = 20$ calculated by Lorentz-Mie theory is depicted in Fig. 4.3. However, the plot does not converge at high frequencies due to the peaks and nulls generated by the interference of the internal partial waves.

For lossy dielectric sphere, these oscillations do not persist and the solution converges at high frequencies [10]. The monostatic RCS of the lossy uniaxial dielectric sphere with $\sigma = 0.2, 0.5$ and 0.75 is shown in Figs. 4.4. The results indicate that the backscattered field of the lossy uniaxial sphere converges as frequency increases and is equal to high frequency formula derived in (4-73).
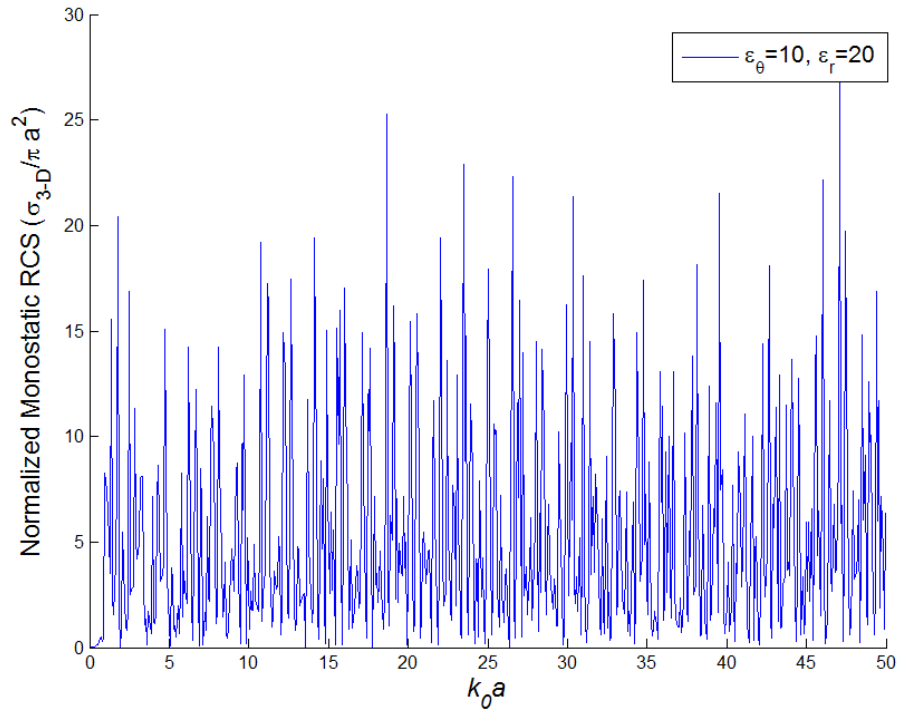
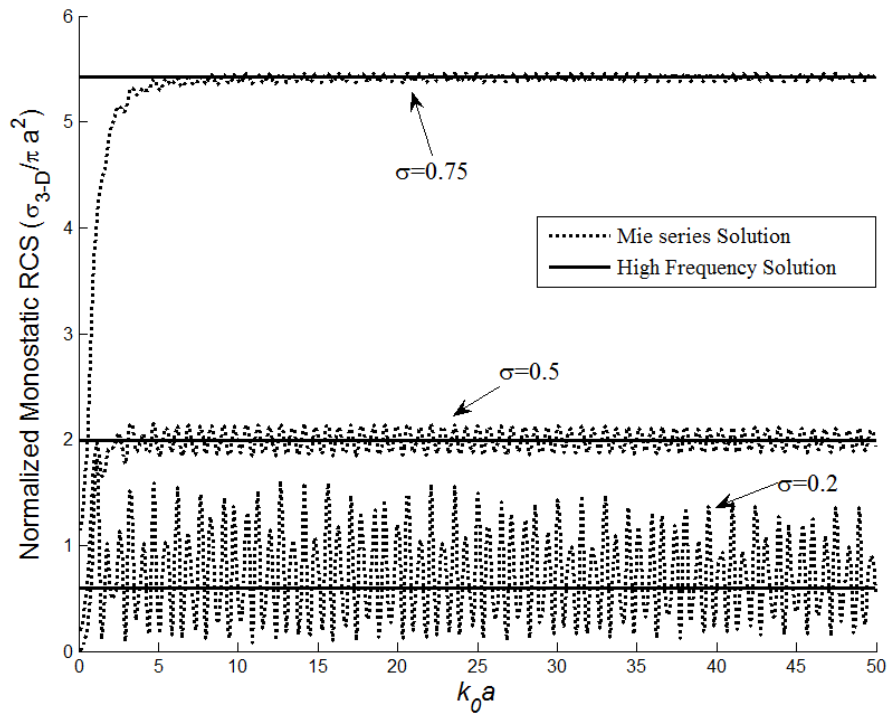Fig. 4. 3. The monostatic RCS of lossless uniaxial dielectric sphere

Fig. 4. 4. The monostatic RCS of the lossy uniaxial dielectric sphere with $\sigma = 0.2, 0.5$ and 0.75

97

4.4 Conclusion

High frequency backscattering by a uniaxial dielectric sphere in the presence of a plane electromagnetic wave is presented in this paper. The generalized Debye series for a uniaxial sphere is introduced and it is shown that the generalized Mie series coefficients can be written in terms of infinite partial waves that are reflected, refracted or diffracted after a number of reflections in the sphere. An approximate solution for high frequency backscattered field is proposed in a form convenient for numerical computation. The results reveal that the uniaxiality influences the high frequency backscattered fields and increasing anisotropic ratio of the uniaxial sphere could reduce the geometric optics portion of the backscattered field. This could be of value in the field of cloaking of targets where uniaxial dielectric coating is used to suppress the scattering from various objects. High frequency monostatic RCS of lossy uniaxial spheres are studied and compared with those calculated using Lorentz-Mie theory. The results are confirmed by good agreement between the proposed formula and the Mie series solution at high frequencies.

Chapter 5 Transient Electromagnetic Scattering by a Radially Uniaxial Dielectric Sphere: The Generalized Mie and Debye Series Solutions

In this chapter a theoretical study is carried out to determine the scattering of a transient electromagnetics wave by a radially uniaxial dielectric sphere. This is achieved by inverse Laplace transformation of the frequency domain scattering solution. To improve understanding of the scattering mechanism from a uniaxial dielectric sphere two different frequency domain solutions are employed. In the first approach, the impulse and step responses of a uniaxial dielectric sphere are evaluated by the Mie series solution. Following the high frequency scattering solution of a large uniaxial sphere, the Mie series summation is split into high frequency (HF) and low frequency terms where the HF term is replaced by its asymptotic expression allowing a significant reduction in computation time of the numerical Bromwich integral. In the second approach, the generalized Debye series solution is introduced and the generalized Mie series coefficients are replaced by their equivalent Debye series formulations. The results are then applied to evaluate the transient response of each individual Debye term allowing the identification of impulse returns in the transient response of a uniaxial sphere. The effect of variation in permittivity on the arrival time as well as amplitudes of each impulse return is studied and the results are compared with those computed using the Mie series solution. The numerical results obtained from both methods are in complete agreement.

5.1 Introduction

The electromagnetic plane wave scattering process from a dielectric sphere has been an attractive subject over the past few decades. A rigorous solution for this problem was first

developed by Lorenz and Mie in the form of an infinite series of partial wave contributions [44] and [2]. Although the solution is exact, it does not allow for construction of a physical model of the scattering process. However, this difficulty is partially resolved by introducing other methods e.g., ray tracing and Debye series solution. By the means of the Debye series formulation, each of the Mie series scattered wave amplitudes, b_n and c_n, is decomposed into a series of partial wave contributions that are due to rays which are diffracted, reflected and refracted. The ray characterized by its value of P in Fig. 5.1 has undergone P-1 internal reflections inside the sphere.
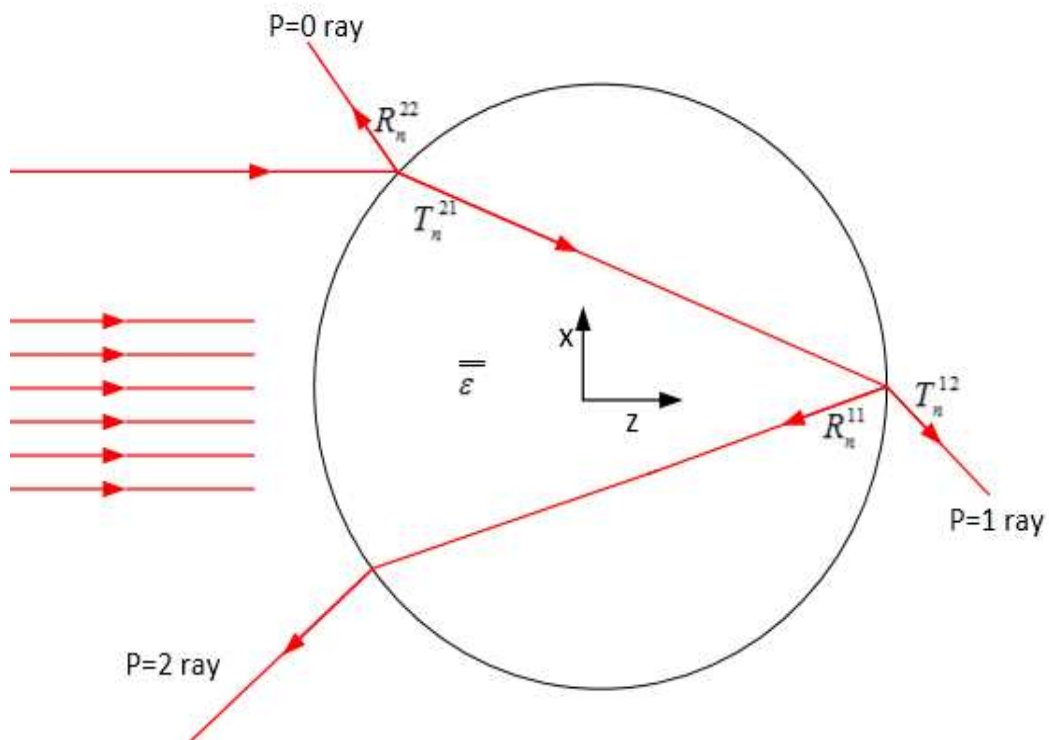

Fig. 5. 1. A plane wave approaching a uniaxial dielectric sphere

Investigating each individual term of the Debye series can improve our understanding of complex scattering processes e.g., the mechanisms causing the atmospheric optical

phenomena such as primary/secondary rainbow, corona and glory [5], as well as the deformation of intricate ripples in the curve associated with the bistatic RCS of the dielectric sphere in Fig. 5.2, [45].

However, there are a number of scattering problems that cannot be examined by Debye series in the frequency domain such as the separation of geometrical wave contributions that belong to the same term of the Debye series and scattering angle but travel along different path lengths as shown in Fig. 5.3. These types of problems have been solved by time domain approach where a short electromagnetic pulse is incident upon the sphere and the delay time is measured for each individual reflected ray [6]–[7].

In recent years, considerable attention has been given to the transient response of various bodies of revolution [4] and [46]. Perhaps the first attempt to calculate the time domain response waveform in the radar scattering context was that of Kennaugh who estimated the impulse response of the field scattered from a perfectly conducting sphere using an extremely simple approximation [8]–[9]. Aly and Wong [10] obtained the transient response of a dielectric sphere using a high frequency scattering approximation. They have shown that the high frequency asymptotic form of the frequency domain representation can be applied beyond a certain point of the contour of the inverse Laplace transformation integral which results in a significant reduction of computation time. Rheinstein [12] investigated the time domain backscattering by perfectly conducting and dielectric spheres illuminated by modulated pulse trains. Using the Fourier series method the scattering of transient EM wave was estimated and various returns were observed in his solutions. However, his achievements were not fully understood due to employing Lorenz-Mie theory which provides no physical interpretation of the scattering
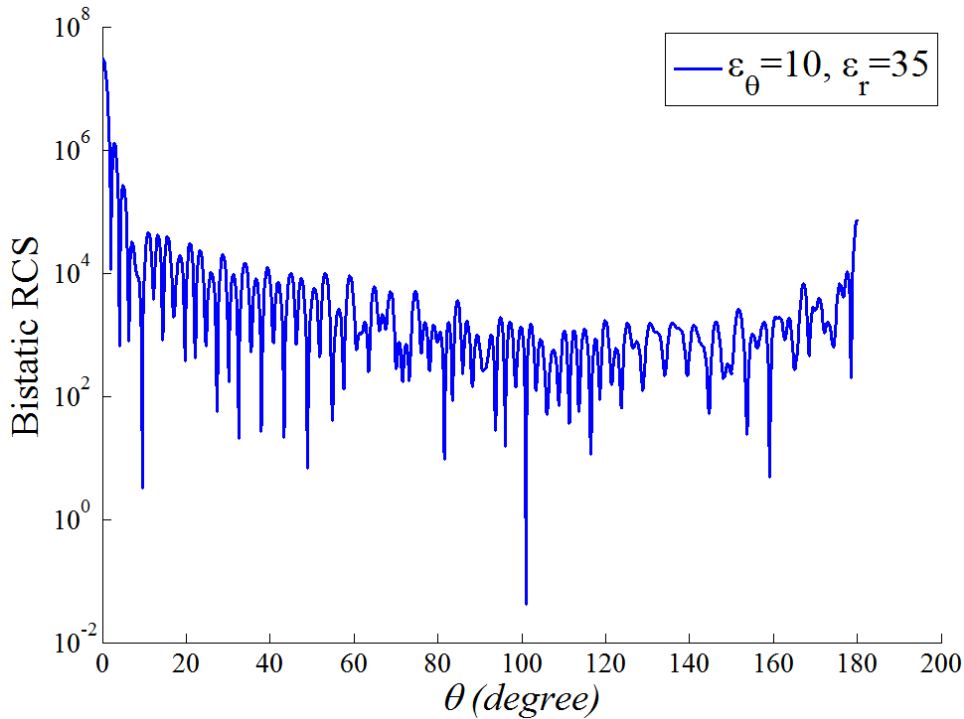
101

mechanisms.

Fig. 5. 2. Bistatic RCS of uniaxial dielectric sphere calculated using Mie series, and $k_0 a = 100$ [45]

To overcome this difficulty, Lock and Laven [6]–[7] estimated the signature of various scattering processes from an isotropic dielectric sphere using the Debye series formulation. This allows the calculation of only a single term of the Debye series at each time rather than the entire Mie series time domain solution which leads to the identification of each individual return in the transient scattering response of the dielectric sphere.

Although the majority of dielectric materials are anisotropic, to the best of our knowledge, the transient response of a uniaxial dielectric sphere using the Mie/Debye series has not yet been investigated. In this chapter, the generalized Mie series solution

102

along with the high frequency approximation from a radially uniaxial dielectric sphere is briefly studied. Using the inverse Laplace transformation and the Mie series-asymptotic combination method [10], the impulse and step responses of a radially uniaxial sphere are calculated in the Second 5.2. In the Section 5.3, the generalized Debye series for the uniaxial sphere is introduced and the results are applied to evaluate the impulse response of each individual term of the Debye series.
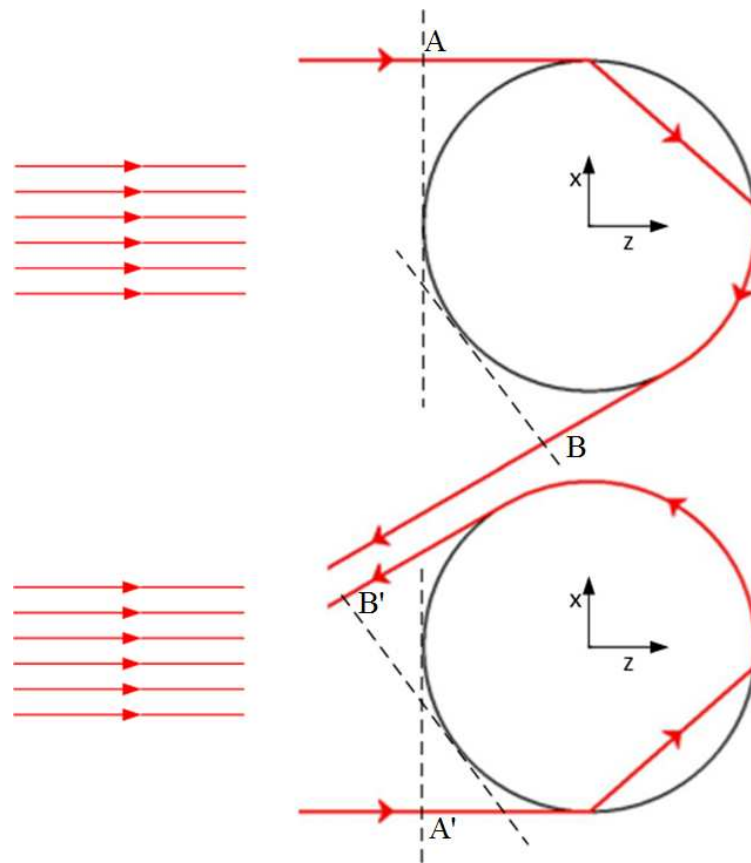

Fig. 5. 3. Pictorial representation of p=1 wave, Shortcut wave

5.2 Mie Series and Watson transformation

Consider a radially uniaxial dielectric sphere with radius a immersed in an incident x-polarized time harmonic plane wave as shown in Fig. 1, traveling in the z-direction where the incident wave is defined by

$$E_i = \hat{a}_x e^{-jk_0 z} = \hat{a}_x e^{-jk_0 r \cos\theta}$$

(5-1)

The sphere has permeability μ_0, and permittivity tensor

$$\bar{\bar{\varepsilon}} = \varepsilon_0 \begin{bmatrix} \varepsilon_r & 0 & 0 \\ 0 & \varepsilon_\theta & 0 \\ 0 & 0 & \varepsilon_\theta \end{bmatrix}$$

(5-2)

where ε_0 is the permittivity of free space and ε_r and ε_θ are the relative permittivities parallel and perpendicular to the optic axis, respectively.

Following the backscattering solution of a radially uniaxial dielectric sphere in the presence of a plane electromagnetic wave derived in Chapter 4, the far-field components are given by

$$E^s = \frac{e^{-jkr}}{jkr} S(\pi)(\cos\phi\, \hat{a}_\theta + \sin\phi\, \hat{a}_\phi)$$

(5-3)

$$S(\pi) = \sum_{n=1}^{\infty} \frac{(-1)^{n+1}}{2} j^n n(n+1)(b_n - c_n)$$

(5-4)

where b_n and c_n are the well-known generalized Mie series coefficients for TM_r and TE_r waves, respectively, and defined as follows

$$
\begin{Bmatrix} b_n \\ c_n \end{Bmatrix}
$$

$$
= \frac{-\begin{Bmatrix} \sqrt{\varepsilon_\theta} \\ 1 \end{Bmatrix} \hat{J}'_n(k_0 a) \begin{Bmatrix} \hat{J}_v(\sqrt{\varepsilon_\theta}k_0 a) \\ \hat{J}_n(\sqrt{\varepsilon_\theta}k_0 a) \end{Bmatrix} + \begin{Bmatrix} 1 \\ \sqrt{\varepsilon_\theta} \end{Bmatrix} \begin{Bmatrix} \hat{J}_v(\sqrt{\varepsilon_\theta}k_0 a) \\ \hat{J}_n(\sqrt{\varepsilon_\theta}k_0 a) \end{Bmatrix}' \hat{J}_n(k_0 a)}{\begin{Bmatrix} \sqrt{\varepsilon_\theta} \\ 1 \end{Bmatrix} \hat{H}_n^{(2)'}(k_0 a) \begin{Bmatrix} \hat{J}_v(\sqrt{\varepsilon_\theta}k_0 a) \\ \hat{J}_n(\sqrt{\varepsilon_\theta}k_0 a) \end{Bmatrix} - \begin{Bmatrix} 1 \\ \sqrt{\varepsilon_\theta} \end{Bmatrix} \begin{Bmatrix} \hat{J}_v(\sqrt{\varepsilon_\theta}k_0 a) \\ \hat{J}_n(\sqrt{\varepsilon_\theta}k_0 a) \end{Bmatrix}' \hat{H}_n^{(2)}(k_0 a)} a_n
$$
(5-5)

where $a_n = \frac{j^{-n}(2n+1)}{n(n+1)}$ $v = \sqrt{n(n+1)AR + \frac{1}{4}} - \frac{1}{2}$ and the anisotropic ratio AR is defined

by $AR = \frac{\varepsilon_\theta}{\varepsilon_r}$. The backscattering transient response $E(t)$ can be evaluated from (5-1) and

(5-3) using the inverse Laplace transformation

$$
E(t) = \frac{1}{2\pi j} \int_{\sigma - j\infty}^{\sigma + j\infty} E(s) e^{st} ds
$$
(5-6)

Where $E(s)$ is given by

$$
E(s) = \frac{E^s(s)}{E^i(s)}
$$
(5-7)

Substituting (5-1) and (5-3) into (5-7) and calculating the backscattering direction

$(\theta = \phi = \pi)$ gives

$$
E(s) = \frac{\sum_{n=1}^{\infty}(-1)^{n+1} j^n n(n+1)(b_n - c_n)}{2rs/c}
$$
(5-8)

Where $s = j\omega$ and c is velocity of light. Equation (5-8) can be expressed as

$$
rE(t) = \frac{1}{2\pi j} \int_{\sigma - j\infty}^{\sigma + j\infty} \frac{\sum_{n=1}^{\infty}(-1)^{n+1} j^n n(n+1)(b_n - c_n)}{\frac{2s}{c} \cdot \frac{a}{c}} e^{st} d(as/c)
$$
(5-9)

Introducing the normalized variables of $\bar{s} = (\sigma + j\omega)a/c$ and $\bar{t} = \left[t - \frac{r}{c} \right] \frac{c}{a}$ (5-9)can be

written as

$$\frac{r}{c}\overline{\boldsymbol{E}}(\bar{t}) = \frac{1}{2\pi j} \int_{\sigma-j\infty}^{\sigma+j\infty} \frac{\sum_{n=1}^{\infty}(-1)^{n+1}j^n n(n+1)(b_n - c_n)}{2\bar{s}} e^{\bar{s}\bar{t}} d\bar{s} \qquad (5\text{-}10)$$

where $\overline{\boldsymbol{E}}(r,\bar{s})$ represents the normalized backscattered field and r is the distance from origin to the observation point and σ represents the loss associated with the dielectric sphere.

The Bromwich integral of (5-10) is determined by numerical techniques such as FFT, Simpson method, etc. However, the computation time can be substantially reduced by employing the asymptotic representation in high frequency region [10]. According to the Aly and Wong's method, the integral in (5-10) is written as the summation of integrals over high and low frequency regions as follows:

$$\frac{r}{c}\overline{\boldsymbol{E}}(\bar{t}) = \frac{1}{2\pi j} \left[\int_{\sigma-j\infty}^{\sigma-j\bar{\Delta}} F_A^S(\bar{s})e^{\bar{s}\bar{t}}d\bar{s} + \int_{\sigma-j\bar{\Delta}}^{\sigma+j\bar{\Delta}} F_M^S(\bar{s})e^{\bar{s}\bar{t}}d\bar{s} \right.$$
$$\left. + \int_{\sigma+j\bar{\Delta}}^{\sigma+j\infty} F_A^S(\bar{s})e^{\bar{s}\bar{t}}d\bar{s} \right] \qquad (5\text{-}11)$$

where F_M^S corresponds to the generalized Mie series solution and F_A^S represents the asymptotic expression in a high frequency region. The convergence result of (5-11) relies on the choice of $\bar{\Delta}$. For the uniaxial sphere, we found that $\bar{\Delta} = 30$ is adequate and increasing this value has no more influence on transient scattering response of the uniaxial sphere. Adding and subtracting the term $\int_{\sigma-j\bar{\Delta}}^{\sigma+j\bar{\Delta}} F_A^S(\bar{s},\theta)e^{\bar{s}\bar{t}}d\bar{s}$ from (5-11), the transient scattering response is expressed as

$$\frac{r}{c}\boldsymbol{E}_\theta^S(\theta,\bar{t}) = \int_{\sigma-j\bar{\Delta}}^{\sigma+j\bar{\Delta}} e^{\bar{s}\bar{t}}(F_M^S(\bar{s}) - F_A^S(\bar{s}))d\bar{s} + L^{-1}(F_A^S(\bar{s})) \qquad (5\text{-}12)$$

106

where L^{-1} denotes the inverse Laplace transform operation and can be calculated analytically.

Following the high frequency scattering approximation for a radially uniaxial dielectric sphere proposed in [47], the generalized Mie series summation is replaced by a rapidly converging contour integral using the modified Watson transformation. The solution is then split into the geometric optics and diffracted field contributions. The coefficients associated with the geometric optics portion are replaced by their equivalent Debye series formulation. The results are simplified and then computed using the saddle point method. An expression for the high frequency backscattered field is proposed as follows

$$F_M^{\bar{s}}(\bar{s},\theta) = -\frac{1}{4}\left[\frac{N - \sqrt{1 + \frac{AR - 1}{4(Nk_0a)^2}}}{N + \sqrt{1 + \frac{AR - 1}{4(Nk_0a)^2}}} + \frac{N - 1}{N + 1}\right]e^{2\bar{s}}g(s) \qquad (5\text{-}13)$$

where $N = \sqrt{\varepsilon_\theta}$ and $AR = \frac{\varepsilon_\theta}{\varepsilon_r}$ and $g(s) = 1 - O((\bar{s})^{-1})$. For the choice of $\bar{\Delta} = 30$, (5.13) can be approximated as

$$F_M^s(\bar{s},\theta) \approx -\frac{1}{2}\frac{N-1}{N+1}e^{2\bar{s}} \qquad (5\text{-}14)$$

Substituting (5-14) into (5-12), we obtain

$$\frac{r}{c}E_\theta^s(\theta,\bar{t}) = \int_{\sigma-j\bar{\Delta}}^{\sigma+j\bar{\Delta}} e^{st}(F_M^s(\bar{s},\theta) - F_A^s(\bar{s},\theta))d\bar{s} - \frac{1}{2}\frac{N-1}{N+1}\delta(\bar{t}+2) \qquad (5\text{-}15)$$

where the second term of (5-15) displays the contribution of the geometrical optics portion. The integral of (5-15) is carried out using numerical techniques with the limits determined by asymptotic solution. The transient response of the isotropic and uniaxial dielectric spheres characterized by $\varepsilon_\theta = 10$, $\varepsilon_r = 10$ and 35 for the first four returns are plotted in Fig. 5.4.
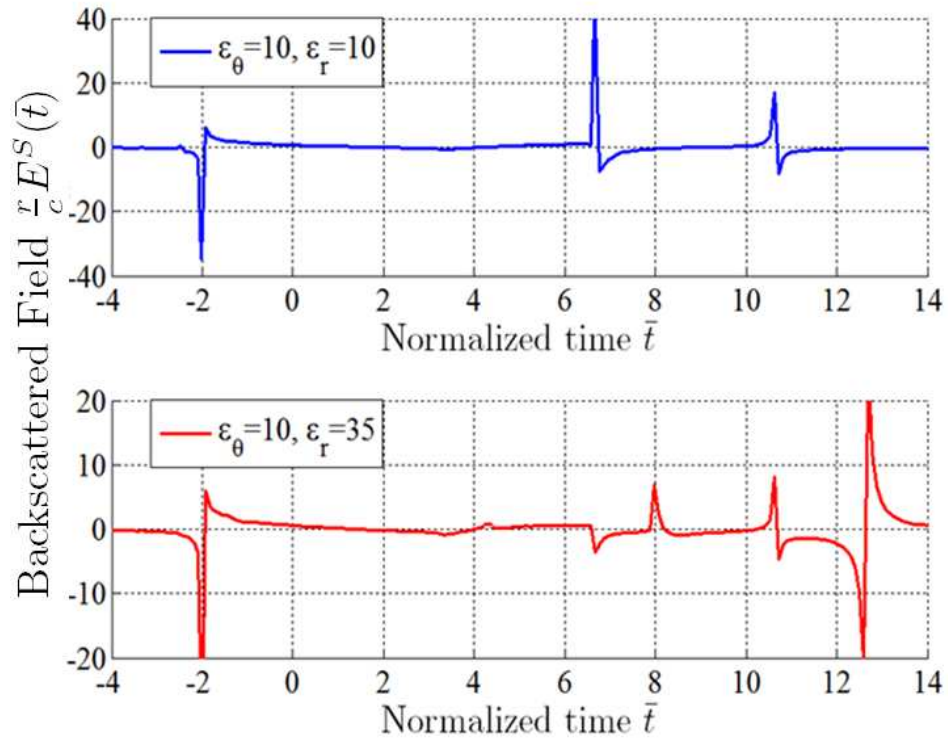

Fig. 5. 4. Transient scattering from isotropic and uniaxial spheres using the Mie series solution

The main features of the transient response from isotropic sphere are already identified in [10]. As observed, the first return from isotropic and uniaxial spheres due to paraxial rays reflected from the front surface of sphere, geometrical optics reflection (GO), appears at $\bar{t} = -2$. The optical path of all other returns will be referenced to this return. After GO

return, the second impulse from isotropic/uniaxial sphere arrives at $\bar{t} = \pi$. This return accounts for the arrival of the exterior creeping waves which originate from the incident rays traveling along the exterior surface of the sphere. Comparing the signature of isotropic sphere with that of obtained from uniaxial sphere reveals that the arrival time of the surface waves has weak dependence on the uniaxiality. However, the energy coupled to these waves is found to be a strong function of ε_r as well as ε_θ [10]. As observed in Fig. 5.5, the amplitude of the exterior creeping waves reduces/strengthens with increasing/decreasing ε_r for a fixed value of ε_θ.

The third and fourth returns from isotropic sphere are generated by short cut and upper apex waves respectively as shown in Fig. 5.6, and their arrival time can be expressed as [10]

$$\bar{t}_{sc} = 2\sqrt{\varepsilon_\theta - 1} + \left(\pi - 2\cos^{-1}\frac{1}{\sqrt{\varepsilon_\theta}}\right)$$

(5-16)

$$\bar{t}_{ua} = 4\sqrt{\varepsilon_\theta} - 2$$

(5-17)

The shortcut and upper apex waves are also replicated as negative and positive smeared impulse returns from the uniaxial sphere respectively but their magnitudes are degraded when compared to those obtained from the isotropic sphere. However, there are some unknown returns in the response of positive/negative uniaxial sphere arriving after/before shortcut and upper apex waves. By varying ε_r, we found that the arrival time of shortcut and upper apex waves are not sensitive to anisotropy, but depending on the type of uniaixality the location of unknown waves move forward/backward along time axis

which concludes the strong dependency of unknown waves to the variation of ε_r. However, there is no general rule of characterizing the unknown returns in terms of the arrival time, the magnitude and origin of these waves, using Mie series solution. Therefore further studies are required to improve our understanding of unknown waves.
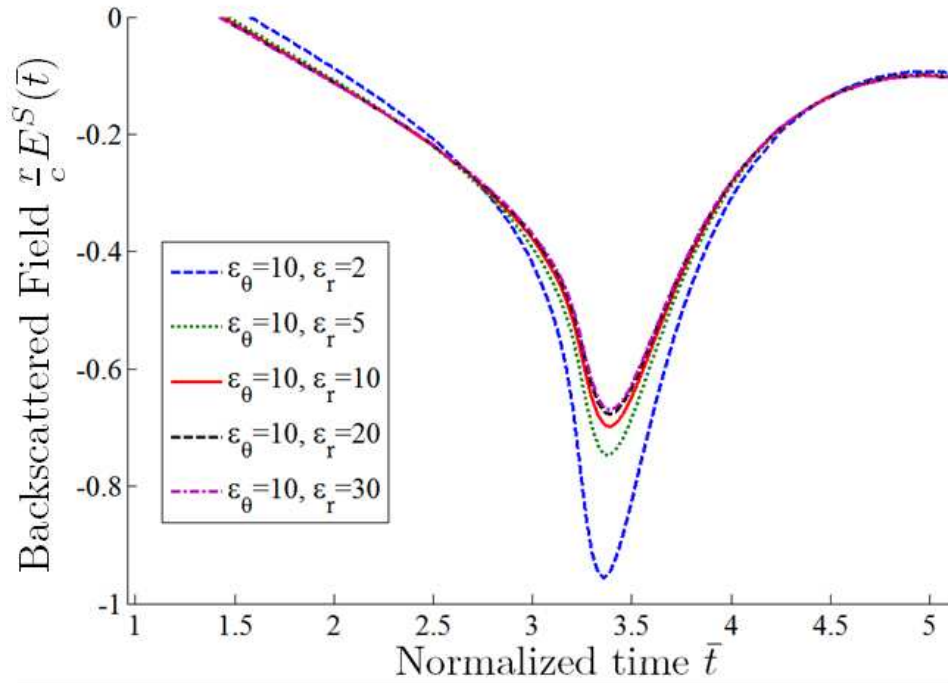

Fig. 5. 5. The effect of ε_r variation on creeping wave

The transient response of uniaxial dielectric sphere in the presence of other incident fields such as short electromagnetic pulse, step excitation, ramp excitation, etc. can now be evaluated by convolution theorem. The step response of a uniaxial and isotropic spheres characterized by $\varepsilon_\theta=10$, $\varepsilon_r=35$ and 10 are depicted in Fig. 5.7. It is observed that several positive/negative jumps appear in the step response of uniaxial as well as isotropic spheres accounting for the arrival of geometrical optics, shortcut and upper apex waves, respectively [10]. It is of interest to note that there are some additional positive

110

and negative jumps appear at $\bar{t}=8$ and 12.6. These jumps are corresponding to unknown returns that appear in impulse response of uniaxial sphere.
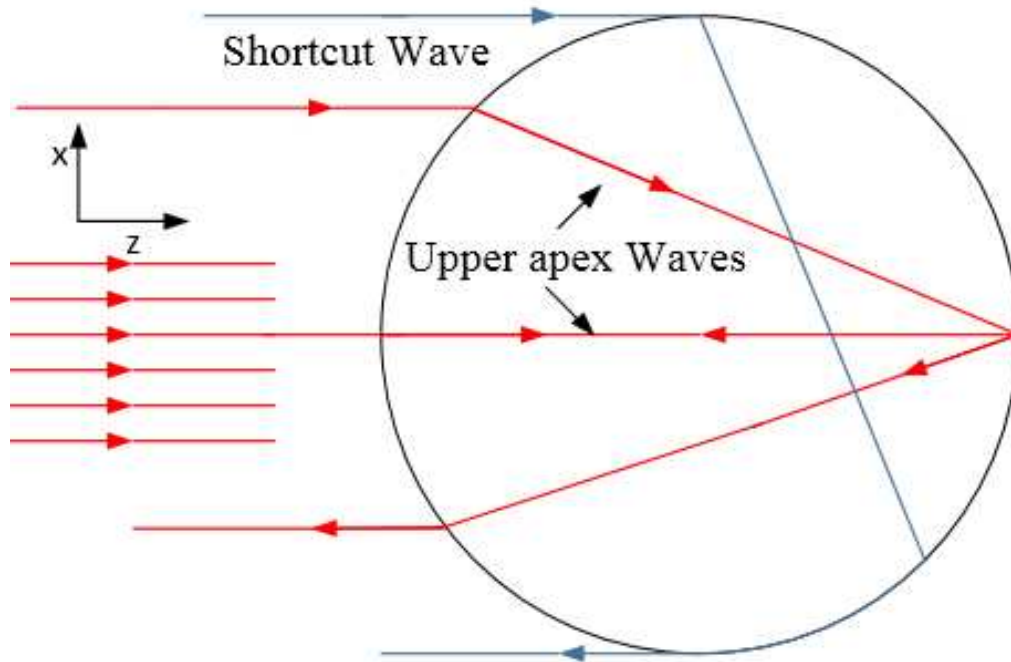

Fig. 5. 6. Pictorial representation of shortcut and upper apex waves

In order to identify the unknown returns and provide a physical interpretation of the problem, the generalized Debye series for uniaxial sphere is introduced in the next section and this method is applied to characterize each individual return that appears in transient response of uniaxial sphere.
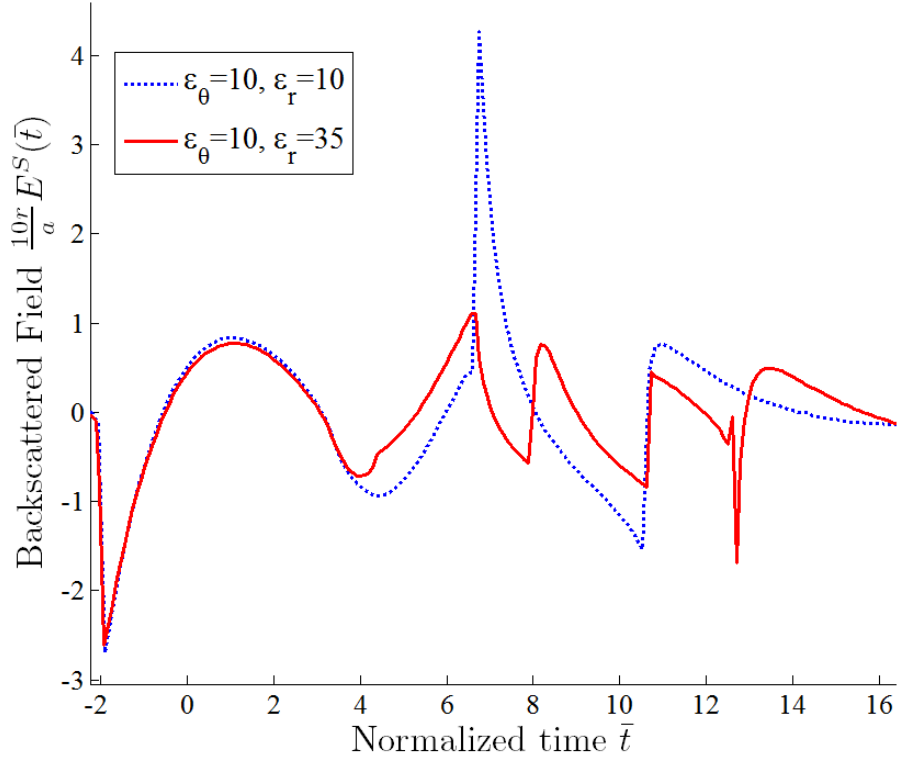
Fig. 5. 7. Impulse and step responses of isotropic and uniaxial sphere

5.3 The transient scattering response of the uniaxial sphere using generalized Debye series solution

To improve our understanding of the scattering process from uniaxial dielectric sphere, the transient response of a uniaxial sphere is evaluated using Debye series solution. This can be achieved by replacing the Mie series coefficients of (5-5) by their equivalent Debye series summation of (3-90) and evaluating the transient response of each individual term of Debye series using numerical techniques. This leads to the identification of each individual return in the transient response of uniaxial dielectric sphere rather than the entire Mie series time domain solution.

The first three terms of the generalized Debye series are depicted in Fig. 5.8. The

sphere is characterized by ε_θ=10, ε_r=35, and $\bar{\sigma}$=0.07. Except for P=0 wave, two impulse returns for each internally reflected wave of order P are observed in backscattered direction confirming the birefringency phenomenon in the uniaxial medium. This suggests the existence of ordinary and extraordinary waves in the transient response of the uniaxial dielectric sphere.

For P=1, the ordinary wave (O-wave) represents the shortcut wave appearing in the isotropic sphere response and arrives at 6.5 whilst extraordinary wave (E-wave) arrives at 8. The time delay between these returns is initially due to the possible velocity and shortcut path differences of E- and O-waves.
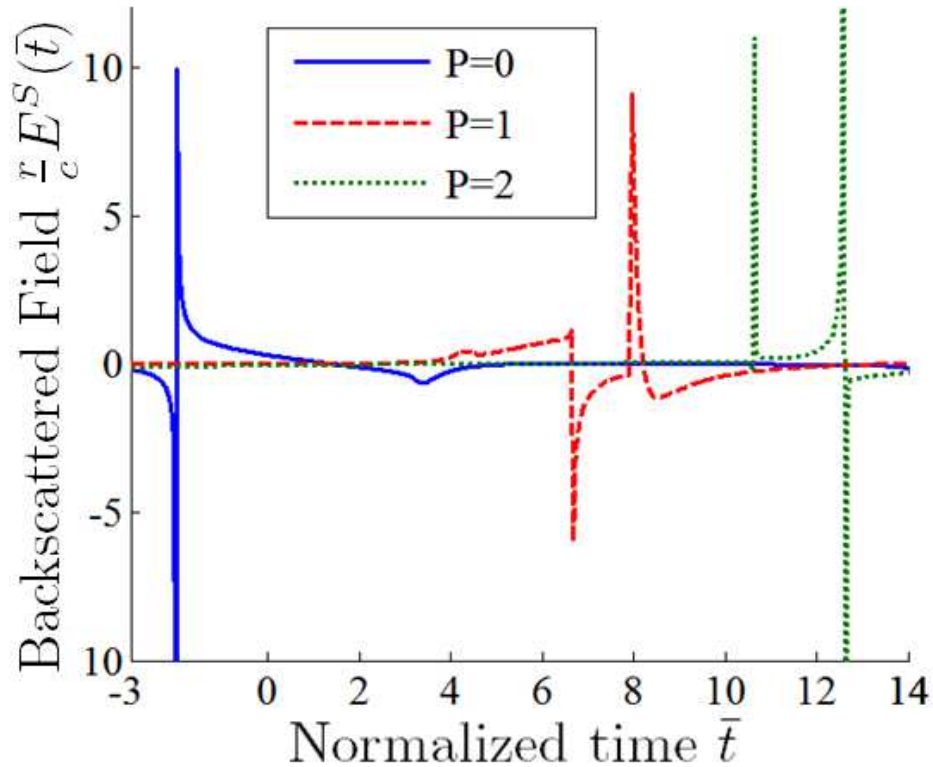

Fig. 5. 8. The first three terms of Debye series for a uniaxial sphere characterized by ε_θ=10, ε_r=35

For P=2, the O-wave appears at 10.65 which is identical to the arrival time of upper apex waves by ray tracing theory in (5-17) whilst the E-wave appears at 12.6.

The uniaxial sphere is characterized by $\varepsilon_\theta=10$ and $\varepsilon_r=2$, 15, 25, 35, and 50. By increasing ε_r, the arrival time of E-wave returns is significantly increased whilst variation of ε_r has no influence on the arrival time of O-wave return which is equal to $\bar{t}=6.65$. These results were also observed earlier in the transient response of the uniaxial sphere using Lorentz-Mie theory. Note that increasing ε_r reduces the E-wave amplitudes and has a small effect on O-wave amplitudes. The results are summarized in Table 5.1.
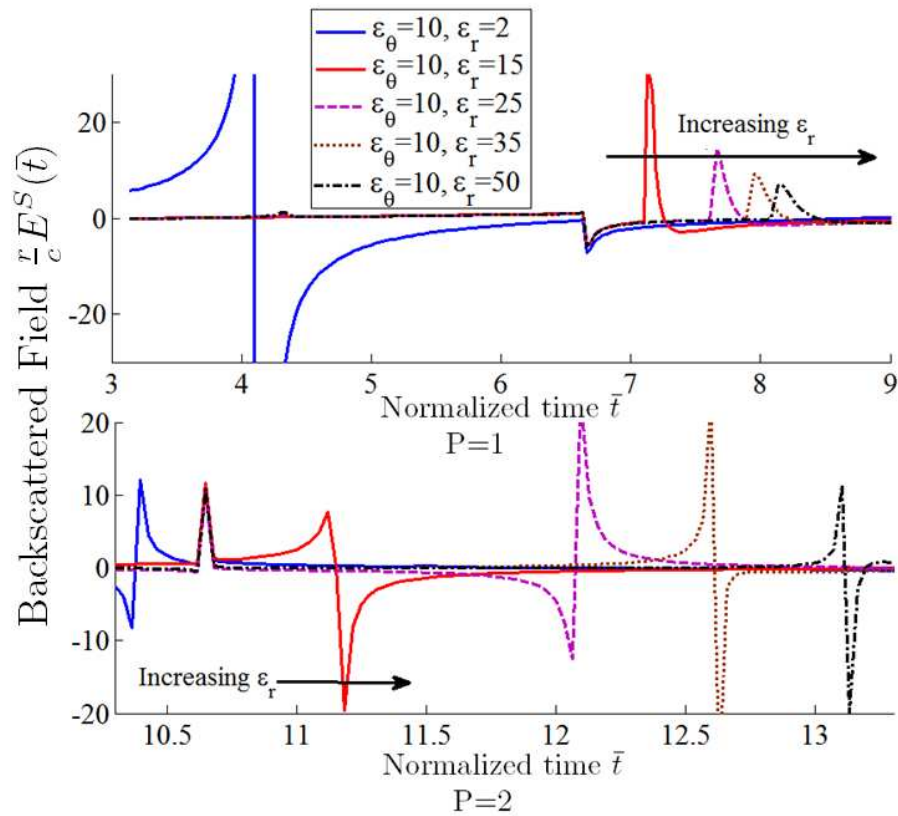

Fig. 5. 9. The effect of ε_r variation on P=1–2 E-waves

It is also of interest to note that the E-wave returns arrive before O-wave returns with

relatively larger amplitude when sphere is negative uniaxial $\varepsilon_r < \varepsilon_\theta$. This implies that the velocity and traveling path associated with E-waves in negative uniaxial sphere are faster/shorter when compared to the positive uniaxial case.

TABLE 5.1

The arrival time of the first three impulse returns for various ε_r values

ε_θ	ε_r	P=0 Arrival Time	P=1 Arrival Time		P=2 Arrival Time	
			O-Wave	E-Wave	O-Wave	E-Wave
10	2	-2	6.65	4.1	10.65	10.3
10	10	-2	6.65	6.65	10.65	10.65
10	15	-2	6.65	7	10.65	11.2
10	25	-2	6.65	7.6	10.65	12.1
10	35	-2	6.65	8	10.65	12.6
10	50	-2	6.65	8.1	10.65	13.2

5.4 Conclusion

The scattering of a transient electromagnetic wave by a radially uniaxial dielectric sphere is evaluated using two well-known methods: Lorenz-Mie theory and Debye series formulation. In the first approach, the time domain scattering by a uniaxial dielectric

sphere is computed using the Mie series solution and the results are compared with those obtained for the isotropic dielectric sphere. Except for some unknown waves, the impulse returns of isotropic sphere are replicated in the response of the uniaxial dielectric sphere. However, the Mie series solution does not provide any physical interpretation of the problem and subsequently the characteristics of unknown returns were not fully understood using this method. To overcome this difficulty, the generalized Debye series for the uniaxial sphere is introduced and the results are applied to study each individual term in the Debye series. This allows the identification of unknown returns observed in the Mie series solution. The results confirm the birefringency phenomenon in the uniaxial sphere and unknown returns are equivalent to extraordinary waves. The effect of ε_r variation on P=1–2 waves are also investigated.

Chapter 6 Transient Electromagnetic Scattering by a Radially Uniaxial Dielectric Sphere: Ray Tracing Theory

Ray tracing theory for a radially uniaxial dielectric sphere illuminated by an incident beam of parallel rays is presented in this paper. Reflection and transmission of plane waves obliquely incident on the spherical interface between air-uniaxial is briefly examined and the general formulations for phase velocities as well as the refractive indices of the ordinary and extraordinary waves propagating in a birefringent medium are investigated. The ray tracing method is implemented for both ordinary and extraordinary rays and the results are applied to evaluate the propagation paths and arrival times of the shortcut and upper apex wave returns appearing in the transient scattering response of a uniaxial dielectric sphere. The effect of the variation in relative permittivity on the arrival times of P=1 waves is studied and the results of the ray tracing method are compared with those computed using Mie and Debye series solutions with good agreement.

6.1 Introduction

The process of electromagnetic scattering by isotropic and nonisotropic dielectric spheres has been an attractive subject over the past few decades. A rigorous EM scattering solution by an isotropic dielectric sphere is introduced in [1]. Wong and Chen [2] developed a generalized Mie series scattering solution for the anisotropic dielectric sphere by deriving the spherical potential wave functions in a radially uniaxial sphere and computing the scattering wave coefficients in the uniaxial-air boundary surface. Although the Mie series solution is exact, the lack of constructing a physical model of the scattering process along with its computational complexity limits the application of this method on

describing the mechanisms causing many optical phenomena such as primary/secondary rainbow, corona and glory. These difficulties were partially resolved by introducing the Debye series method for plane wave scattering by an isotropic dielectric sphere [5]. According to this method, the Mie series coefficients can be represented by an infinite series of partial wave contributions that are diffracted, reflected and refracted following by p-1 internal reflections in the sphere as shown in Fig. 6.1. This procedure was also applied to a radially uniaxial dielectric sphere by deriving the magnetic and electric vector potentials both inside and outside the sphere and calculating the generalized Fresnel coefficients at the air-uniaxial boundary interface of the sphere in [45]. However, there are a number of scattering problems that cannot be examined by a frequency domain solution of the Mie and Debye series methods and consequently, other powerful methods such as time domain representations of the Mie and Debye series solutions were introduced.

The time domain response waveform in the radar scattering context was first introduced by Kennaugh who estimated the impulse response of the field scattered from a perfectly conducting sphere using an extremely simple approximation [8] and [9]. Aly and Wong [10] obtained the transient response of a dielectric sphere using a high frequency scattering approximation. This problem was also studied by Lock and Laven [6] and [7] using the Debye series formulation. This allowed the identification of each individual impulse return observed in the transient response of a dielectric sphere.

The transient scattering response of a radially uniaxial dielectric sphere for the first four impulse returns was also studied by authors using Lorentz-Mie theory in [48]. The result revealed the presence of some unknown returns in the transient response of the

uniaxial sphere arriving after/before shortcut and upper apex waves. To characterize the unknown returns, the problem was investigated using the Debye series method. It was shown that two impulse returns appear for each internally reflected wave of order P confirming the birefringency phenomenon in the uniaxial sphere. Although the Mie and Debye theories were successful in describing several particular features of the transient EM scattering by the uniaxial sphere, lack of a simple graphical computation for determining the features of impulse returns, e.g., arrival time, travel path, velocity, refractive index, etc., required the ray tracing modeling in the uniaxial dielectric sphere.

In the past, ray tracing has been frequently used to describe many complex scattering problems. In 1637, Descartes used ray tracing to understand the formation of primary and secondary rainbows [49]. Newton subsequently extended the theory to explain the colors of the rainbow. Laven [4] applied ray tracing along with the Debye series solution to compute the arrival time of each individual ray of order P in the transient response of the isotropic dielectric sphere and proposed a simple description of the formation of optical phenomena such as glory and corona. Ray tracing was also studied for an anisotropic plane parallel plate by Simon in [50]. This was achieved by computation of the reflection and refraction wave angles in the air-anisotropic and anisotropic-air boundaries in [51]. Although ray tracing cannot match the accuracy of Mie and Debye theories, it remains a valuable tool because it can provide intuitive explanations of many features of the field scattered by a sphere without requiring the use of complicated mathematics.

To improve our understanding of the impulse returns observed in the transient response of the uniaxial dielectric sphere, ray tracing in the uniaxial sphere is introduced in this dissertation. In the following section, the generalized Snell's laws for the air-uniaxial and

uniaxial-air boundaries of the sphere are briefly studied and general formulas for velocity and refractive indices of ordinary and extraordinary waves are derived. Ray tracing for ordinary and extraordinary wave returns of order P=1 are investigated in the Section 6.3 and the results are applied to propose general formulations for computing the arrival times of extraordinary and ordinary waves in the uniaxial sphere. The results are validated by good agreement between Mie, Debye, and ray tracing methods.

6.2 Waves and Rays in a birefringent medium

Consider a radially uniaxial dielectric sphere with radius a immersed in an incident x-polarized time harmonic plane wave traveling in the z-direction where the incident wave is defined by

$$\boldsymbol{E_i} = \hat{a}_x e^{-jk_0 z} = \hat{a}_x e^{-jk_0 r \cos\theta}$$

(6-1)

The sphere has permeability μ_0 and a permittivity tensor of the form

$$\bar{\bar{\varepsilon}} = \varepsilon_0 \begin{bmatrix} \varepsilon_r & 0 & 0 \\ 0 & \varepsilon_\theta & 0 \\ 0 & 0 & \varepsilon_\theta \end{bmatrix}$$

(6-2)

where ε_0 is the relative permittivity in the air and ε_r and ε_θ are the relative permittivities parallel and perpendicular to the optic axis respectively. The EM wave in the air region is modeled as a beam of parallel rays incident on the sphere as shown in Fig. 6.1. Each individual ray is characterized by its impact factor b. The central ray in Fig. 6.1 is denoted by b=0, whilst $b = \pm 1$ represent the edge rays tangential to the top and bottom of the dielectric sphere respectively.

When an incoming ray encounters the interface of the uniaxial sphere at r=a, two rays,

120

namely, ordinary and extraordinary waves propagate inside the sphere and after a number of reflections, they are transmitted out of the sphere. The solution of the Maxwell equations in a radially uniaxial sphere yields two possible phase velocities as follows [51]

$$u' = u_o$$

(6-3)

$$u'' = \sqrt{u_e^2 + (u_0^2 - u_e^2)(\widehat{\boldsymbol{S}}.\widehat{\boldsymbol{r}})^2}$$

(6-4)

where u' and u'' are the velocities of the ordinary and extraordinary rays respectively. $u_0^2 = \frac{1}{\mu_0 \varepsilon_0 \varepsilon_\theta}$, $u_e^2 = \frac{1}{\mu_0 \varepsilon_0 \varepsilon_r}$ and $\boldsymbol{S}$ is the unit vector normal to the wave front. It is of interest to note that the value of u'' varies between u_o and u_e. For $\boldsymbol{S} \parallel \boldsymbol{r}$ and $\boldsymbol{S} \perp \boldsymbol{r}$ this value is equal to u_o and u_e respectively whilst the velocity of the ordinary wave u' is constant and independent of the wave propagation direction.

Following the constitutive relationship of the principal $\boldsymbol{E}$ and $\boldsymbol{H}$ components in this medium, the electric field components of the ordinary wave $\boldsymbol{E}'$ and $\boldsymbol{D}'$ lie in a plane perpendicular to the optic axis. Therefore the unit vectors representing the wave propagation S and energy flow R_o of the ordinary wave are in the same direction as shown in Fig. 6.2.
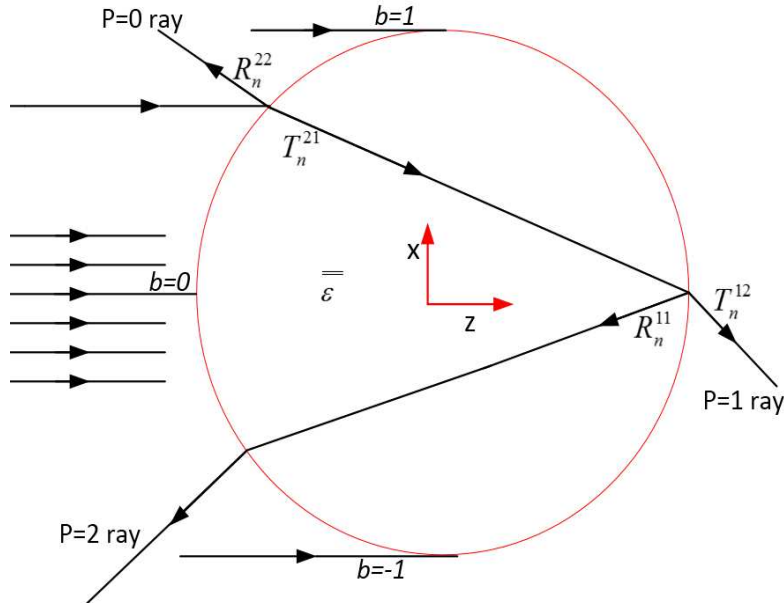
Fig. 6.1. A plane wave approaching a radially uniaxial dielectric sphere

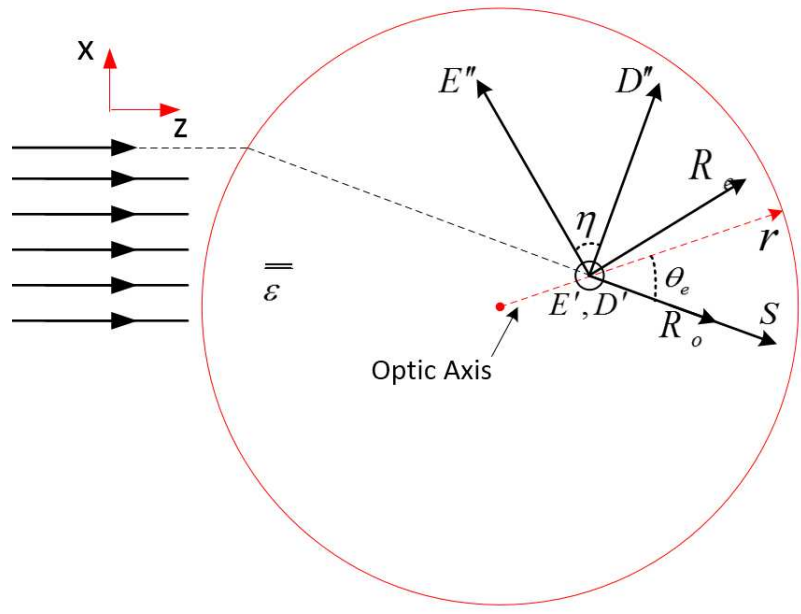Fig. 6.2. Wave and ray in a radially uniaxial sphere

The extraordinary wave however is linearly polarized by both $\boldsymbol{E''}$ and $\boldsymbol{D''}$ perpendicular

to the unit vector $\boldsymbol{S}$ but these components are no longer in the same direction. As a result,

the directions of wave propagation S and energy flow R_e are not parallel and the angle between them is given by [51]

$$\eta = \pm \cos^{-1} \frac{n_o^2 + (n_e^2 - n_o^2) \cos \theta_e{}^2}{\sqrt{n_o^4 + (n_e^4 - n_o^4)(\cos \theta_e)^4}} \tag{6-5}$$

where the positive/negative sign refers to negative/positive uniaxiality and θ_e is the angle between unit normal vector S and optic axis r as shown in Fig. 6.2. A ray velocity is also defined in [51] due to the optical path difference of the wave and energy flux (ray) as follows

$$v'' = \frac{u''}{\cos \eta} \tag{6-6}$$

6.3 Reflection and refraction in the air-uniaxial boundary of the uniaxial sphere

We define a local coordinate system $r' - \theta'$ with origin located at the point of ray incidence on the boundary surface of the uniaxial sphere. The r' axis is parallel to the radius of the sphere at the point of incidence and the $r' - \theta'$ plane is assumed to be the plane of incidence in our local coordinate system.

Consider a linearly polarized plane wave with a unit vector of S_i normal to the incident wave front where θ_i is the incident angle as shown in Fig. 6.3. We denote by S_r, S_o, and S_e the unit vectors normal to the reflected wave front and refracted wave fronts of the ordinary and extraordinary waves where θ_r is defined as the reflected wave angle, and θ_o and θ_e are the refracted angles of the ordinary and extraordinary waves respectively. R_o and R_e, are also defined as the unit vectors normal to the ordinary and extraordinary ray

123

fronts. Writing the electric and magnetic field boundary conditions at the air-uniaxial interface and applying the phase matching conditions, we found

$$S_i.\,\theta' = S_r.\,\theta' \qquad (6\text{-}7)$$

$$\frac{1}{u_o}(S_o.\,\theta') = (S_i.\,\theta') \qquad (6\text{-}8)$$

$$\frac{1}{v''}(S_e.\,\theta') = (S_i.\,\theta') \qquad (6\text{-}9)$$

where the first equation is recognized as Snell's law and the second and third equations are known as the generalized Snell's law [51].

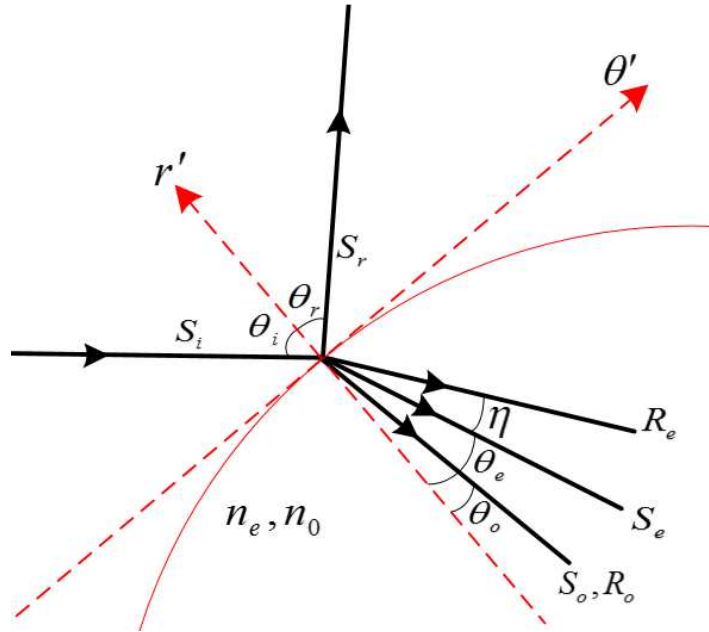Fig. 6.3. Incident wave approaching the air-uniaxial interface

Note that $S_e.\,\theta' = \sin\theta_e$ where where θ_e is shown in Fig. 6.3. Applying (6-3)–(6-5) to (6-7)–(6-9), θ_e and θ_o for a given θ_i are expressed as

124

$$\sin \theta_i = n_o \sin \theta_o \tag{6-10}$$

$$\sin \theta_i = N'' \sin \theta_e \tag{6-11}$$

where $n_o = c/u_o$, $n_e = c/u_e$ and c is the speed of light and $N'' = c/u''$ which can be written as follows:

$$N'' = \frac{n_e n_o}{\sqrt{n_o^2 + (n_e^2 - n_o^2)cos^2\theta_e}} \tag{6-12}$$

Substituting (6-12) into (6-11) gives

$$\cos \theta_e = \frac{\sqrt{n_e^2 n_o^2 - n_o^2 \sin^2 \theta_i}}{\sqrt{n_e^2 n_o^2 + (n_e^2 - n_o^2) \sin^2 \theta_i}} \tag{6-13}$$

or

$$\sin \theta_e = \frac{n_e \sin \theta_i}{\sqrt{n_e^2 n_o^2 + (n_e^2 - n_o^2) \sin^2 \theta_i}}. \tag{6-14}$$

6.4 Internal reflection in the uniaxial-air boundary interface of a uniaxial sphere

Following the reflection and transmission in the boundary of uniaxial-air media reported by Simon [51], four possible internal reflection cases in the boundary surface of the uniaxial dielectric sphere should be considered

1. The incident and reflected waves are ordinary (O-O wave)

2. The incident wave is ordinary and reflected wave is extraordinary (O-E wave)

125

3. The incident wave is extraordinary, and the reflected wave is ordinary(E-O wave)

4. The incident and reflected waves are both extraordinary (E-E wave)

6.4.1   The incident and reflected waves are ordinary

Let u_o be the phase velocity of the incident and reflected waves and let $\boldsymbol{S_o}$ and $\boldsymbol{S'_o}$ be the unit vectors normal to the incident and reflected wave fronts in Fig. 6.4. Applying the phase matching conditions of the tangential electric fields yields

$$\frac{\boldsymbol{S_o}.\boldsymbol{\theta'}}{u_o} = \frac{\boldsymbol{S'_o}.\boldsymbol{\theta'}}{u_o}$$

(6-15)

which implies that θ_o and θ'_o are identical.
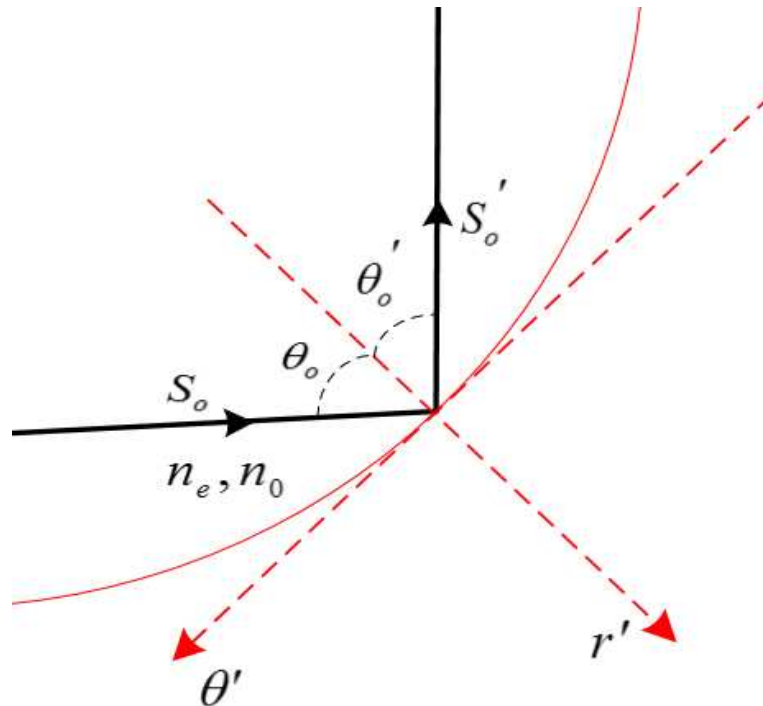

Fig. 6.4. The incident and refracted waves are ordinary in a uniaxial-air boundary surface

126

6.4.2 The incident wave is extraordinary and reflected wave is ordinary

We define $\boldsymbol{S_e}$ and $\boldsymbol{R_e}$ as the unit vectors normal to the incident wave and ray fronts respectively and u'', v'' as their corresponding phase velocities in Fig. 5. $\boldsymbol{S_o'}$ and u_o' are also employed as the unit vector normal to the reflected wave and its phase velocity respectively. Applying the boundary conditions gives

$$\frac{\boldsymbol{S_e}.\boldsymbol{\theta'}}{u''} = \frac{\boldsymbol{S_o'}.\boldsymbol{\theta'}}{u_o'}$$

(6-16)

Substituting (6-4) into (6-16) and deriving the angles correspond to $\boldsymbol{S_e}.\boldsymbol{r'}$ and $\boldsymbol{S_o'}.\boldsymbol{r'}$, the (6-16) becomes

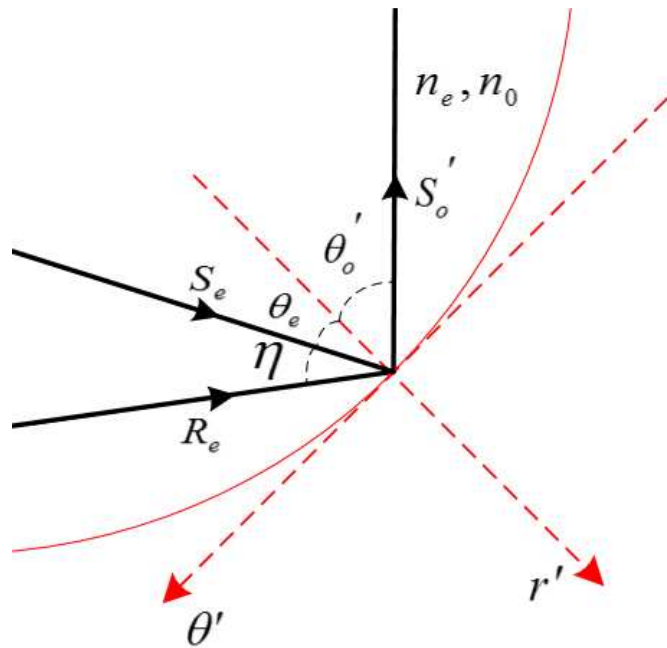$$N'' \sin \theta_e = n_o. \sin \theta_o'$$

(6-17)

Fig. 6.5. The incident and reflected waves are extraordinary and ordinary respectively

127

Therefore, θ'_o for a given θ_e is found by the following equation

$$\sin \theta'_o = \frac{n_e}{\sqrt{n_o^2 + (n_e^2 - n_o^2)cos^2\theta_e}}$$

(6-18)

6.4.3 The incident wave is ordinary and reflected wave is extraordinary:

We denote by N_o and u_o the refractive index and velocity of incident ordinary wave and by S'_e and u'_e the refractive index and phase velocity of the reflected extraordinary wave in Fig. 6.6.
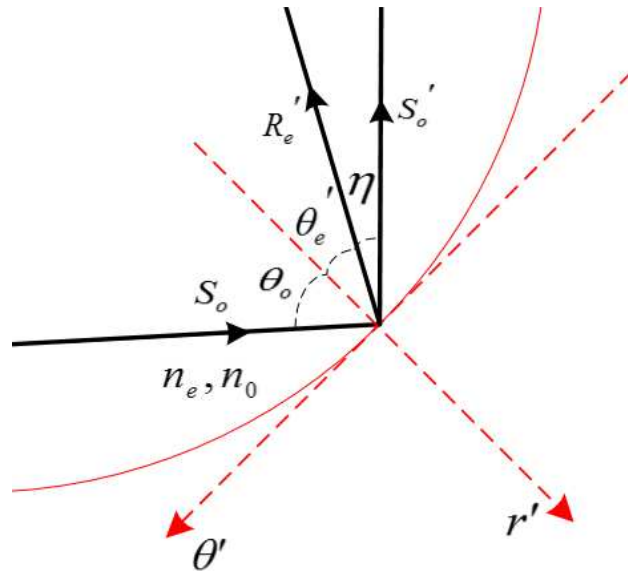

Fig. 6.6. The incident and reflected waves are ordinary and extraordinary respectively
Applying the boundary condition at the uniaxial-air boundary, we found

$$n_o \sin \theta_o = N'' \sin \theta'_e$$

(6-19)

128

where θ_o and θ_e' are the incident and reflection angles respectively. Equation (6-19) can be written as

$$\cos \theta_e' = \frac{\sqrt{n_e^2 - n_o^2 \sin^2 \theta_o}}{\sqrt{n_e^2 + (n_e^2 - n_o^2) \sin^2 \theta_o}} \qquad (6\text{-}20)$$

or

$$\sin \theta_e' = \frac{n_e \sin \theta_o}{\sqrt{n_e^2 + (n_e^2 - n_o^2) \sin^2 \theta_o}} \qquad (6\text{-}21)$$

6.4.4 The incident wave is extraordinary and reflected wave is extraordinary:

Using the phase matching condition in the boundary interface of the uniaxial sphere, we obtain

$$N'' \sin \theta_e = N'' \sin \theta_e' \qquad (6\text{-}22)$$

where θ_e and θ_e' are incident angle and reflection angles shown in Fig. 6.7. Equation (6-22) implies that incident and reflection angles in this case are identical.
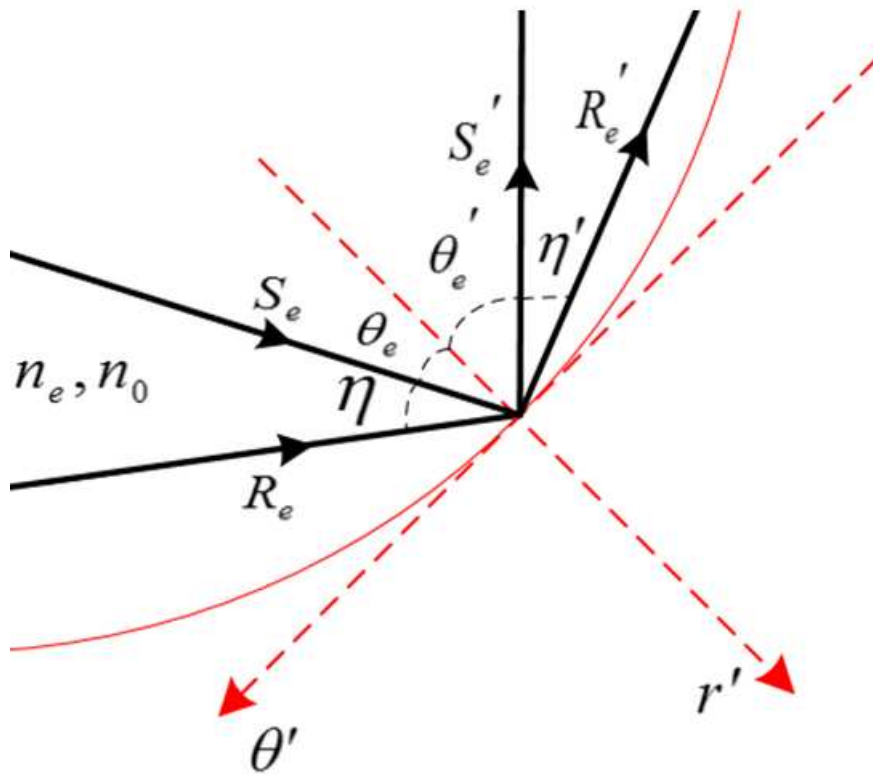
Fig. 6.7. The incident and reflected waves are both extraordinary

6.5 Waves and rays propagating in a radially uniaxial sphere

Using the results obtained in the previous section, the ray tracing for the shortcut waves in a radially uniaxial sphere is evaluated. Our investigations reveal that unlike other types of uniaxial media, the extraordinary wave and ray paths no longer propagate on a straight line when traveling in a radially uniaxial sphere due to the continuous variation of the angle between wave propagation and optic axis, e.g., $\theta_e(n)$, $\theta_e(m)$, $\theta_e(k)$ in Fig. 6.8 Consequently the energy flux and wave propagation travel on plane curves, which depending on the type of uniaxiality, positive/negative, are concave /convex curve toward the center of the sphere.

To determine the wave and ray paths corresponding to the extraordinary wave, the propagation path is split into N equal sections and introducing a fictitious boundary between each segments, the sphere is divided into small dielectric rings as shown in Fig. 6.9.
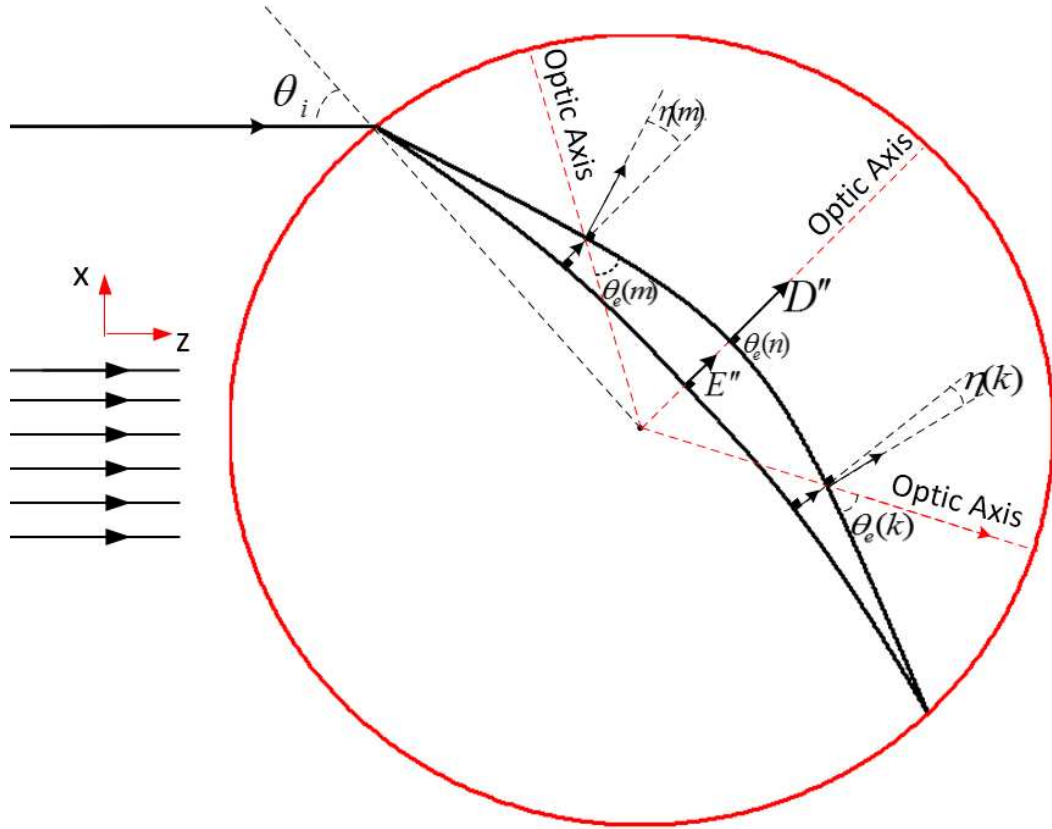
Fig. 6.8. Extraordinary wave and ray in a uniaxial dielectric sphere

Assuming negligible variation of θ_e and η over the sections, the rings can now be characterized by electric permittivity tensor of $\bar{\bar{\varepsilon}}$ but different optic axis directions, e.g., $r'(1), r'(2), r'(3)$ in Fig. 6.9. Starting from the incident point of each ray on the boundary surface of air-uniaxial, the refraction angle is obtained using (6-13) or (6-14) where the incident angle is acquired by $\theta_i = \frac{\pi}{2}b$ in which b represents the impact factor.

Using (6-5) the angle between $\boldsymbol{E}''$ and $\boldsymbol{D}''$ of the first segment is computed and by updating the wave and ray paths in the first section, they are now preserved as the incident wave and ray for the second medium, m=2. The same procedure is applied to determine the refraction angle as well as the angle between $\boldsymbol{E}''$ and $\boldsymbol{D}''$ of the next segments. Applying boundary conditions on the fictitious interfaces, the refraction angles of the segments are given by

$$\frac{\boldsymbol{S}_e(m).\boldsymbol{\theta}'(m)}{u''(m)} = \frac{\boldsymbol{S}_e(m+1).\boldsymbol{\theta}'(m+1)}{u''(m+1)} \qquad (6\text{-}23)$$

where m represents the segment number and $\boldsymbol{S}_e(m)$ and $\boldsymbol{r}'(m)$ are the unit vectors normal to the wave fronts and fictitious boundaries of the mth segment respectively. Substituting (6-4) into (6-23) and deriving the angles corresponding to $\boldsymbol{S}_e(m).\boldsymbol{\theta}'(m)$ and $\boldsymbol{S}_e(m+1).\boldsymbol{\theta}'(m+1)$, (6-23) becomes

$$\frac{\sin(\theta_e(m) + \theta_2(m))}{\sqrt{n_o^2 + (n_e^2 - n_o^2)cos^2\theta_e(m)}} = \frac{\sin\theta_e(m+1)}{\sqrt{n_o^2 + (n_e^2 - n_o^2)cos^2\theta_e(m+1)}} \qquad (6\text{-}24)$$

where $\theta_e(m) + \theta_2(m)$ and $\theta_e(m+1)$ are the incident and refraction angles at the boundary of m–m+1 media respectively and

$$\theta_2(m) = \tan^{-1}\frac{x(m+1) - x(m)}{z(m+1) - z(m)} \qquad (6\text{-}25)$$

where $(x(m), z(m))$ are the Cartesian coordinates of the points on the wave propagation path. Using (6-24) the refraction angle of the $m+1$ medium is expressed by

$$\begin{aligned}&\cos\theta_e(m+1)\\ &= \sqrt{\frac{n_e^2 cos^2\theta_e(m) + n_o^2(cos^2(\theta_e(m) + \theta_2(m)) - cos^2\theta_e(m))}{n_e^2 - (n_e^2 - n_o^2)(cos^2(\theta_e(m) + \theta_2(m)) - cos^2\theta_e(m))}}.\end{aligned} \qquad (6\text{-}26)$$

132
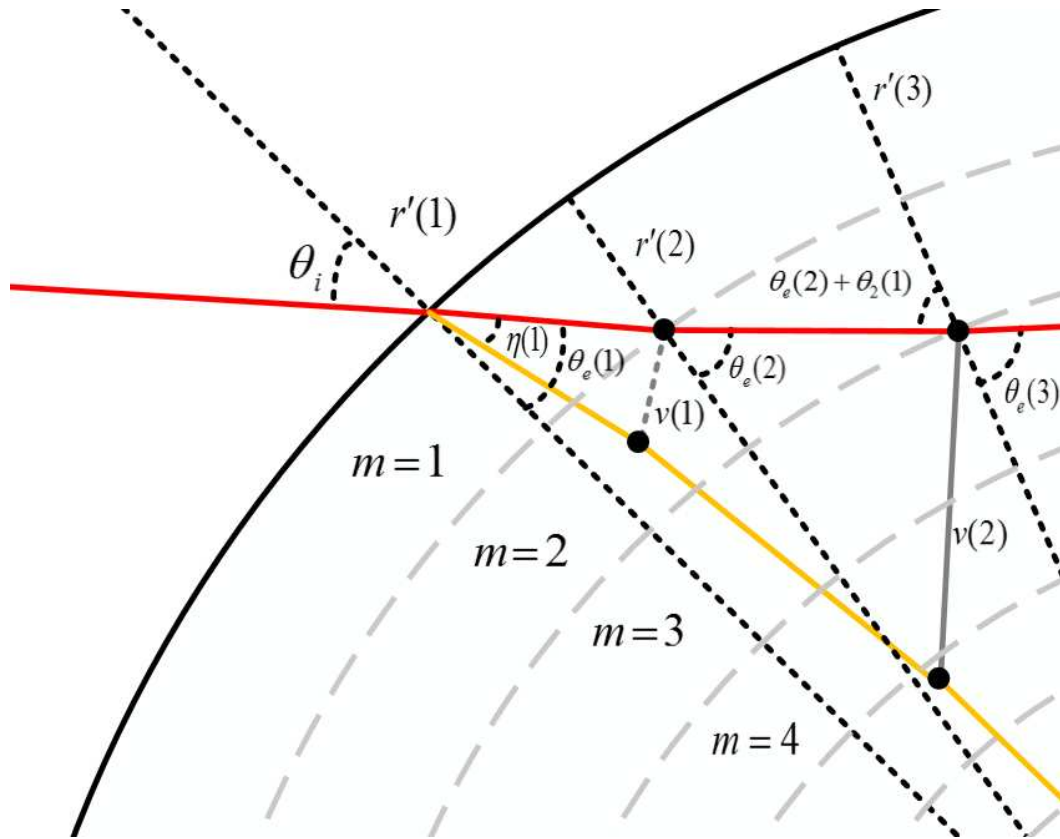
Fig. 6.9. Updating the wave and ray propagation path by dividing the propagation path into N equal segments

6.5.1 The travel time of the shortcut waves in the backscattering direction

Following the ray tracing theory in the isotropic dielectric sphere, the shortcut wave (P=1) comes from the incident tangential rays whose impact parameters are $b = {}^{+}_{-}1$. By traveling along the surface of dielectric sphere, these rays enter the sphere at the lit-shadow boundary region by critical angle. After crossing the dielectric sphere, they tangentially emerge on the other side of the boundary surface and regenerate the surface waves as demonstrated in Fig. 6.10.
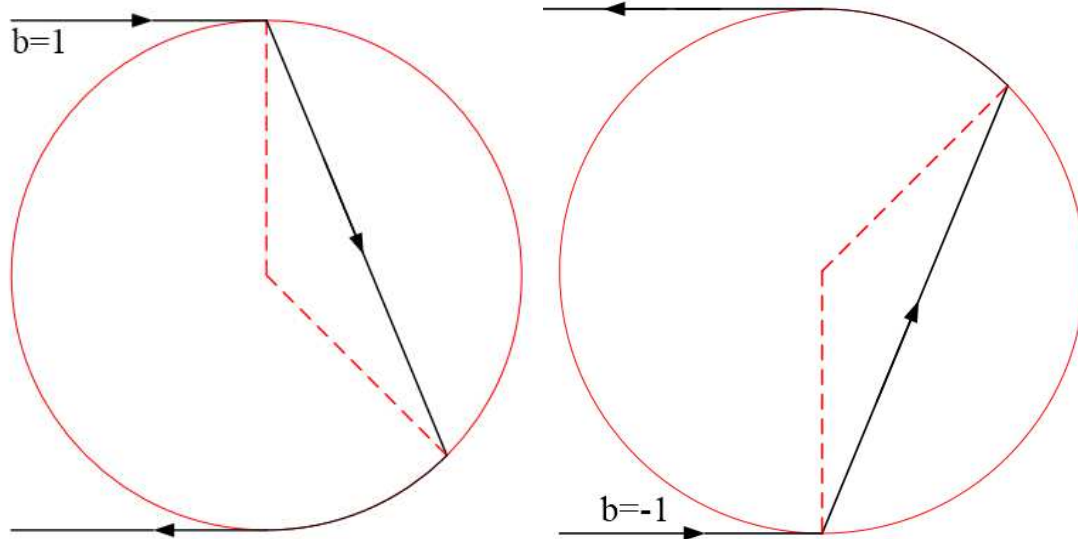
Fig. 6.10. The two possible examples of p=1 rays in uniaxial dielectric sphere

In the uniaxial sphere, however, two shortcut waves namely ordinary and extraordinary propagate in the sphere and it is found that they are not necessarily generated by incident tangential rays. As shown in Fig. 6.11, the incident ray generating the backscattered shortcut wave varies by ε_r values. It is of interest to note that the incident angle of these rays in the negative and weak positive uniaxial sphere is still the same as for the isotropic sphere and is equal to $\frac{\pi}{2}$. However, larger values of ε_r significantly reduce the angle of the incident ray generating the back scattered shortcut wave as summarized in Table 6.1.
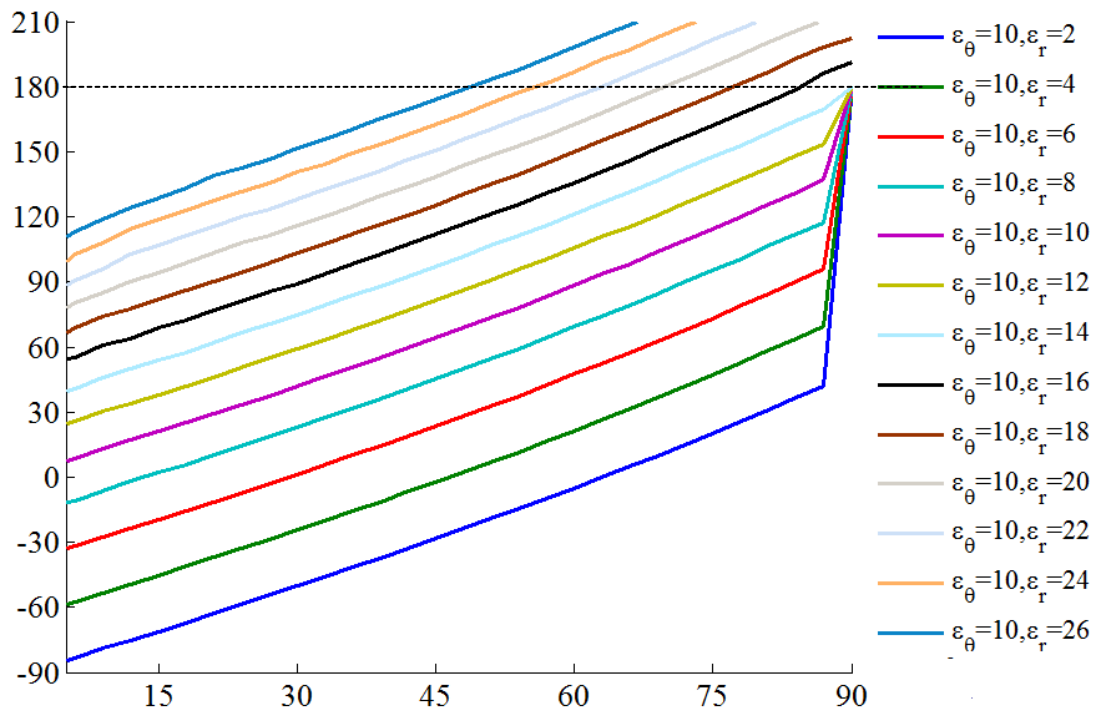
Fig. 6.11. Incident angle versus scattering angle of the shortcut waves

Table 6.1

The incident and scattering angles of the shortcut wave in various uniaxial spheres

ε_θ	ε_r	Incident angle (Degree)	scattering Angle (Degree)
10	2	90	180
10	4	90	180
10	6	90	180
10	8	90	180
10	10	90	180
10	12	90	180
10	14	90	180
10	16	84	180
10	18	71.5	180
10	20	66	180
10	22	59	180
10	24	52	180
10	26	48	180

135

The effect of variation in ε_r on the wave and ray paths is shown in Fig. 6. 12 and Fig. 6. 13. It is found that, by increasing/decreasing the value of ε_r, the curvature of the extraordinary wave and ray grow rapidly and therefore the path lengths corresponding to the extraordinary wave and ray increase accordingly. However, this variation has no influence on the ordinary wave path length and as a result the arrival time corresponding to these waves does not depend on the value of ε_r.

For the ordinary wave, the ray and wave propagate in the same direction and therefore their arrival time for the back scattering direction is identical and expressed as [10]

$$\bar{t} = 2\sqrt{(\varepsilon_\theta - 1)} + (\pi - 2\cos^{-1}(\theta_{o_c}))$$

(6-27)

where the first and second terms represent the traveling time of shortcut and surface wave respectively and $\theta_{o_c} = \sin^{-1} 1/n_o$. However, the arrival times of the extraordinary waves/rays are no longer identical to those of the ordinary waves. By varying the relative permittivities of the uniaxial sphere, we found that the arrival time of the extraordinary ray is extremely sensitive to both ε_r and ε_θ.

Using the Cartesian coordinates of N points on the extraordinary wave and ray paths and assuming a negligible phase velocity variation along each segment, the normalized arrival time of the extraordinary backscattered waves whose incident angle is $\frac{\pi}{2}$ can be derived by

$$\bar{t}$$

$$
= \begin{cases}
\left| \tan^{-1} \dfrac{z_r(N)}{x_r(N)} \right| \\
\quad + \displaystyle\sum_{m=1}^{N} N''(m) \cos \eta(m) \sqrt{\Delta x_r^2(m) + \Delta z_r^2(m)}, & x_r(N) < 0 \\[2mm]
\dfrac{\pi}{2} + \left| \tan^{-1} \dfrac{x_r(N)}{z_r(N)} \right| \\
\quad + \displaystyle\sum_{m=1}^{N} N''(m) \cos \eta(m) \sqrt{\Delta x_r^2(m) + \Delta z_r^2(m)}, & x_r(N) > 0
\end{cases} \tag{6-28}
$$

where the first and second terms are associated with the surface and shortcut wave travel times respectively, $\Delta x_r(m) = x_r(m+1) - x_r(m)$, $\Delta z_r(m) = z_r(m+1) - z_r(m)$, where $(x_r(m), z_r(m))$ are the Cartesian coordinates of the points on the ray path and $N''(m)$ and $\eta(m)$ are determined by (6-4)– (6-5). Note that $\bar{t} = \dfrac{c}{a} t$ and it can also be determined by the geometrical path along the normal wave front. Using the relation between u'' and v'' in (6-6) and knowing that

$$
\cos \eta(m) = \frac{\sqrt{\Delta x^2(m) + \Delta z^2(m)}}{\sqrt{\Delta x_r^2(m) + \Delta z_r^2(m)}} \tag{6-29}
$$

(6-28) can also be expressed as

$$
\bar{t} = \begin{cases}
\left| \tan^{-1} \dfrac{z(N)}{x(N)} \right| \\
\quad + \displaystyle\sum_{m=1}^{N} N''(m) \sqrt{\Delta x^2(m) + \Delta z^2(m)}, & x(N) < 0 \\[2mm]
\dfrac{\pi}{2} + \left| \tan^{-1} \dfrac{x(N)}{z(N)} \right| \\
\quad + \displaystyle\sum_{m=1}^{N} N''(m) \sqrt{\Delta x^2(m) + \Delta z^2(m)}, & x(N) > 0
\end{cases} \tag{6-30}
$$

where each term in the summation of (6-30) represents the travel time along a segment of the wave path and (x(m), z(m)) are the Cartesian coordinates of the points on the wave path. For high positive uniaxiality where the backscattered shortcut wave is generated by incident wave with impact parameter of $|b| < 1$, the normalized arrival time can be expressed as

$$\bar{t} = -\cos\theta_i + \sum_{m=1}^{N} N''(m)\cos\eta(m)\sqrt{\Delta x_r^2(m) + \Delta z_r^2(m)} \qquad (6\text{-}31)$$

or

$$\bar{t} = -\cos\theta_i + \sum_{m=1}^{N} N''(m)\sqrt{\Delta x^2(m) + \Delta z^2(m)} \qquad (6\text{-}32)$$

where θ_i is the incident angle of the wave generating the backscattered shortcut wave.
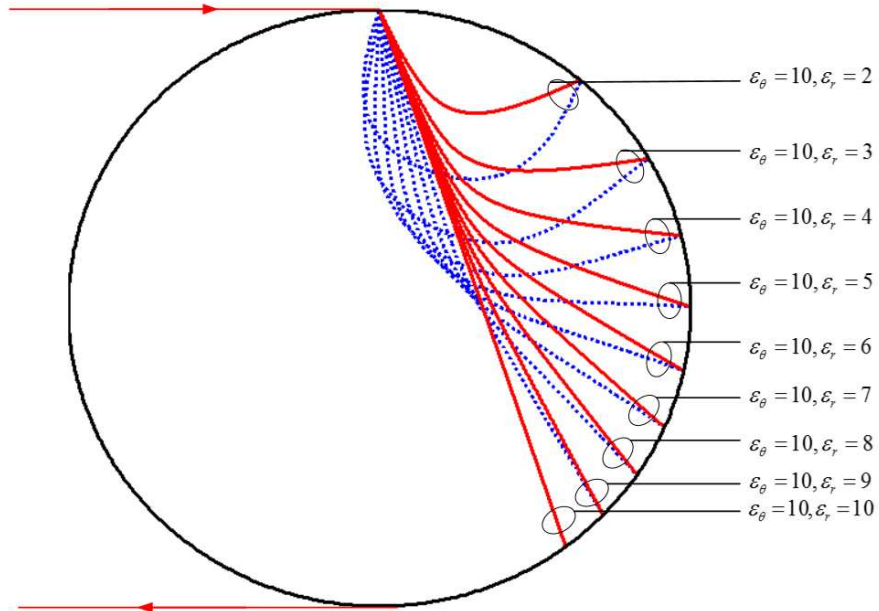
Fig. 6. 12. The shortcut wave and ray in various negative uniaxial spheres (solid line represents the wave propagation path and dotted line is ray path)

138
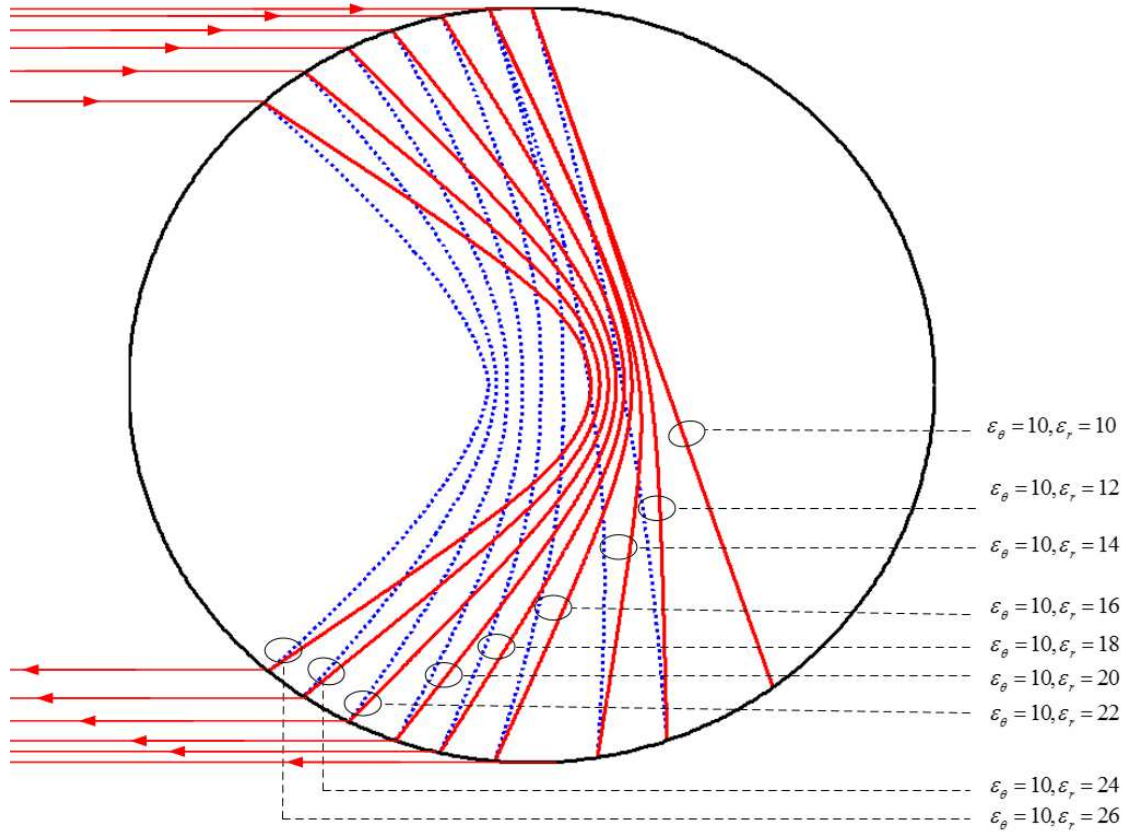
Fig. 6. 13. The shortcut wave and ray in various positive uniaxial spheres (solid line represents the wave propagation path and dotted line is ray path)

To validate (6-28)–(6-32), the arrival times of the P=1 ray for different values of ε_r are evaluated for N=2300 and compared with those computed using Mie and Debye series theories with good agreement as summarized in Table 6.2.

Table 6.2
The Arrival Time of the Shortcut Wave for various ε_r values

		P=1 Mie and Debye series Methods		P=1 Ray tracing Method	
ε_θ	ε_r	O-Wave	E-Wave	O-Wave	E-Wave

10	2	6.65	4.11	6.65	4.10
10	3	6.65	4.78	6.65	4.81
10	4	6.65	5.33	6.65	5.31
10	5	6.65	5.63	6.65	5.66
10	6	6.65	5.91	6.65	5.94
10	7	6.65	6.18	6.65	6.17
10	8	6.65	6.37	6.65	6.35
10	9	6.65	6.54	6.65	6.51
10	10	6.65	6.65	6.65	6.65
10	12	6.65	6.85	6.65	6.86
10	14	6.65	7.04	6.65	7.04
10	16	6.65	7.23	6.65	7.26
10	18	6.65	7.32	6.65	7.36
10	20	6.65	7.51	6.65	7.55
10	22	6.65	7.60	6.65	7.61
10	24	6.65	7.61	6.65	7.62
10	26	6.65	7.69	6.65	7.68

6.6 Conclusion

Ray tracing theory for a radially uniaxial dielectric sphere is implemented in this paper. The phase velocities as well as the refractive indices of the ordinary and extraordinary waves and rays in a radially birefringent medium are briefly studied and the results are applied to evaluate the arrival times and propagation paths of the shortcut wave returns. The effect of the variation in relative permittivities on the properties of these returns is investigated and it is found that the extraordinary wave and ray no longer propagate on a straight line when traveling in a radially uniaxial medium. The curvature of the extraordinary wave and ray paths grow rapidly with increasing/decreasing ε_r indicating increased/decreased path lengths of the extraordinary wave and ray. The angle of the incident ray whose scattering angle is in the backward direction is computed for various dielectric constants and its travel time is computed and compared with that obtained using Mie and Debye series solutions with satisfactory agreement.

References

[1] J. A. Stratton, Electromagnetic Theory, New York: McGraw-Hill, 1941.

[2] K. L. Wong and H. T. Chen, "Electromagnetic scattering by a uniaxially anisotropic sphere," *IEE Proceedings H,* Microwaves, Antennas and Propagation, vol. 139, no. 4, 1992.

[3] *J.* Lock and P. Laven, "Understanding light scattering by a coated sphere Part 1: Theoretical considerations," *J. Opt. Soc. Am.* A 29, 1489–1497, 2012.

[4] P. Laven, "Time domain analysis of scattering by a water droplet," Appl. Opt. 50, F29–F38, 2011.

[5] Philip Laven, "Simulation of rainbows, coronas and glories using Mie theory and the Debye series," *Journal of Quantitative Spectroscopy and Radiative Transfer*, Vol. 89, no. 1–4, pp. 257–269, 2004.

[6] J. Lock and P. Laven, "Mie scattering in the time domain. Part 1. The role of surface waves," J. Opt. Soc. Am. A, 28, 1086-1095, 2011

[7] J. Lock and P. Laven, "Mie scattering in the time domain Part II: the role of diffraction," J. Opt. Soc. Am. A 28, 1096–1106, 2011.

[8] E. M. Kennaugh, D. L. Moffatt, "Transient and impulse response approximations," *Proceedings of the IEEE*, vol.53, no.8, pp.893–901, Aug. 1965.

[9] E. M. Kennaugh and R. L. Cosgriff, "The use of impulse response in

electromagnetic scattering problems," *IRE Nat'l Conv. Rec.*, pp.72–77, 1958.

[10] M. S. Aly and T. T. Y. Wong, "Scattering of a transient electromagnetic wave by a dielectric sphere," *Microwaves, Antennas and Propagation, IEE Proceedings H*, vol. 138, no. 2, pp. 192–198, Apr 1991.

[11] H. Inada and M. A. Plonus, "The geometric optics contribution to the scattering from a large dense dielectric sphere," *Antennas and Propagation, IEEE Trans.*, vol. 18, no. 1, pp. 89–99, Jan 1970.

[12] J. Rheinstein, "Backscatter from spheres: A short pulse view," *IEEE Transactions on*, *Antennas and Propagation,* vol.16, no.1, pp. 89–97, Jan 1968.

[13] C. Jr. Bennett, W. L. Weeks, "Transient scattering from conducting cylinders," *Antennas and Propagation, IEEE Transactions on*, vol.18, no.5, pp. 627–633, Sep. 1970.

[14] H. C. Strifors, G. C. Gaunaurd, "Scattering of electromagnetic pulses by simple-shaped targets with radar cross section modified by a dielectric coating," *Antennas and Propagation, IEEE Transactions on* , vol.46, no.9, pp. 1252–1262, Sep 1998.

[15] P. Laven and J. Lock, "Understanding light scattering by a coated sphere Part 2: Time domain analysis," *J. Opt. Soc*. Am. A 29, 1498–1507, 2012.

[16] M. C. Simon, "Image formation through monoaxial plane-parallel plates," Appl. Opt. 27, 4176–4182, 1988.

[17] M. C. Simon, K. V. Gottschalk, "Waves and rays in uniaxial birefringent crystals," Optik International Journal for Light and Electron Optics, Volume 118, Issue 10, pp. 457–470, Oct. 2007.

[18] M. Avendaño-Alejo, O. Stavroudis, and A. Boyain y Goitia, "Huygens's principle and rays in uniaxial anisotropic media. I. Crystal axis normal to refracting surface," *J. Opt. Soc*. Am. A 19, 1668–1673, 2002.

[19] M. Avendaño-Alejo and O. Stavroudis, "Huygens's principle and rays in uniaxial anisotropic media. II. Crystal axis orientation arbitrary," *J. Opt. Soc.* Am. A 19, 1674–1679, 2002.

[20] J. Van Bladel, Electromagnetic Fields. New York: McGraw-Hill, 1964, p. 496, no. 161 and p. 494, #149.

[21] R. F. Harrington, Time-Harmonic Electromagnetic Fields, New York: McGraw-Hill, 1961.

[22] C.-W. Qui, S. Zouhdi, and A. Razek, "Modified spherical wave functions with anisotropy ratio: Application to the analysis of scattering by multilayered anisotropic shells*," IEEE Trans. Antennas Propagat*., vol. 55, no. 12, Dec. 2007.

[23] M. Abramowitz and I. A. Stegun, Editors, Handbook of Mathematical functions. Washington, D.C.: U.S. Government Printing Office, 1964.

[24] D. Worasawate, "Electromagnetic scattering from an arbitrarily shaped three-dimensional chiral body," Ph.D. thesis, Syracuse University, Syracuse, NY, Aug. 2002.

[25] S. Yarga, K. Sertel and J. L. Volakis, "Multilayer Dielectric Resonator Antenna Operating at Degenerate Band Edge Modes," *IEEE Antennas and Wireless Propagation Letters*, vol. 8, pp. 287–290, May 2009.

[26] H. Kettunen, H. Wallén and A. Sihvola, "Cloaking and Magnifying Using Radial Anisotropy," *Journal of Applied Physics,* vol. 114, no. 4, Aug. 2013.

[27] A. Novitsky, C. W. Qiu and S. Zouhdi, "Transformation-based spherical cloaks designed by an implicit transformation-independent method: theory and optimization," *New Journal of Physics,* vol. 11, Nov. 2009.

[28] E. A. Hovenac and J. A. Lock, "Assessing the contributions of surface waves and complex rays to far-field Mie scattering by use of Debye series," J. Opt. Soc. Am. A*, vol. 9, no. 5, pp. 781–795, May 1992.

[29] H. Kettunen, H. Wallén, and A. Sihvola, "Cloaking and magnifying using radial anisotropy," *Journal of Applied Physics,* vol. 114, no. 4, Aug. 2013.

[30] B. Ivsic, T. Komljenovic, and Z. Sipus, "Performance of uniaxial multilayer cylinders and spheres used for invisible cloak realization," *Antennas and Propagation (EUCAP), Proceedings of the 5th European Conference on*, pp.1092–1096, Apr. 2011.

[31] N. G. Alexopoulos, "High-frequency backscattering from a perfectly conducting sphere coated with a radially inhomogeneous dielectric," *Radio Science*, Vol. 6, no. 10, pp. 893–901, 1971.

[32] P. L. E. Uslenghi, "Electromagnetic scattering from radially inhomogeneous

media," Rep. 8658-1-T, NSF Grant GK-1408, University of Michigan, Radiation Laboratory, 1967

[33] G. N. Watson, "The diffraction of electric waves by the earth," *Proc. Roy. Soc. London*, Ser. A. 95, PP. 83–99, 1918.

[34] T. B. A. Senior and R. F. Goodrich, "Scattering by a sphere," in *Proc. Inst. Elect. Eng.*, vol. 111, May 1964.

[35] V. H. Weston and R. Hemenger, "High-frequency scattering from a coated sphere," *J. Res. Nat. Bureau of Standards-D. Radio Propagat.*, vol. 66D, no. 5, 1962.

[36] H. T. Kim, "High-frequency analysis of EM scattering from a conducting sphere coated with a composite material," *IEEE Trans. Antennas Propagation*, vol. 41, pp. 1665–1674, Dec. 1993.

[37] P. L. E. Uslenghi, V. H. Weston, "High-frequency scattering from a metal-like dielectric lens," *Applied Scientific Research,* pp. 147–163, 1971.

[38] R. F. Goodrich and N. D. Kazarinoff, "scalar diffraction by prolate spheroids whose eccentricities are almost one," *Proc. Cambridge Philos*. Soc. 59, pp. 167–183, 1963.

[39] H. M. Nussenzveig, "High-Frequency scattering by a transparent sphere. I. direct reflection and transmission," *Journal of Mathematical Physics*, vol. 10, pp. 82-

124, 1969.

[40] M. Abramowitz and I. A. Stegun, *Handbook of mathematical functions: with Formulas, Graphs, and Mathematical Tables*, Dover Books on Mathematics, 1961.

[41] G. N. Watson, *A treatise on the theory of Bessel functions*, Cambridge University press, Cambridge, England, 1952.

[42] S.I Rubinow, "Scattering from a penetrable sphere at short wavelengths," *Annals of Physics*, Vol. 14, pp. 305–332, 1961.

[43] J. M. C. Scott, "An asymptotic series for the radar scattering cross section of a spherical target," *Atomic Energy Research Establishment, Tech. Memo*. T/M 30, 1949.

[44] R. F. Harrington, *Time-Harmonic Electromagnetic Fields*, Wiley IEEE-press, Sep. 2001.

[45] M. Yazdani, J. Mautz, L. Murphy, and E. Arvas, "Electromagnetic backscattering from uniaxial sphere: Debye series solution" Accepted in *International Microwave Symposium*., Jan. 2014.

[46] V. H. Weston, "Pulse return from a sphere," *Antennas and Propagation, IRE Transactions on* , vol. 7, no. 5, pp. 43–51, December 1959.

[47] M. Yazdani, J. Mautz, L. Murphy, and E. Arvas, "High Frequency scattering from radially uniaxial dielectric sphere" under review in *IEEE Transactions on Antennas and Propagation*, Feb. 2014.

[48] M. Yazdani, J. Mautz, J. K. Lee, and E. Arvas, "Transient electromagnetic scattering by a radially uniaxial dielectric sphere: Mie and Debye series solutions," under review in *IEEE Trans*. on antenna and propagation, March 2014.

[49] L. C. Van de Hulst, *Light Scattering by Small Particles*, 1981.

[50] M. C. Simon, "Image formation through monoaxial plane-parallel plates," Appl. Opt. 27, 4176–4182, 1988.

[51] M. C. Simon, K. V. Gottschalk, "Waves and rays in uniaxial birefringent crystals," Optik International Journal for Light and Electron Optics, Volume 118, Issue 10, pp. 457–470, Oct. 2007.

Mohsen Yazdani

CURRICULUM VITAE

3-204 Center of Science & Technology, Syracuse University, Syracuse NY 13244

myazdani@syr.edu   (315)-744-5981

Professional Summary

Doctoral student with academic and industrial background in the fields of RF/Microwave circuits, antennas and electromagnetics. Over 20 papers (including 11 journal papers) published and/or under review in various refereed journals and conferences.

Education

- *2011-present:* Ph.D., Electrical Engineering, Syracuse University, Syracuse, NY. August 2014
    - Advisors: Prof. Ercument Arvas and Dr. Joseph R. Mautz.
    - Ph.D. Dissertation: Time domain scattering from anisotropic dielectric sphere
- *2007-2009*: Master of Science, Electrical Engineering, Iran University of Science and Technology (IUST), Tehran, Iran.
    - MS Thesis: The design of double ridge waveguide filter using conventional stepped impedance low-pass filter method

Job Experience

2012 – Present: R&D Engineer, Dielectric Laboratories, Inc., Cazenovia, NY

- Designing, simulating, and testing of the following microwave products:
- Compact Ultra-low phase noise dielectric cavity resonator oscillators, Reference: conference NO. 15.
- Thin film low-pass and band-pass microwave filters, Reference: Journal NO. 2 conference NO. 16, 18, and 19.
- Microwave couplers, power dividers, and phase shifters
- Dielectric resonator antenna, Reference: conference NO. 10-11.

2011–Present: Graduate/Teaching Assistant, PhD study Syracuse University, Dept. of EECS, Syracuse

Published and presented scientific papers on Microwave and Electromagnetics problems. Detailed list of publications can be found further below.

- Conducting research on time domain scattering from anisotropic objects
  A theoretical study is carried out to determine the scattering of a transient electromagnetic wave by a radially uniaxial dielectric spheres using three methods, Mie, Debye and ray tracing. This is achieved by inverse Laplace transformation of the frequency domain scattering solution. In the first approach, the impulse and step response of uniaxial dielectric spheres are evaluated by Mie series asymptotic high frequency solutions. In the second approach, the generalized Debye series solution is introduced and the generalized Mie series coefficients are replaced by their equivalent Debye series formulations. The results are then applied to evaluate the transient response of each individual Debye term allowing the identification of impulse returns in the transient response of a uniaxial sphere. In the third approach the ray tracing is introduced in uniaxial dielectric spheres and the time arrival of each individual impulse return is calculated using this method.
- Teaching assistant: Taught lectures/recitations for Circuits I/II, sophomore-level electrical engineering courses, as well as prepared teaching materials (handouts, exams, quizzes, and homework).

2010-2011: Teaching assistant, Dept. of EECS, Huntsville, AL

- Taught lectures for Circuit Labs I/II, sophomore-level electrical engineering courses.

2007-2009: Antenna laboratories, IUST

- Design, Simulation, Fabrication and test of 3D Inclined Slot Array Waveguide Antenna (11x35 elements)
- Mutual Coupling Reduction in Patch Antenna Arrays Using EBG Structures

Class Projects

- Comparison between TLM & FDTD & FEM methods in computing Resonance Frequency of Rectangular Cavity (Numerical techniques in electromagnetics class).
- 3D objects Scattering Wave Analysis with arbitrary cross sections by Magnetic Field Integral Equation (MFIE) & Electric Field Integral Equation (EFIE) (Numerical techniques in Electromagnetics class).

Professional Skills

- Programming & Software: Ansoft HFSS, Genesys, AWR, ADS, Matlab, Autocad, Sonnet, hobbies, AWAS, CST.
- Tools: Hands-on experience with the RF/Microwave test equipment, TDR, phase noise analyzer, spectrum analyzer, pico probing, network analyzer, signal generator, antenna tester, LPKF, Microwave Power meter, amplifier NF measurement.

Awards and Certificates

- Phi Kappa Phi (honor society) awarded 2014.
- Certificate of attending the poster session, IEEE UWB, Syracuse, NY, 2012.
- Awarded departmental recognition for outstanding student, academic year 2010-11, UAHuntsville.

Professional Roles and Memberships

- Program assistant for the IEEE International Microwave Symposium Tampa, FL, 2014.
- Program assistant for the 11th IEEE International Conference on Ultra-Wideband, ICUWB 2012,
- Reviewer for PIER & JEMWA (Progress in Electromagnetics Research & Journal of Electromagnetic Wave and Applications.
- Student Member of IEEE

Journal Articles (Published/Accepted/Under Review)

1. M. Yazdani, L. Murphy, A. Mallahzadeh, E. Arvas, and J. Mautz. "The design of double ridge waveguide filter using conventional stepped impedance low-pass filter method," *Microwave and Optical Technology Letters*. Vol. 56, No. 1, Jan. 2014, pp. 120-124.

2. L. Murphy, M. Yazdani, J. Mautz, E. Arvas, and S. Tozin. "Design of a Dielectric Waveguide Filter with Embedded Metamaterial using Mode Matching Technique," *Microwave and Optical Technology Letters*. Vol. 2, Issue 2, pp. 443-446, 2014.

3. M. Khalaj-Amirhosseini, M. Yazdani, "To Compact Branch-Line Coupler using Parallel High-Impedance Transmission Lines," *Microwave and Optical Technology Letters*, Volume 53, Issue 3, page 700, March 2011.

4. F. Hosseini, M. Khalaj-Amirhosseini and M. Yazdani, "A Miniaturized Wilkinson Power Divider Using Nonuniform Transmission Line," *Journal of Electromagnetic and Microwave Application (JEMWA),* Volume 23, Number 7, 2009, pp. 917-924(8).

5. F. Hosseini, M. Khalaj-Amirhosseini and m. Yazdani, "To Compact circular Branch Line Coupler Using Nonuniform Transmission Line," *Microwave and Optical Technology Letters*, Volume 51, Issue 11, Nov. 2009, pp. 2679-2682.

6. M. Yazdani, J. Mautz, L. Murphy, and E. Arvas, "High Frequency scattering from Radially Uniaxial Dielectric Sphere," Second review on *IEEE transactions on antenna and propagation*, 2014.

7. M. Yazdani, J. Mautz, J. K. Lee, and E. Arvas, "Transient scattering from a radially uniaxial dielectric sphere: Mie and Debye series solutions," Under review on *IEEE transactions on antenna and propagation*, 2014.

8. M. Yazdani, J. K. Lee, J. Mautz, and E. Arvas, "Transient scattering from a radially uniaxial dielectric sphere: Ray tracing method," to be submitted on *IEEE transactions on antenna and propagation*, 2014.

9. L. Murphy, J. Mautz, M.Yazdani, E. Arvas, and S. Tozin. "Uniaxial Dielectric Waveguide Filter Design Accounting for Losses Using Mode Matching Technique," *ACES Journal*. Under review 2013.

10. M. Yazdani, D. Bates, and L. Murphy, "A new method of excitation in Cubic DRA," to be submitted on *Antennas and wireless propagation Letters*, 2014.

11. M. Yazdani, D. Bates, and L. Murphy, "Beam forming and steerability of cubic DRA," to be submitted on *Antennas and wireless propagation Letters*, 2014.

Conference papers (Published/Accepted/Under Review)

12. Murphy, J. Mautz, M.Yazdani, E. Arvas, and S. Tozin, "Design of an Uniaxial Dielectric Waveguide Filter with Embedded Metamaterial using Mode Mathcing Technique," *ACES Conf. on App. Comp. Electomag*. Jacksonville, Fl. March, 2014.

13. M. Yazdani, J. Mautz, L. Murphy, and E. Arvas, "Electromagnetic Wave Scattering by a Uniaxial Dielectric Sphere: Debye series solution," Accepted on *International Microwave symposium*, Tampa, FL, 2014.

14. M. Yazdani, J. Mautz, L. Murphy, and E. Arvas, "Scattering from a large uniaxial dielectric sphere," Accepted on *Antenna and propagation Symposium*, Memphis, TN, 2014.

15. M. Yazdani, D. Bates, and L. Murphy, "The Design and Fabrication of a Compact Low Phase Noise Dielectric Cavity Resonator Oscillator," accepted on *European Microwave Conference*, Rome, Italy, 2014.

16. L. Murphy, J. Mautz, M.Yazdani, E. Arvas, S. Tozin, and D. Bates. "Design of V-Band Dielectric Filled Waveguide Filters with Improved Loss and Suppression of Parasitic Waves." accepted on *European Microwave Conference*, Rome, Italy, 2014.

17. M. Yazdani, F. Khajeh mirzaee Yazdi, "A UWB 1 to 4 Wilkinson Power Divider With Triple High-Q Band-Notched Characteristic Using U-Shaped DGS," *ICUWB* 2012, Syracuse.

18. L. Murphy, M. Yazdani, and E. Arvas, "Compact Low Pass Filter with Ultra-Wide Pass and Stopbands using Stepped Impedance Resonators and Novel Techniques," *ARMMS Conference*, Bedfordshire UK, November 2012.
19. L. Murphy, M. Yazdani, and E. Arvas, "Ultra-wide stopband in a Compact Low Pass Filter using Stepped Imedance Resonators and Novel Techniques," *IEEE Confr. on UWB*, Syracuse NY, pp. 92-94, 2012.
20. M. Yazdani, M. Khalaj-Amirhosseini and F. Hosseini, "Size Reduction and Harmonic Suppression of Narrow Band-Pass Waveguide Filter Using Nonuniform Transmission Line Theory," *Progress In Electromagnetics Research (PIER)*, Cambridge, USA, July 5-8, 2010.
21. F. Hosseini, M. Khalaj-Amirhosseini and M. Yazdani, "Novel Compact Branch-Line Coupler Using Nonuniform Transmission Line," *Asia Pacific Microwave Conference (APMC)*, 2009.

Poster Presentations

1. M. Yazdani, L. Murphy, and E. Arvas, "The design of microwave passive components using non-uniform transmission lines," The Annual Conference of SU's CASE Center, The NEXT, Liverpool, NY, 2014.
2. M. Yazdani, D. Bates, L. Murphy, and E. Arvas, "Design of low phase noise oscillators using two and four port cavity resonators," The Annual Conference of SU's CASE Center, The NEXT, Liverpool, NY, 2014.
3. L. Murphy, M. Yazdani, J. Mautz and E. Arvas **"**Metamaterials in Waveguides filled with Uniaxial Dielectric," The Annual Conference of SU's CASE Center, The NEXT, Liverpool, NY, 2014.
4. M. Yazdani, L. Murphy, and E. Arvas "Size reduction and harmonic suppression of band-pass filters Using Non-Uniform Transmission Line Technique," *IEEE Confr. on UWB*, Syracuse NY, 2012.
5. L. Murphy, M. Yazdani, and E. Arvas "The design of Compact Low Pass Filter using Stepped Impedance Resonators," *IEEE Confr. on UWB*, Syracuse NY, 2012.
6. M. Yazdani, M. El-Sabbagh, "New Excitation for Cubic Dielectric Resonator Antenna to Produce Omnidirectional Pattern," NUNAN poster, Syracuse University, Syracuse, NY, 2012.

Research Talk and Presentation

"Design of ultra-low phase noise Microwave oscillators," annual meeting at Syracuse University Cognitive Wireless Systems and Networks Group, Jan. 2014.

Selected Graduate Courses

Fundamental of Microwave, Advanced Microwave, Electromagnetics, Advanced Electromagnetics, Antenna I, Antenna II, Bases of Radar Systems, Numerical

Techniques in Electromagnetics, Advanced RADAR techniques, advanced digital signal processing, Modern antennas, Microwave measurement, optical communication systems, Surface plasmonics and methamaterials, Advanced Antenna.